A DATA-DRIVEN APPROACH TO GLYCEMIC DISTURBANCE MITIGATION, RECONSTRUCTION, AND PATTERN RECOGNITION

By John P. Corbett

A dissertation submitted in partial fulfillment of the requirements for the degree of

Doctor of Philosophy

University of Virginia

AUGUST 18, 2021

UNIVERSITY OF VIRGINIA
Department of Engineering Systems and Environment

To the Faculty of University of Virginia,

This dissertation has been read and approved by the following members of the examining committee.

X

Mehdi Boukhechba, Ph.D.
Committee Chair

X

Marc Breton, Ph.D.
Advisor

X

Mark DeBoer, M.D.

X

Stephen Patek, Ph.D.

X

Rupa Valdez, Ph.D.

Acknowledgments

I would like first to thank my parents. They taught me that we all face challenges in our lives, and how we deal with them makes us who we are. I learned how to accept how I was different and appreciate that through their words and actions. I would also like to thank my brother Joe. He has shown me how, even when situations are not easy and even when others do not see the struggle you are going through, it is important to persevere. In all that you all do, you bring kindness and tenacity. I hope to do the same in my own life.

Dr. Marc Breton has been a mentor personally and academically since I was a clueless 19-year-old intern. Now that I am 27 years old and slightly less clueless, I can really appreciate all that you have done to teach me how to be a better thinker, engineer, and scientist. Even though it was not always easy, I know that you always had my best interest at heart, and for that, I am extraordinarily appreciative. There is no one who would have done a better job at training me to make an impact in the field of diabetes technology. I would also like to thank my committee members Drs. Boukhechba, DeBoer, Patek, and Valdez. Each of you has helped me learn and become a better researcher in your own ways and for that I am very grateful.

It is very rare that a group of people can be accurately described as world-class, but I think this is an appropriate adjective for my colleagues at the Center for Diabetes Technology. You all are exceptional in your passion and technical ability. Working with this extraordingary team has made my experience so much better and the impact of the work that is very personal to me so much more profound. Thank you for all that you all do.

In memory of Nicole Perrot "Nikki" Foster

August 18, 1985 – December 17, 2010

Your kindness has had such a profound impact on my life and inspired me to help others like you helped me. You made this challenging disease, much less so, even though it was so difficult for you. You brought so much light to this world, and I hope you know that some good came from it. This was for you.

With love your cousin,

- Jack

"If people bring so much courage to this world the world has to kill them to break them, so of course it kills them. The world breaks everyone and afterward many are strong at the broken places. But those that will not break it kills. It kills the very good and the very gentle and the very brave impartially."

– Ernest Hemingway

Abstract

The outline of the following chapters is listed below.

Chapter 1 states the problem that is addressed by this dissertation and the contents of each of the specific aims.

Chapter 2 provides background on the physiology of glucose homeostasis in the human body. A review of diabetes pathology, simulation modeling of type one diabetes, challenges with self-reported data, and meal detection is also included.

Chapter 3 describes the design and evaluation of an automatic bolus priming system focused on safety. This chapter also includes the results of a pilot clinical study where the automatic bolus priming system was integrated into an MPC-based automatic insulin dosing system and compared to a state-of-the-art artificial pancreas control system.

Chapter 4 explains the design of two glycemic disturbance detection algorithms. There is also a comparison of these two algorithms provided in this chapter.

Chapter 5 details how historical data was used to create individualized profiles representing patterns of disturbances experienced by people with type 1 diabetes and how these profiles were integrated into a multistage model predictive control system to anticipate glycemic disturbances such as meals. The results of a simulation experiment designed to evaluate the impact of the bolus priming system and the anticipatory disturbance profiles on glycemia are also discussed.

Chapter 6 summarizes the findings of this dissertation and reflects on its impact. Additionally, there are some further applications of this work that are presented.

Table of Contents

Table of Figures

List of Abbreviations

ADA	American Diabetes Association
BG	Blood Glucose
BMI	Body Mass Index
BPS	Bolus Priming System
CGM	Continuous Glucose Monitoring
CV	Coefficient of Variation
DiAs	Diabetes Assistant
DSS2	Decision Support System Project 2
EEG	Electroglottography
EMG	Electromyography
FDA	Food and Drug Administration
GRID	Glucose Rate of Increase Detector
GV2a	Glucose Variability 2 Study Part A
HbA1c	Hemoglobin A1c
IOB	Insulin on Board
LDL	Low-density Lipoproteins
MPC	Model Predictive Control
MS-MPC	Multistage Model Predictive Control
PAIN	Parameter-invariant
RCKT+	Rocket+ Project
ROC	Receiver Operating Characteristic
SD	Standard Deviation
SMBG	Self-monitoring of Blood Glucose
SOGMM	Subcutaneous Oral Glucose Minimal Model
T1D	Type 1 Diabetes
T2D	Type 2 Diabetes
TDI	Total Daily Insulin

Introduction

Glycemic disturbances such as meals and exercise are the primary causes of hypoglycemia and hyperglycemia for those with type 1 diabetes (T1D). Currently available automatic insulin dosing systems (i.e., hybrid artificial pancreas systems) cannot sufficiently mitigate the unwanted effects of these disturbances without user input. Because meals are entered manually by the user, there are errors regarding the timing and size estimates of these events, which causes issues with both real-time control of blood glucose (BG) and retrospective data analysis. To create a fully closed-loop artificial pancreas system, techniques to automatically detect, anticipate, and reject disturbances must be developed.

This dissertation strives to advance diabetes technology by developing a method to detect glycemic disturbances in real-time and create a strategy to automatically dose insulin when appropriate. Additionally, methods to improve data quality by retrospectively detecting positive glycemic disturbances will be defined and compared. Finally, this work describes a procedure to recognize patterns in behaviors relevant to glycemic control and characterize those patterns in a way that is usable in a closed-loop system to anticipate disturbances. These advances will be used for real-time disturbance detection and dosing, data reconstruction, and disturbance mitigation through anticipatory behavioral profiles.

The primary hypotheses of this work are: (1) events where insulin doses can be administered safely and would improve control of plasma BG can be detected in real-time using machine learning, and a strategy for automatically dosing insulin can be determined from the output of this detection algorithm; (2) data-driven methodologies can be used to detect and reconstruct past disturbance events accurately; and finally (3) reconstructed records can be used to create profiles of glycemic disturbances to inform the planning of insulin treatment strategies (i.e., model predictive controllers that can anticipate meals). The chapters related to the specific aims of this work detail how each of these hypotheses was evaluated.

Background

Physiology of Glucose Homeostasis

In a healthy state, the human body can maintain tight control of plasma BG levels. This process involves input and response from several physiological components. Glucose regulation is achieved through a sophisticated interplay between various hormones and neuropeptides released and regulated by the brain, pancreas, liver, intestine, and muscle and adipose tissue. The pancreas plays a vital role in this process by producing insulin, which lowers BG, and glucagon, which raises it. These two hormones serve as counterbalances in raising and lowering plasma BG as deemed appropriate. Both T1D and type two diabetes (T2D) are characterized by defective insulin production. Those with T1D have little to no endogenous insulin production, and those with T2D have impaired regulation due to reduced insulin production and increased resistance to insulin.[1] Defective glucose regulation causes hypoglycemia and hyperglycemia in both conditions. Figure 1 shows the components involved in the glucose homeostasis process. This system involves the kidneys, pancreas, liver, and tissue (e.g., brain, muscle). The processes that raise BG are shown in blue, and the processes that lower BG are shown in orange.

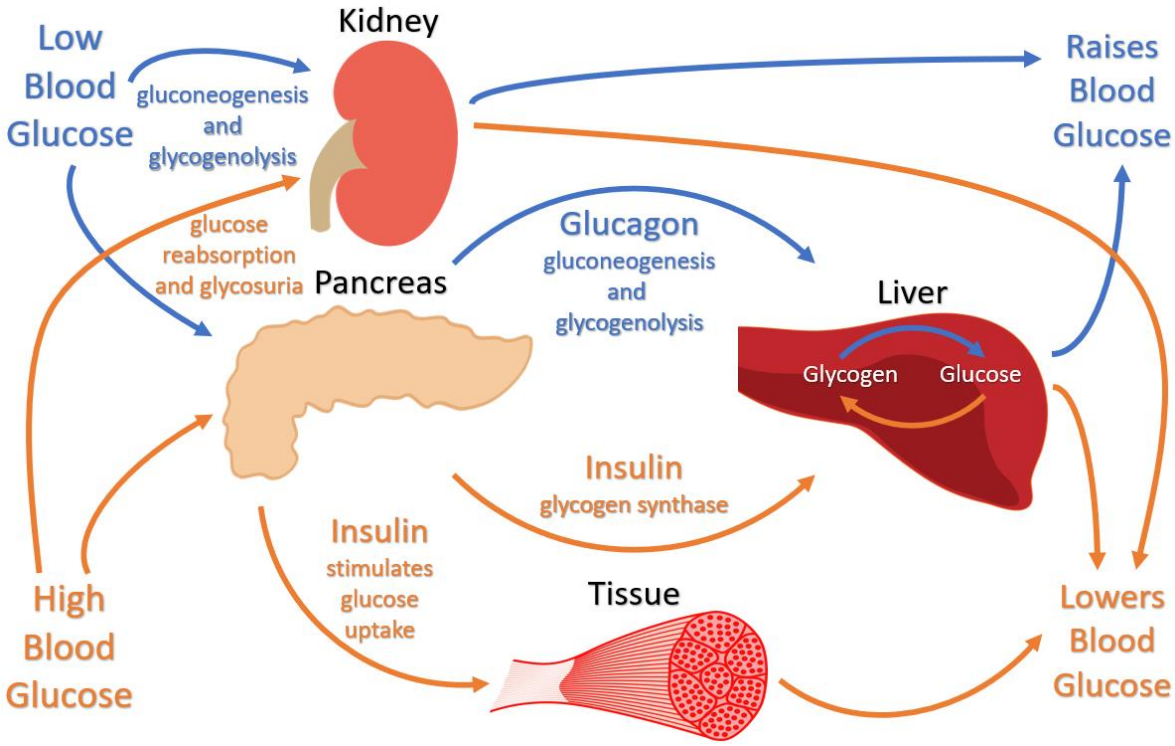

Figure 1 – A diagram of the insulin-glucose system. The processes shown in orange represent actions that lower blood glucose. The processes in blue raise blood glucose.

Pancreas

The pancreas is located in the left upper abdominal cavity behind the stomach and is responsible for releasing digestive enzymes and hormones. Five types of cells produce hormones in the pancreas, α-cells that make glucagon, β-cells that generate amylin and insulin (which is released with c-peptide), ɣ-cells that make pancreatic polypeptide, somatostatin producing δ-cells, and ε-cells that make ghrelin. The body maintains BG within a narrow range from the balancing effects of glucagon and insulin. Glucagon raises BG by stimulating hepatic glycogenolysis as well as hepatic and renal gluconeogenesis. The production of glucagon is inversely proportional to BG.

Conversely, insulin secretion is stimulated by elevated BG and reduced when BG is decreased. Insulin lowers BG by enabling the insulin-dependent uptake of glucose into muscle and adipose tissues. This action, in turn, decreases BG values by removing exogenous glucose from plasma blood. The release of insulin also signals α-cells to downregulate glucagon production.[1,2]

Liver

The liver plays an essential role in glucose homeostasis through two mechanisms: gluconeogenesis and glycogenolysis. Glycogenolysis is the transformation of glycogen to free glucose. Gluconeogenesis is the formation of glucose from precursors (e.g., lactate, glycerol, amino acids) and the conversion of that glucose (i.e., glucose-6-phosphatase) to free glucose.[3] In the fasted state, the liver can release glucose from stored glycogen through the process of glycogenolysis. Glycogenolysis is triggered by glucagon's presence and releases glucose that can be consumed by the brain, red blood cells, and muscles.[4] After eating, glucose is stored in the liver in the form of glycogen. Insulin signaling, which occurs after eating, activates glycogen synthase, allowing the conversion of glucose to glycogen. Plasma BG levels are reduced by converting free glucose to glycogen, which is stored in the liver.[5]

Kidneys

The kidneys contribute to the homeostasis process by releasing glucose into blood plasma via gluconeogenesis and absorbing glucose to maintain renal functionality through glucose uptake. Besides the liver, the kidneys are the only organ capable of significant gluconeogenesis, which allows the release of glucose into circulation. In addition to gluconeogenesis, the kidneys are also capable of glycogenolysis, where glycogen stored renally is transformed into free glucose in the blood plasma.[3] Some studies have shown that the kidneys may be responsible for up to 40% of all gluconeogenesis.[6] The kidneys also contribute to glucose homeostasis by filtering and reabsorbing glucose. Under normal glycemic conditions, the kidneys absorb as much glucose as is available. In a hyperglycemic state,

usually, when BG is greater than 200 mg/dL, glucose transporter proteins become overwhelmed, and glucosuria occurs.

Tissue

Following eating, skeletal muscles are a significant consumer of glucose through insulin-dependent glucose uptake. In euglycemic conditions where plasma insulin levels are high, skeletal muscles are responsible for approximately 80% of all glucose uptake. In muscle and adipose tissue, GLUT4 is mainly responsible for glucose transport. GLUT4 is insulin sensitive and allows for postprandial glucose to be absorbed into adipose and skeletal muscle tissue.[7] The brain is a large consumer of glucose and uses roughly 20% of all energy derived from glucose.[8] The degree to which the brain affects glucose homeostasis is somewhat controversial, but there is some evidence to support its role.[9] The adipose tissue accounts for 10% to 15% of glucose disposal after a meal. It has been shown that both too little fat (i.e., lipodystrophy) and excess fat (i.e., obesity) are linked to insulin resistance and hyperglycemia.[10] Altogether, tissues are responsible for a large portion of glucose absorption and play a role in glucose homeostasis by removing free glucose from plasma.

Diabetes

Type One Diabetes

The process of glucose homeostasis is substantially disrupted for individuals with T1D. T1D is a chronic autoimmune disease characterized by the destruction of insulin-producing β-cells in the pancreas. The exact cause of T1D is unclear but is likely due to the interplay of environmental, immune, and genetic factors.[11] In addition to attenuated or a complete lack of insulin production, glucagon amounts can be increased inappropriately for the prevailing plasma BG levels, and endogenous glucose output is higher in T1D than in health.[12] The smooth transition of insulin and glucagon secretion present in health is dysfunctional for those with T1D. Eating and the subsequently absorbed glucose do not stop endogenous glucose output, and there is some evidence to support that it accelerates this process.

Additionally, for people with T1D, eating is not compensated for through total glucose disposal because of the lack of naturally produced insulin in the system. The disruption in glucose homeostasis makes individuals with T1D prone to hyperglycemia because of their lack of insulin production. To manage BG, those with T1D inject exogenous insulin and monitor BG levels. Miscalculations in insulin doses can lead to both hypoglycemia and hyperglycemia. Dysregulation of BG to the degree of T1D can be experienced by those who have severely progressed T2D.[12]

Type Two Diabetes

People with T2D generally have fasting insulin secretion rates and glucagon concentrations that are higher than in health. When the renal glucose absorption rates are at a maximum, glycosuria provides a glucose disposal method through urine, as it does in T1D. In T2D, insulin resistance is usually present in the peripheral tissues and liver.[12] Those with T2D often experience postprandial plasma glucose concentrations that are higher than what is found in health. Several factors contribute to this occurrence. In the fed state, glucagon levels may be elevated for those with T2D.

Additionally, in T2D, glucose-induced insulin secretion, GLP-1 response, and glucagon suppression are attenuated, eliminating some of the endocrine system's ability to regulate BG. An overarching issue of T2D is that hyperglycemia does not prevent the liver from releasing glucose. Those with T2D also have higher insulin levels in the presence of elevated plasma glucose, thus indicating insulin resistance. Furthermore, glucose clearance is reduced in peripheral tissues.[12] The combination of these factors that disrupt glucose homeostasis makes people with T2D more prone to hyperglycemia.

Prevalence

Although the exact quantity is unknown, the International Diabetes Federation estimated that in 2019 there were 463 million people with diabetes worldwide.[13] Globally this accounts for 9.3% of the population, and it is projected that 10.9% of the world will have diabetes by 2045. The increasing prevalence of obesity, hypertension, urbanization, alcohol use, and diagnostic testing, as well as decreasing consumption of fruits and vegetables, may contribute to the increase in T2D.[14] The cause of increasing rates of T1D is not clear. It has been hypothesized that viruses, hygiene, vitamin D deficiency, and even the consumption of breast and cow milk may affect the pathogenesis of T1D, but a consensus has not been reached among scientists.[15]

There are 26.9 million people in the United States with diagnosed diabetes, which accounts for 8.2% of the total population.[16] Of those people, nearly 6% (1.6 million) have T1D. Based on the laboratory criteria for diabetes, an additional 7.3 million Americans in 2018 had diabetes but were unaware of their disease.

Due to complications associated with the disease, people with diabetes have a notable increase in the risk of all-cause mortality.[17,18] It has been estimated that 4.2 million people, ages 20 to 79, died as a result of diabetes in 2019.[19] Globally, diabetes contributes to 11.3% of death with disparities in various continents, regions, and countries. In Europe, diabetes is a factor in 31.4% of deaths for people under

60, whereas this percentage is 73.1% in Africa. The estimated worldwide expenditure on diabetes in 2019 was $760 billion.

Complications

The hemoglobin A1c (HbA1c) test is the most widely accepted measurement of glycemic control in diabetes. This test measures the amount of glucose attached to hemoglobin in the blood and typically indicates glycemic control over the last three months.[20–22] HbA1c is so widely used because its value is strongly linked to the risk of developing complications from diabetes.[23–25] Only 52.5% of adults with T2D and 21% of adults with T1D are meeting the goals set forth by the American Diabetes Association of having an HbA1c value of less than 7%.[26,27] When the criteria for diabetes management are extended to other factors significant to the development of complications for T2D, such as low-density lipoproteins (LDL) cholesterol and blood pressure, only 18.8% of the population met the benchmarks.

The complications related to hyperglycemia are severe and can be fatal. Prolonged hyperglycemia can result in numerous vascular complications, including.[28] Hypoglycemia may lead to short and long-term complications such as myocardial infarction, neurocognitive dysfunction, cerebrovascular disease, retinal cell death, and vision loss.[29] Severe hypoglycemia can result in coma, seizure, brain damage, or even death.[30] There is also growing evidence to link diabetes to some cancers, dementia, infections, and liver disease.[28] It is believed that people with diabetes can avoid glycemia-related complications through intensive insulin therapy and careful management of BG levels.[23]

People with diabetes are also more likely to suffer from psychological conditions such as anxiety, depression, and disordered eating.[31] These problems can often stem from diet issues, management tasks such as measuring BG and administering insulin, and a lack of support from family members and health care providers. There is a defined relationship between worse glycemic control and increased psychological symptoms.[32] Depression and anxiety can increase the occurrence of severe hypoglycemia and diabetic ketoacidosis, both of which can be fatal.[33] Additionally, people living with diabetes have a lower quality of life than those without it.[34]

3.8% of females and 1.5% of males between the ages of 13 and 18 in the US exhibit some form of disordered eating.[35] Rates of disordered eating are 2.4 times higher in women with T1D than in the population without diabetes in the US.[36] Furthermore, preteen and teenage girls with T1D were more likely to exhibit a combination of two or more disordered eating behaviors than their peers without diabetes.[37] Empirically, it has been shown that risk factors associated with eating disorders, such as

higher body mass index (BMI), depression, and monitored eating, are often more prevalent in the lives of those with T1D.[38] People with T1D can also restrict insulin to lose weight, which is a modality of unhealthy weight control not available to the population without diabetes. Those who limit insulin injections compared to other women with T1D have a threefold increase in mortality after controlling for BMI, HbA1c, and age.[39] It has been posited that increased rates of disordered eating could be a result of management tasks related to T1D, such as dietary restraint and monitoring.[40–42]

Management of Type One Diabetes

To supplement halted or attenuated insulin production, people with T1D administer exogenous insulin through either insulin injections or continuous subcutaneous insulin infusion via an insulin pump. When people eat glucose, it is absorbed and released into circulation. To compensate for the ensuing rise in plasma glucose, people with diabetes must inject insulin when they eat (i.e., meal boluses). People with T1D also administer correction boluses to mitigate hyperglycemia. For those who take multiple daily injections, a dose of long-acting insulin is given either once or twice daily. Pump users have insulin continuously infused. This "basal rate" varies from person to person and may change throughout the day.[43]

To ensure that proper amounts of insulin are being delivered and BG concentration is in the euglycemic range, people with T1D measure glucose concentrations throughout the day. While HbA1c provides information about relative levels of glycemic control over a long time, it does not give information about the effect of specific activities (e.g., eating, physical activity) or intraday patterns of glycemia. Self-monitoring of blood glucose (SMBG) is a method for measuring capillary glucose concentrations where an individual pricks his or her finger, produces a droplet of blood, and places that droplet on the end of a disposable strip protruding from a glucose meter. SMBG allows people to monitor BG levels whenever they need to with a meter that can be transported easily. A challenge associated with glucometers is that they must be calibrated using a control solution periodically, and it has been shown that 58% of patients or their caregivers never do.[44]

It is recommended that people with diabetes use some glucose monitoring method like SMBG to keep BG values within an acceptable range. SMBG can improve the management of diabetes by collecting information to determine long-term patterns in glycemia, allow for people with diabetes and their families to make day-to-day decisions regarding treatment, prevent unwanted glycemic events (i.e., hypoglycemia and hyperglycemia), and educate people on how activities (e.g., eating and exercise) affect BG.[45] The frequency at which individuals measure their BG through SMBG is positively correlated

with positive glycemic outcomes for people with T1D and T2D.[46] The American Diabetes Association (ADA) recommends that people who use insulin to manage their diabetes should measure their BG "prior to meals and snacks, at bedtime, occasionally postprandially, prior to exercise, when they suspect low blood glucose, after treating low BG until they are normoglycemic, and prior to and while performing critical tasks such as driving."[47] The ADA estimates that this would require six to ten finger sticks per day.

Although helpful, SMBG can be invasive and painful. It also does not fully describe trends, variability, and glycemic excursions throughout the day. Additionally, SMBG does not alert individuals to current or imminent hypoglycemia or hyperglycemia without their prompting. Continuous glucose monitoring (CGM) measures glucose with a small sensor inserted in the interstitium (i.e., just under the skin). The values measured in this manner are then converted to estimates of plasma BG levels. These devices collect measurements frequently, usually every five minutes, and transmit them using a Bluetooth transmitter to a device where they are displayed. The device where BG values are displayed can be a CGM-specific receiver, smartphone, or a connected insulin pump.

Figure 2 shows an example of the differences between CGM and SMBG measurements for one day. The CGM measurements are shown with the blue markers, and the SMBG measurements are shown in red. Here the difference in sampling is clear. If SMBG measurements are only taken before meals, the rise and variability following those events would be unknown to the individual. Even the mean between the two methods of measurement is notably different in this example. The average CGM value is 136 mg/dL, whereas the average SMBG value is 32 mg/dL lower.

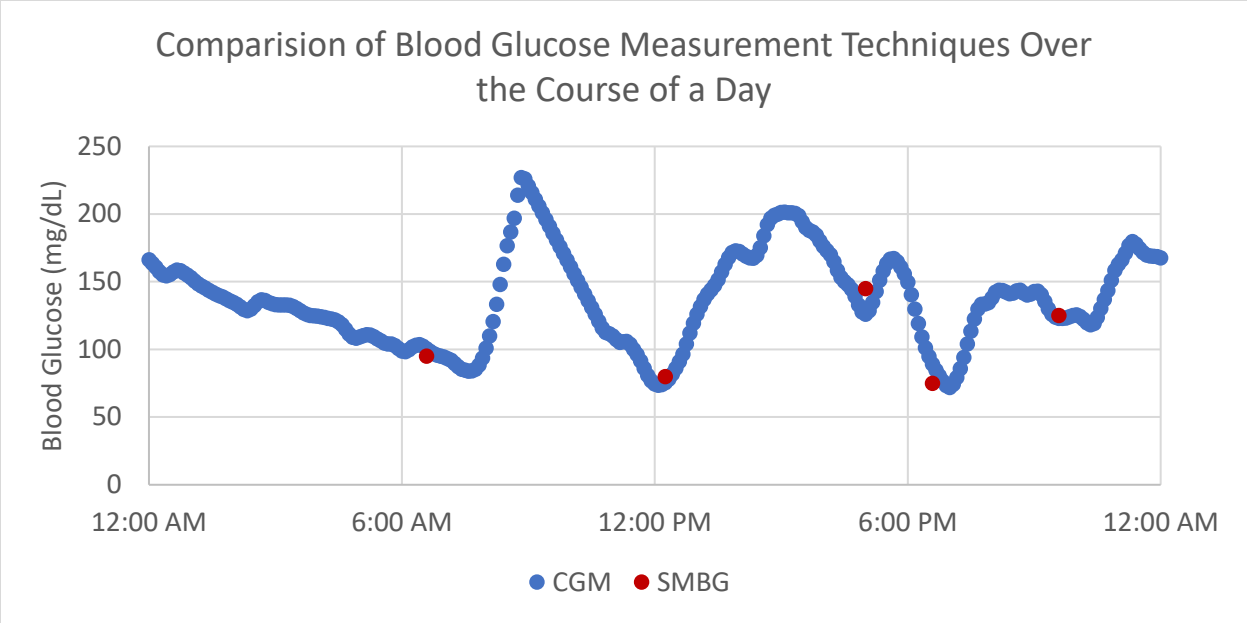

Figure 2 – An example of SMBG in red and CGM values in blue throughout a day.

A vast body of research supports that CGM's improve glycemic control for those using intensive insulin therapy.[48,49,58,59,50–57] CGM's have proven effective in reducing both hypoglycemia, hyperglycemia, and HbA1c overall. Those who use their CGM device the most regularly experienced the greatest benefit in terms of glycemic control.[48,50,57] It is also believed that CGM's can reduce diabetes-related complications and medical costs as well as improve quality of life over the lifetime of a person with diabetes compared to SMBG.[60,61] A recent study has shown that the prevalence of people using insulin pumps and CGMs is increasing, and those who use those advanced devices have better glycemic management overall.[27]

Feedforward Control for Prandial Insulin Dosing

The dynamics associated with insulin and glucose create a pernicious problem from a control perspective. In the context of T1D management, the actuator, which is insulin administration, has somehow slower time dynamics than the disturbances that it is attempting to mitigate (i.e., meals and exercise), thus justifying the use of feedforward control. Intensive insulin therapy (a.k.a. functional insulin therapy) has been used widely for the past decades as a method of preventing postprandial hyperglycemia. This feedforward strategy requires people with T1D to quantify the magnitude of a disturbance in real-time in the form of carbohydrate amounts, and then an insulin dose is calculated to prevent future hyperglycemia caused by this disturbance. The formula for functional insulin therapy is,

$$J = \frac{CHO}{CR} + \frac{BG - BG_{target}}{CF} - IOB,$$

where J (u) is the insulin dose, CHO (g) is the number of carbohydrates consumed, CR (g/u) is the carbohydrate to insulin ratio, BG (mg/dL) is the current BG value, BG_{target} (mg/dL) is the target BG value, CF (mg/dL/u) is the correction factor, and IOB (u) is an estimate of the amount of insulin currently in the system.

Traditionally, the CR and CF parameters were changed by physicians empirically based on observation and clinical experience. Paul Davidson pioneered a formulaic approach to determining these values from clinical observations in the 1980s.[62] The so-called "1500 rule" is,

$$CF = \frac{1500}{TDI},$$

where TDI (u) is the patient's average total daily insulin amount. Similarly, Walsh and Roberts introduced the "450 rule" based on Walsh's clinical experience.[63] This rule to determine appropriate CR is,

$$CR = \frac{450}{TDI}.$$

These guidelines did not consider the patient's size or the type of insulin being used. The "1500 rule" was initially construed for regular insulin and updated when insulin analogs and insulin pumps became more prevalent.[64] Based on a retrospective clinical study with 167 insulin pump patients, the formulas for CR and CF became,

$$CR = \frac{2.8 \cdot BW}{TDI},$$

$$CF = \frac{1717}{TDI},$$

with BW (lb) representing the patient's body weight. These formulas are based on the basal insulin requirement accounting for 48% of the TDI. Others have also tried to develop formulaic rules for prandial insulin dosing using clinical trials and retrospective data analysis.[65] In all of these studies, the formulas derived disregard known fluctuations in intraday and interday insulin sensitivity. Additionally, none take into account differences in individuals, hormone fluctuations, or the macronutrient content of what is being eaten. These empirical rules may serve as a good starting point for physicians to select

parameters if there is little or no data available but are crude and ignore many factors that affect the insulin need of individuals.

Automatic Insulin Delivery

CGM's and insulin pumps have been integrated to assist those with T1D further than traditional intensive insulin therapy. Threshold suspend and predictive suspend systems, anticipate BG values in the near future, and reduce or stop basal delivery of insulin to prevent hypoglycemia. These systems are available commercially to individuals in the United States through several medical device manufacturers (e.g., Tandem Diabetes Care, Medtronic) and have been shown to reduce the time and intensity of hypoglycemia.[66,67] The US Food and Drug Administration (FDA) approved the first hybrid closed-loop insulin dosing system, the Medtronic 670G HCL, which in addition to preventing hypoglycemia by reducing insulin, is capable of increasing insulin to prevent hyperglycemia. Clinical trials of this product showed improvements in HbA1c, reduction in hypoglycemia, and an increased percentage of BG values in a euglycemic range.[68] The FDA approved a second hybrid closed-loop insulin dosing system, Tandem Control-IQ, in 2019 for adults and adolescents and 2020 for school-aged children. The algorithm used in this product was developed to a large degree at the University of Virginia (UVA) and licensed by Tandem to make it available to consumers.

Research efforts regarding automatic insulin delivery systems, also known as artificial pancreases, have expanded to systems that anticipate meals, adapt continuously, and adjust for exercise based on detections and announcements.[69–73] The two main strategies in automatic insulin delivery development are single hormone and dual hormone control. Single-hormone systems infuse one hormone to regulate BG levels, which is always insulin. Dual hormone control uses multiple hormones to lower BG with insulin and a second hormone (e.g., pramlintide, glucagon) to either raise BG or change the dynamics of glucose absorption. Recent meta-analyses have shown an improvement of 10% to 15% in the amount of time when the users' BG was between 70 and 180 mg/dL (i.e., time in range) when artificial pancreases are used compared to conventional therapy or sensor-augmented pump therapy. Time in range can be further increased when a second hormone is implemented in the system.[74]

Several automatic insulin dosing systems that do not require users to input meal amounts have been tested. In 2014, Harvey et al. evaluated a fully closed-loop artificial pancreas system on 12 adult participants with T1D in an inpatient clinical trial.[75] Overall, this system produced glycemic control with 80% of all BG readings in the 70 to 180 mg/dL range but caused high postprandial glucose values following unannounced meals. Forlenza et al. presented the performance of a fully closed-loop system

that preempted predefined postprandial excursions in a 72-hour hotel-based study, reporting a time in range of 63.6 ± 9.2%.[76] However, in the four hours following unannounced meals, the time above range (i.e., >180mg/dL) was 60.9 ± 23.3%. A recent study by Dovc et al. used two formulations of insulin, FIASP, and Aspart, in a 27-hour inpatient admission study of their fully closed-loop artificial pancreas system.[77] They reported time in range of 53.3% and 57.9% for Aspart and FIASP insulins, respectively. Their approach relied on a meal detection algorithm but similarly faced difficulty with unannounced meals. Multi-hormone approaches have reported better performances, with recent early outpatient results.[78] In 2021, Haidar et al. conducted a 30 participant open-label crossover trial and showed that an automatic insulin dosing system using simple meal announcements and empagliflozin was non-inferior to a hybrid system with meal announcements. The dual hormone system achieved a mean BG of 153 ± 25.2 mg/dL compared to the hybrid system, which had a mean BG of 153 ± 27.0 mg/dL.[79] Majdpour et al. demonstrated the non-inferiority of an insulin-pramlintide fully closed-loop artificial pancreas to a hybrid system in another 2021 pilot study.[80] In this study, the fully closed-loop system had a time in range of 81%, whereas the subjects were in range 83% of the time using the hybrid closed-loop system.

Simulation Modeling of Type One Diabetes

The University of Virginia/Padova Type One Diabetes Simulator

In 2008, the US FDA accepted a T1D simulation platform designed through a collaboration of researchers from the UVA and the University of Padova for testing new insulin dosing strategies in place of animal trials.[81] This platform, known as the UVA/Padova T1D Simulator, can accurately represent the effects of insulin and ingested carbohydrates for people with T1D. It contains a 300-subject population of virtual subjects consisting of 100 adults, 100 adolescents, and 100 children with parameterizations based on observed metabolic characteristics of the T1D population.

The UVA/Padova T1D Simulator can represent the features of various commercially available insulin delivery methods (i.e., insulin pumps) and glucose measurement devices (i.e., CGM's). Updates to the platform have improved the accuracy of the model's glucose dynamics as well as allow for the simulation of multiple sequential meals and intraday fluctuations of insulin sensitivity.[82,83] The original paper describing the UVA/Padova T1D Simulator has over 700 citations, and this simulator has been used to verify the safety and efficacy of numerous closed-loop insulin dosing systems preceding human clinical trials. A limitation of this method is that this platform helps determine a treatment's effect in an overall sense but does not match specific in silico subjects to in vitro individuals, thus demonstrating the effect it would have on them in real life. Other limitations are that it does not incorporate aspects of

diabetes management like the effect of exercise, hormonal changes (e.g., sickness, menstruation), device failures, and behavioral characteristics frequently observed in the population (e.g., inaccurate carbohydrate counting, missed or late boluses).

Insulin-Glucose Dynamics

A two-compartment model represents the glucose subsystem in the UVA/Padova T1D Simulator. This model is defined as,

$$\dot{G}_p(t) = EGP(t) + Ra_{meal}(t) - U_{ii}(t) - E(t) - k_1 \cdot G_p(t) + k_2 \cdot G_t(t),$$

with EGP (mg/kg/min) as the endogenous glucose production, Ra_{meal} (mg/kg/min) as meal glucose rate of appearance, U_{ii} (mg/kg/min) representing the insulin-independent glucose utilization, E (mg/kg/min) as the renal excretion, $k_{1,2}$ (1/min) as time constants, and G_t (mg/dL) representing the glucose mass in the rapidly and slowly equilibrating tissues. G_t is shown as,

$$\dot{G}_t(t) = -U_{id}(t) + k_1 \cdot G_p(t) - k_2 \cdot G_t(t),$$

with U_{id} (mg/kg/min) as the rate of insulin-dependent glucose uptake. The measured BG value, G (mg/dL), is found through the equation,

$$G(t) = \frac{G_p(t)}{VG},$$

where VG (dL/kg) is the distribution volume of glucose.

Glucose Rate of Appearance in Blood Plasma

The physiological model used for intestinal glucose absorption in the UVA/Padova T1D simulator was described first by Dalla Man et al.[84] This representation describes how glucose is transferred through the digestive system by representing the stomach with two compartments and a single compartment for the gut. The stomach compartments are represented as,

$$Q_{sto}(t) = Q_{sto1}(t) + Q_{sto2}(t),$$

$$\dot{Q}_{sto1}(t) = -k_{gri} \cdot Q_{sto1}(t) + D \cdot \delta(t),$$

$$\dot{Q}_{sto2}(t) = -k_{empt}(Q_{sto}) \cdot Q_{sto2}(t) + k_{gri} \cdot Q_{sto1}(t),$$

where k_{gri} (1/min) and $= -k_{empt}(Q_{sto})$ (1/min) are rate constants describing grinding and gastric emptying. D (mg) is the amount of ingested glucose, and δ is the impulse function. The gut compartment is represented as,

$$\dot{Q}_{gut}(t) = -k_{abs} \cdot Q_{gut}(t) + k_{empt}(Q_{sto}) \cdot Q_{sto2}(t),$$

with k_{abs} (1/min) representing the rate constant for intestinal absorption. Glucose rate of appearance this then found using,

$$Ra(t) = \frac{f \cdot k_{abs} \cdot Q_{gut}(t)}{BW},$$

where f (unitless) is the fraction of absorbed glucose and BW (kg) is the individual's body weight.

The Subcutaneous Oral Glucose Minimal Model

The subcutaneous oral glucose minimal model (SOGMM) is a framework to represent the effects of ingested carbohydrates and subcutaneously injected insulin on plasma BG levels.[85] The SOGMM is an extension of previous compartmental models, namely those developed by Bergman et al. and Dalla Man et al.[86,87] The core minimal submodel model equations are given as,

$$\dot{G}(t) = -\Big(S_g + X(t)\Big) \cdot G(t) + S_g \cdot G_b + \frac{R_a(t)}{V_g},$$

$$\dot{X}(t) = -p_2 \cdot X(t) + p_2 \cdot S_I(I(t) - I_b),$$

where G (mg/dL) is the plasma glucose concentration. R_a (mg/dL/min) represents the glucose rate of appearance. G_b(mg/dL) is the basal plasma glucose value associated with the individual's basal insulin rate. S_g (1/min) is the fractional glucose effectiveness, which represents how well glucose can stimulate glucose disposal and reduce endogenous glucose production and V_g (kg/dL) is the distribution volume of glucose in the blood plasma. X (1/min) is the proportion of insulin in the remote compartment. I (mU/L) is the concentration of insulin in the plasma. I_b (mU/L) is the individual's plasma insulin requirement. p_2 (1/min) is the rate constant for the remote insulin compartment and S_I (1/min/mU/L) is the insulin sensitivity factor which represents the individual's ability dispose of glucose from injected insulin. Glucose rate of appearance, R_a, is found by,

$$R_a(t) = \frac{(Q_2(t) \cdot k_{abs} \cdot f)}{BW},$$

with Q_2 as the second "gut" compartment. k_{abs} (1/min) represents the rate constant for oral glucose absorption. f (dimensionless) is the proportion of intestinal absorption of glucose that appears in plasma, and BW (kg) is the individual's body weight. Insulin concentration, I (mU), is determined as,

$$I(t) = \frac{I_p(t)}{V_I \cdot BW},$$

where V_I (L/kg) is the distribution volume of insulin, and I_p (mU) which is the plasma insulin concentration.

The gastrointestinal submodel is comprised of two compartments and represents the transport of oral carbohydrates. The model equations are as follows,

$$\dot{Q_1}(t) = -k_\tau \cdot Q_1(t) + \omega(t),$$

$$\dot{Q_2}(t) = k_{abs} \cdot Q_2(t) + k_\tau \cdot Q_1(t),$$

where Q_1 (mg) and Q_2 (mg) are the first and second compartments of oral glucose transport. k_τ (1/min) is the rate constant for oral glucose absorption, and ω (mg/min) is the rate of meal carbohydrate absorption.

The subcutaneous insulin kinetic submodel is a three-compartment model that describes the insulin pathway from subcutaneous injection to the blood plasma. The model equations are,

$$\dot{I}_{sc1}(t) = -k_d \cdot I_{sc1}(t) + J_{ctrl}(t),$$

$$\dot{I}_{sc1}(t) = -k_d \cdot I_{sc2}(t) + k_d \cdot I_{sc1}(t),$$

$$\dot{I}_{sc1}(t) = -k_{cl} \cdot I_p(t) + k_d \cdot I_{sc2}(t),$$

where I_{sc1} (mU) and I_{sc2} (mU) are the interstitial insulin compartments. k_d (1/min) and k_{cl} (1/min) are the rate constants related to subcutaneous insulin transport. J_{ctrl} (mU/min) is the insulin injected and I_P (mU) is the plasma insulin concentration.

Because inputs such as insulin and meals and BG measurements are recorded discretely, the SOGMM has a linearized and discretized form. The system is linearized around basal plasma insulin concentration, I_b (mU), and the basal glucose concentration, G_b (mg/dL). This new linear continuous form is represented as,

$$x_c = \left[\partial G(t), \partial X(t), \partial I_{sc1}(t), \partial I_{sc2}(t), \partial I_p(t), \partial G_{sc}(t), \partial Q_1(t), \partial Q_2(t)\right]^T,$$

$$\dot{x}_c(t) = A_c \cdot x_c(t) + B_c \cdot u_c(t) + G_c \cdot \omega(t),$$

$$y_c(t) = C_c \cdot x_c(t),$$

where x_c is the patient's metabolic state vector. The different states are defined as:

1. Differential BG concentration, $\partial G(t)$
2. Differential insulin action in the remote compartment, $\partial X(t)$
3. Differential interstitial insulin in the first compartment, $\partial I_{sc1}(t)$
4. Differential interstitial insulin in the second compartment, $\partial I_{sc2}(t)$
5. Differential plasma insulin, $\partial I_p(t)$
6. Differential interstitial glucose concentration, $\partial G_{sc}(t)$
7. Differential gut mass in the first compartment, $\partial Q_1(t)$
8. Differential gut mass in the second compartment, $\partial Q_2(t)$

Because the system is linearized around the operating points related to basal glucose and insulin concentration values (i.e., G_b and I_b) the new states are defined as differential values related to:

1. Differential insulin input which is relative to the individual's preprogrammed basal rate profile
2. Differential subcutaneous glucose which is relative to G_b

The coefficient matrices for the linear form are,

$$A = \begin{bmatrix} S_g & -G_b & 0 & 0 & 0 & 0 & 0 & \frac{k_{abs} \cdot f}{BW \cdot V_G} \\ 0 & -p_2 & 0 & 0 & \frac{p_2 \cdot S_I}{V_I \cdot BW} & 0 & 0 & 0 \\ 0 & 0 & -k_d & 0 & 0 & 0 & 0 & 0 \\ 0 & 0 & k_d & -k_d & 0 & 0 & 0 & 0 \\ 0 & 0 & 0 & k_d & -k_{cl} & 0 & 0 & 0 \\ k_{sc} & 0 & 0 & 0 & 0 & -k_{sc} & 0 & 0 \\ 0 & 0 & 0 & 0 & 0 & 0 & -k_\tau & 0 \\ 0 & 0 & 0 & 0 & 0 & 0 & k_\tau & -k_{abs} \end{bmatrix},$$

$$B = [0 \quad 0 \quad 1 \quad 0 \quad 0 \quad 0 \quad 0 \quad 0]^T,$$

$$G = [0 \quad 0 \quad 0 \quad 0 \quad 0 \quad 0 \quad 1 \quad 0]^T,$$

$$C = [0 \quad 0 \quad 0 \quad 0 \quad 0 \quad 1 \quad 0 \quad 0].$$

The linear time-invariant model is made discrete using the zero-hold order method.

Personalized Simulation Platforms

More recently, new simulation platforms based directly on field-collected data, and therefore potentially specific to individual subjects or subgroups, have been developed.[85,88] The primary technological innovation of these platforms is the estimation of an additional input signal designed to capture system disturbances unrepresented in traditional insulin-glucose models, like exercise, unreported meals, or hormonal changes. This estimation procedure is achieved using a deconvolution method that relates CGM readings with insulin and meal records through the SOGMM. The unknown input that explains observed data from recorded inputs is called the oral carbohydrate net effect signal or simply the "net effect." This signal can then be used to change insulin or carbohydrate amounts and determine how those changes would impact that particular subject on that specific day based on how they absorbed insulin and carbohydrates. This highly personalized tool helps impart unmodeled real-world dynamics into a simulation environment capable of determining the effects of changing treatments.

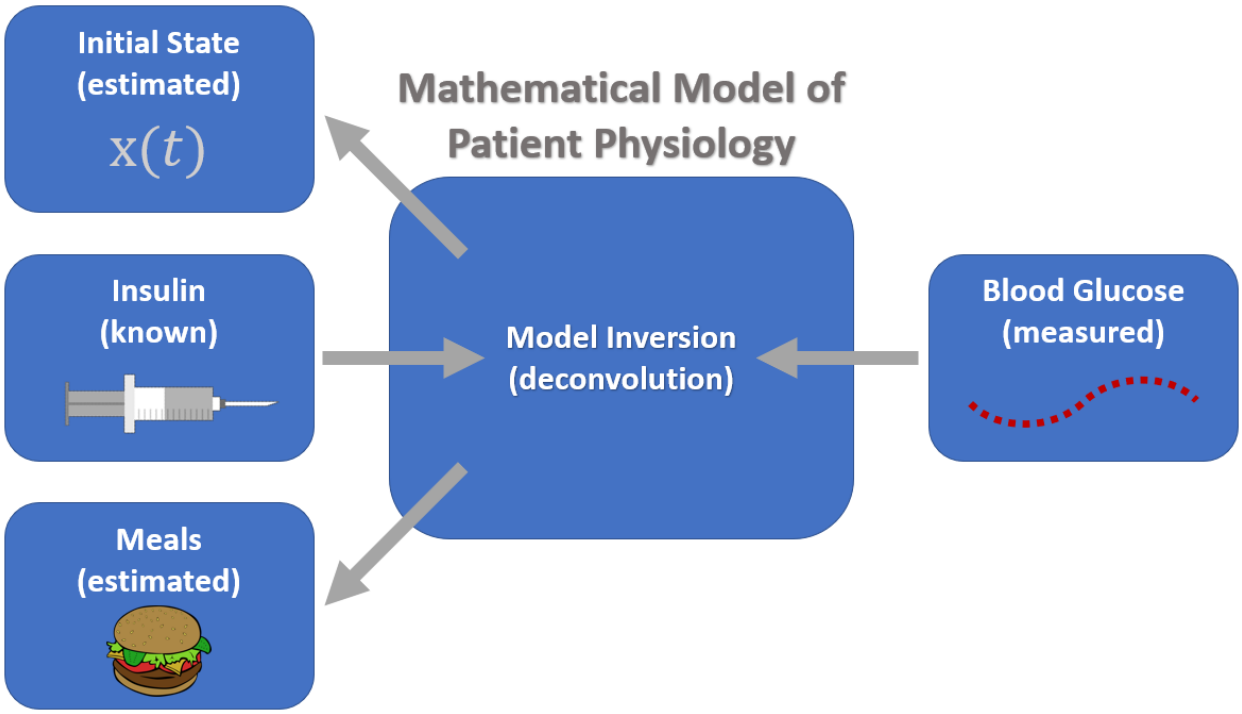

Figure 3 – A diagram of the "net effect" methodology adapted from Patek et al.[85]

Figure 3 shows a diagram of the "net effect" methodology. This depiction shows how when there is a record of subcutaneous glucose concentrations measured with a CGM and known insulin infusions; the unknown disturbance can be estimated. By solving for the unknown inputs using the

model, this methodology can be inverted. In this process, the historical inputs, like recorded meals or boluses, can be altered, and glucose predictions can be made as a result of the changes. In this way, previous situations can be "replayed," allowing for a simulation of how treatment changes would have affected BG values. Figure 4 shows an example of how the net effect simulator was used to replay the glucose trace following a meal using a different prandial insulin dose. In this example, the historical data is shown in blue, and the simulated data is in orange. It can be seen in this example how when the insulin dose was increased and the glucose trace was re-simulated, BG values were lower than the original. This tool is useful in determining the effect of a treatment change in a specific real-life situation.

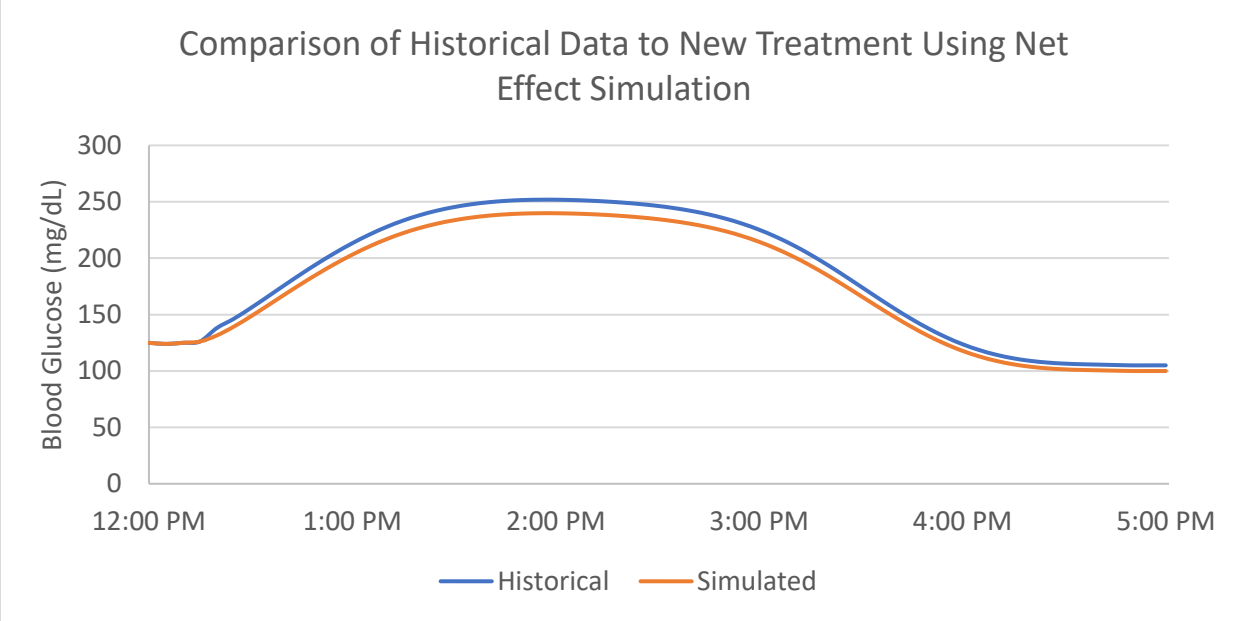

Figure 4 – A net effect re-simulation example comparing historical data shown in blue to simulated data using the net effect with a different insulin dose following a meal shown in orange.

Challenges with Self-Reported Data

The most widely used models of the insulin-glucose system have traditionally been nonlinear, dynamic models.[82,85,87,89,90] These models attempt to represent glucose using insulin and consumed glucose as inputs and a series of differential equations to represent the digestive process, endogenous glucose production, and insulin-dependent and independent glucose uptake in the tissue and muscles. Without appropriate inputs (i.e., meal and insulin records), glucose predictions cannot accurately be obtained using these models. Additionally, reconstruction of past data using these white-box models relies on accurate meal and insulin records, which are often unavailable. In recent years, data-driven black-box models have also been developed to represent the insulin-glucose system.[91] These are even

more reliant on precise data.[92] There are a plethora of examples from the machine learning community that stress the importance of data quality and the impact of erroneous data on the effectiveness of data-driven techniques.[93–95]

Data records collected from patients in an at-home setting are fraught with errors. These issues stem from a variety of causes. Individuals record meal amounts at the time of insulin doses, so if they do not deliver insulin at the exact time when they begin to eat, this error is reflected in the data. When reviewing meal record data, it is difficult to assess if these events were recorded at the proper time and can cause cascading errors in models seeking to interpret BG data. Peters et al. showed that in a survey of 21,533 people with T1D, 32% admit to delivering insulin after or during a meal.[96] Because meal and insulin records are most easily obtained by downloading insulin pumps or now connected pens, meal events are frequently recorded after they occurred for a significant proportion of the T1D population.

Self-reported carbohydrate amounts are also a source of inaccuracy. Meade and Rushton conducted an experiment where 61 adult participants familiar with carbohydrate counting filled out a questionnaire to assess their ability to estimate the number of carbohydrates in everyday foods.[97] On average, the participants could only guess the carbohydrate amount of 59% of the foods listed. Another study by Brazeau et al.'s 2013 showed that when 50 adults were asked to estimate the carbohydrate amounts of the meals they had eaten in the last 72 hours, they made errors of 20.9 ± 9.7%.[98] Furthermore, 38% of patients claim to forget to administer insulin for meals at least once a week, meaning that those meals would not be reported at all.[99] Issues with meal records cause serious problems when trying to create new technologies to manage T1D. Without trustworthy mealtimes and amounts, the dynamics of the system are unexplainable with white-box or black-box models. These issues with data have major implications in model fitting and in the design of data-driven approaches.

Meal Detection

Meal detection has long been a focus in the diabetes technology community. Many of the papers in this field aim to incorporate meal detection into closed-loop insulin dosing systems to eliminate the need for patients to acknowledge meals manually. In all commercially available systems, the user estimates the number of carbohydrates he or she is about to eat and delivers insulin using a functional insulin therapy calculator. This process is burdensome, especially if someone eats many small meals throughout the day, and also it presents an opportunity for a lapse in focus to create a significant problem. If someone forgets to take insulin at the time of a meal on accident, BG levels following the meal can reach dangerously high levels.[100] Automatic meal detection would result in a considerable

reduction in the work required of people with T1D to manage their disease and prevent the negative effects of forgotten insulin injections.

Seminal work in CGM-only meal detection was done by Dassau and colleagues.[101] In this approach, where meals were detected based on a voting algorithm with rules defined by different evaluations of glucose rate of change. The Glucose Rate of Increase Detector (GRID) method was able to detect meals, where the associated bolus was withheld for an hour, with a great deal of certainty. For this specific instance where glucose rose rapidly following a meal, GRID detected more than 90% of meals within 30 minutes of the onset of eating.

This method was refined in a later work by Harvey et al. in 2014.[102] The GRID+ method eliminated the voting algorithm and used only a filtered glucose rate of change to detect meals. This new formulation of the algorithm was able to detect 87.5% of meals in a training dataset of real and virtual patients where insulin was given at the time. The mean time to detection was 42 minutes.

Other research groups have attempted to use insulin-glucose models to determine when and if meals occurred using insulin and meal records as well as CGM values. Turksoy et al. used CGM measurements as well as a formulation of the Bergman minimal model with the addition of an unscented Kalman Filter for state estimation.[103] From this, the estimated rate of appearance of glucose was used for meal detection. This algorithm was evaluated on nine subjects, and the results indicate that the method works with high accuracy. On average, glucose only changed by 16 ± 9.42 mg/dL from the mealtime to the detection for 61 detected meals and snacks. This algorithm was developed to be integrated into an artificial pancreas controller to dose insulin for meals automatically.

Weimer has proposed a method of detecting meals that is agnostic to patient-specific parameters usually incorporated in other model schemes.[104] The physiological parameter-invariant (PAIN) detector was based on a minimal insulin-glucose model. This detector does not require patient-specific customization as some other methods do. This algorithm achieved a near-constant false alarm rate across all subjects and was compared to three existing meal detection algorithms using a clinical T1D dataset. The PAIN detector achieved 86.9% sensitivity and two false alarms on average per day. It also outperformed all three of the other algorithms with regard to false alarm rates. This method has the unique characteristic of maintaining low variance in detection and false alarms for all subjects in the dataset without patient-specific tuning or training.

Many sensor-based methods for meal detection have been applied to a plethora of domains other than diabetes. Instead of an approach strictly based on sensor streams generally related to T1D, many methodologies use other passive sensing techniques to glean information about people's eating habits. Devices such as smart plates and dining tables have been created to detect how much someone is eating.[105,106] Others have tried to create methods for detecting when people eat by using surveillance video and audio recording.[107–115]

Wearables provide the unique benefit of collecting information on a semi-continuous basis and monitoring their users in a minimally invasive fashion.[116,117] Acoustic sensors, visual sensors, inertia sensors, electroglottography (EEG) and electromyography (EMG) based sensors, piezoelectric sensors, sensors that combine multiple sources, electrical proximity sensors, and respiratory inductance plethysmography sensors have also been used to detect eating. A methodology was created and improved upon by Dong et al. to track wrist motion when the user took a bite and was able to detect meals with 80% accuracy under laboratory conditions for certain foods.[118] Additional studies have been done where accelerometers were embedded in a smartwatch or band to detect eating activities.[119,120] Using an EEG sensor, Farooq could detect 89.7% of meal events in females and 90.3% in males.[121] Woda et al. used EMG to determine the effect of food hardness, bite-size, chewing cycles, and sequence duration for various foods and subject behaviors.[122,123]

Other researchers have delved into whether or not piezoelectric materials are a viable way to detect food consumption. Farooq and Sazonoz utilized piezoelectric film sensors to identify jaw movements during chewing.[124] By placing two sensors below one ear, they could detect chewing with an error rate of 8.09%. Kalantarian et al. used piezoelectric materials to detect movement in the throat during swallowing.[125] The authors of this work embedded piezoelectric materials in a necklace to detect changes in the movement of a person's throat. This method recognized swallowing with 86% when it was tested on ten subjects in a laboratory setting.

Fontana et al. proposed a method called the Automatic Ingestion Monitor that used piezoelectric, accelerometer, and proximity sensors to monitor food intake.[126] By using this sensor set, their algorithm detected eating by using a combination of signals that collected information regarding jaw movement, body motion, and hand gestures. This method was 89.8% accurate in a laboratory setting when it was tested on 12 subjects.

The physical sensor-based approaches to meal detection yielded good results but were often invasive, impractical, or uncomfortable. A system used to detect eating events should take all of these ergonomic factors into account. It is paramount that meal detection devices benefit the user and do not place an undue burden on them. Passive sensing techniques are much more practical in terms of what would be a useful and manageable addition to chronic disease treatment in real life.

Overview

The following chapters will address and discuss the challenges presented in the Background. The body of this dissertation is organized into three specific aims. Aim 1 describes the design and evaluation of an automatic bolus priming system (BPS). This chapter also includes the results of a pilot clinical study where the BPS was integrated into a model predictive control (MPC) based automatic insulin dosing system and compared to a state-of-the-art artificial pancreas. Aim 2 explains the design of two glycemic disturbance detection algorithms. There is also a comparison of these two algorithms provided in this chapter. Aim 3 details how historical data was used to create individualized profiles representing patterns of disturbances experienced by people with T1D and how these profiles were integrated into a multistage model predictive control (MS-MPC) system to anticipate glycemic disturbances such as meals. The results of a simulation experiment designed to evaluate the impact of the BPS and the anticipatory disturbance profiles on glycemia are also included in this chapter. The final chapter contains a discussion of how these aims relate and enhance one another, a summary of the findings, future work, additional applications, and concluding remarks.

Aim 1 - Real-time Disturbance Detection and Mitigation

Design of the Real-time Disturbance Detection Algorithm

Current automatic insulin dosing systems require users to manually input when they are eating to deliver a mealtime insulin dose. There are issues with this user-driven approach for many of the same reasons mentioned in the Background (i.e., forgotten or late boluses and inaccurate carbohydrate estimations). Numerous research groups have tried to advance from hybrid closed-loop artificial pancreas systems, which require user input, to fully closed-loop artificial pancreas systems, but none have been able to avoid hyperglycemia caused by meals. The dynamics associated with ingested carbohydrates and insulin require that boluses are ideally at the time of eating, thus making feedback-only approaches to this problem suboptimal.

Our approach to this challenge differed from past attempts in a significant way: we did not try to detect meals per se, but instead periods where it was both safe and effective to deliver an insulin dose. By detecting glycemic disturbances that could lead to a rise in glucose, we sought to avoid hyperglycemia without requiring user interaction. Eating carbohydrates without taking insulin often leads to a rapid increase in BG values, but some meals, if they consist mainly of protein or fat or eaten contemporaneously with physical activity, may not increase BG. It might not be necessary or safe for a person to take insulin with their food in these instances.

This chapter describes a methodology to detect events in real-time that require insulin characterized by large increases in BG and automatically delivers priming doses. A logistic regression-based algorithm with features that represented changing BG was trained to detect significant glycemic disturbances while only using past CGM data to accomplish this goal. The causality of this approach was essential so that the disturbance detection algorithm could run in real-time. The BPS was designed to evaluate the disturbance probability at the time of each CGM measurement and determine if an insulin dose should be delivered to the patient. Insulin doses will be based on the user's average total daily insulin (TDI) to account for personalized factors such as insulin sensitivity and will not rely on the unknown disturbance magnitude. The system was evaluated to ensure that the BPS insulin boluses were delivered only when it was safe to do so.

Feature Selection

The features used in the online disturbance detection algorithm were selected to encompass how BG changes following the consumption of carbohydrates. Approximations of the average and first

and second-order rates of change of glucose values were found by taking the coefficients of a second-order polynomial that was fit on recent BG values. The polynomial equation,

$$y(i) = p_{d,1} + p_{d,2} \cdot i + p_{d,3} \cdot i^2$$

was found by using polynomial least-squares fitting for the most recent CGM values. These CGM values were from the last 30 minutes of available data. The typical sampling time for a CGM is five minutes, so this consisted of seven measurements. The choice to use the last 30 minutes of CGM data will be discussed in a later section. The vectors used for the least-squares fitting were,

$$cgm_{disturbance} = [cgm(t-7), \dots, cgm(t)],$$

$$t_{disturbance} = \begin{bmatrix} t_{disturbance,1} \\ t_{disturbance,2} \\ t_{disturbance,3} \\ t_{disturbance,4} \\ t_{disturbance,5} \\ t_{disturbance,6} \\ t_{disturbance,7} \end{bmatrix} = \begin{bmatrix} -3 \\ -2 \\ -1 \\ 0 \\ 1 \\ 2 \\ 3 \end{bmatrix}.$$

The coefficients from the polynomial describing the CGM signal, $p_{d,1-3}$, were found with the equation,

$$\begin{bmatrix} p_{d,1} \\ p_{d,2} \\ p_{d,3} \end{bmatrix} = (X^T \cdot X)^{-1} \cdot X \cdot cgm_{disturbance},$$

where,

$$X = \begin{bmatrix} 1 & t_{disturbance,1} & t_{disturbance,1}^2 \\ 1 & t_{disturbance,2} & t_{disturbance,2}^2 \\ 1 & t_{disturbance,3} & t_{disturbance,3}^2 \\ 1 & t_{disturbance,4} & t_{disturbance,4}^2 \\ 1 & t_{disturbance,5} & t_{disturbance,5}^2 \\ 1 & t_{disturbance,6} & t_{disturbance,6}^2 \\ 1 & t_{disturbance,7} & t_{disturbance,7}^2 \end{bmatrix}.$$

Figure 5 depicts an example of the function determined using polynomial fitting compared to the actual CGM measurements. The second-order polynomial closely fits the CGM values in the period of time shortly after a meal.

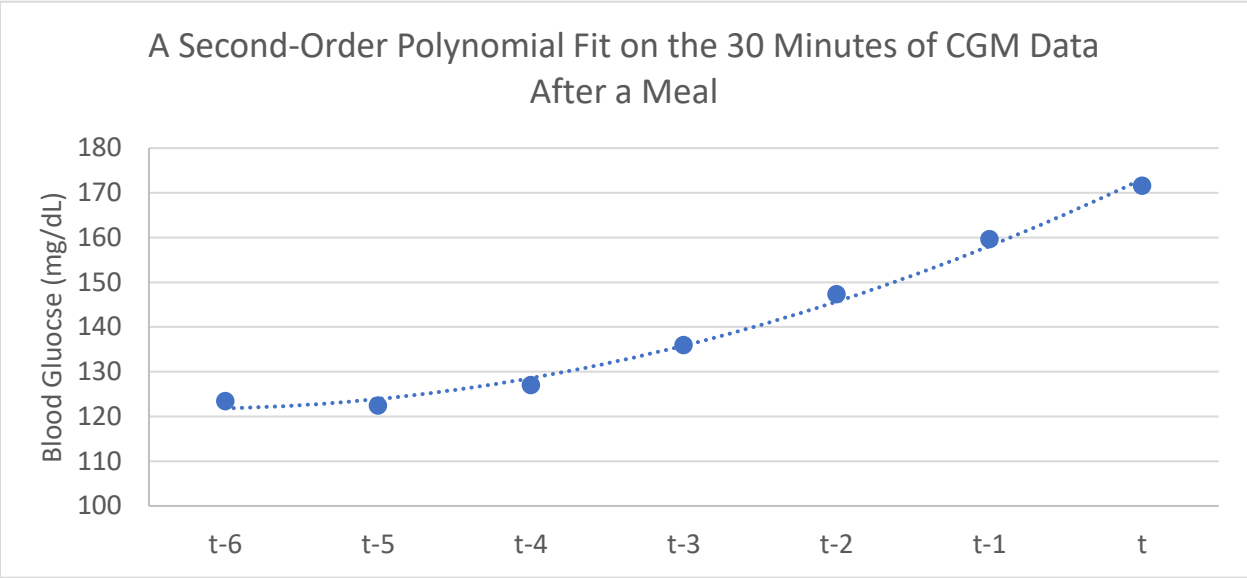

Figure 5 – An example of a second-order polynomial fit on 30 minutes of CGM data using polynomial least-squares. The x-axis represents the time of the seven measurements ranging from 30 minutes (t-6) before the current time to the present, t.

Model Selection

Because the BPS was a multistage approach, the purpose of the classification algorithm used as an input was simple: to provide information that was useful in terms of delivering increasingly large insulin doses safely. With this in mind, the actual classification rate was less important than the suitability of the information being provided. A classification algorithm needed to be selected that gave a range of values as an output, modeled a binary variable, and was easily interpretable. The logistic regression classification algorithm fits each of these criteria.

Logistic regression is one of the most widely used data-driven classification algorithms. Elements of this technique were developed throughout the nineteenth and early twentieth centuries.[127] The logit model used, representing the probability of a discrete binary variable, is generally attributed to Joseph Berkson in 1944. The linear equation of the logistic regression determined log-odds, y, is,

$$y = \beta_0 + \beta_1 x_1 + \cdots + \beta_n x_n.$$

Because there is no closed-form solution to determine the coefficient values, β_{0-n}, are usually defined using maximum likelihood estimation on the data available for training.[128] The logistic function is then used to transform the log odds into a probability, π, between zero and one. The formula for this conversion is,

$$\pi = \frac{1}{1 + e^{-y}}.$$

Here, π represents the probability that the event labeled with the positive class has occurred given the values of the features, $x_1, \ldots, x_n$

Model Training

The coefficients, $p_{d,1-3}$, found from the least squares-fitting were used as features in the logistic regression equation,

$$y_{disturbance}(t) = \beta_{disturbance,0} + \beta_{disturbance,1} \cdot p_{d,1} + \beta_{disturbance,2} \cdot p_{d,2} + \beta_{disturbance,3} \cdot p_{d,3}$$

This value was then transformed using the sigmoid function to the disturbance probability,

$$\pi_{disturbance}(t) = \frac{1}{1 + e^{-y_{disturbance}(t)}}.$$

This probability was informative because it provided a relatively interpretable output from the detector. $\pi_{disturbance}$ was the probability that a sizeable meal-like disturbance occurred in the last 30 minutes based on the CGM values observed.

The coefficients for the logistic regression formula were determined using a dataset generated with the UVA/Padova T1D simulator. In silico data was used because there was no clinical data available representing the context in which the detector was to be used, where insulin will not be taken for meals under fully closed-loop conditions. A dataset was generated where the 100 virtual subjects ate three meals and one snack daily without bolusing for a month. In this simulation setup, the virtual patients used a hybrid closed-loop artificial pancreas but did not announce meals to the system. The unbolused meals caused large and pronounced postprandial excursions. The dataset was labeled so that the five-minute intervals in the one hour following meals were in the positive class, and all other times were labeled as negative. The coefficients of the logistic regression model were determined using this training data and are listed in Table 1.

Table 1 - The coefficients for the logistic regression classification algorithm determined from the simulation dataset.

Coefficient	Value
$\boldsymbol{\beta_{disturbance,0}}$	-2.2825
$\boldsymbol{\beta_{disturbance,1}}$	2.3056
$\boldsymbol{\beta_{disturbance,2}}$	0.3606
$\boldsymbol{\beta_{disturbance,3}}$	0.0012

Figure 6 shows the receiver operating characteristic (ROC) curve for the online disturbance detection algorithm. The ROC curve shows the rates of true and false positives for each five-minute interval for the 25% of the data held out from the training for validation. The area under the curve for the ROC was 0.84. These rates are different from the rate at which meals would be detected because, in this case, the detector is labeling each sampling time as in the postprandial window or not. If a meal was not detected immediately but shortly after the subject ate within the first hour, this would likely result in a few false negatives for the five-minute intervals subsequent to the meal and then a series of true positives. The classification algorithm was trained in this manner so that the classifier would emphasize the characteristics of BG values following eating.

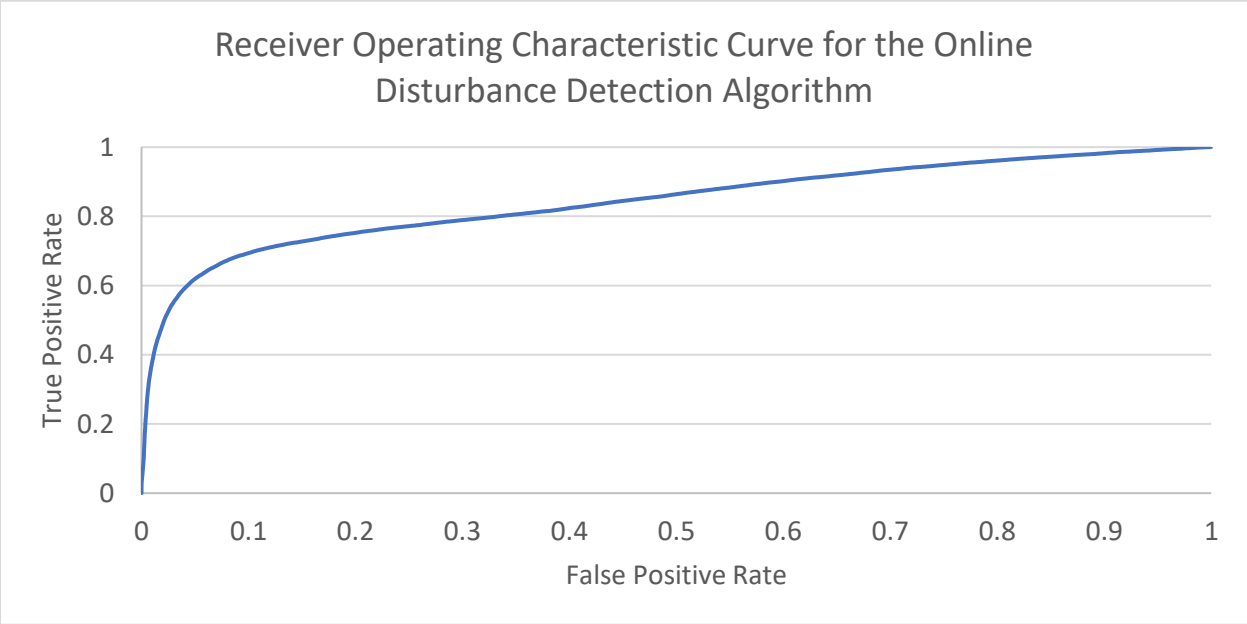

Figure 6 – The ROC curve for the online disturbance detection algorithm generated based on the results from the holdout validation data.

Figure 7 shows an example of the disturbance probability output generated from one day of simulated CGM values in the training dataset. The disturbance probability is shown in blue, and the meals given to the virtual subject are in orange. In this example, it can be observed that the disturbance probability rises following eating when insulin is not given, and BG is increasing. In this situation, the detector's behavior is beneficial for the BPS system because the disturbance probability increases quickly after meals and not in situations where giving an insulin dose could be dangerous.

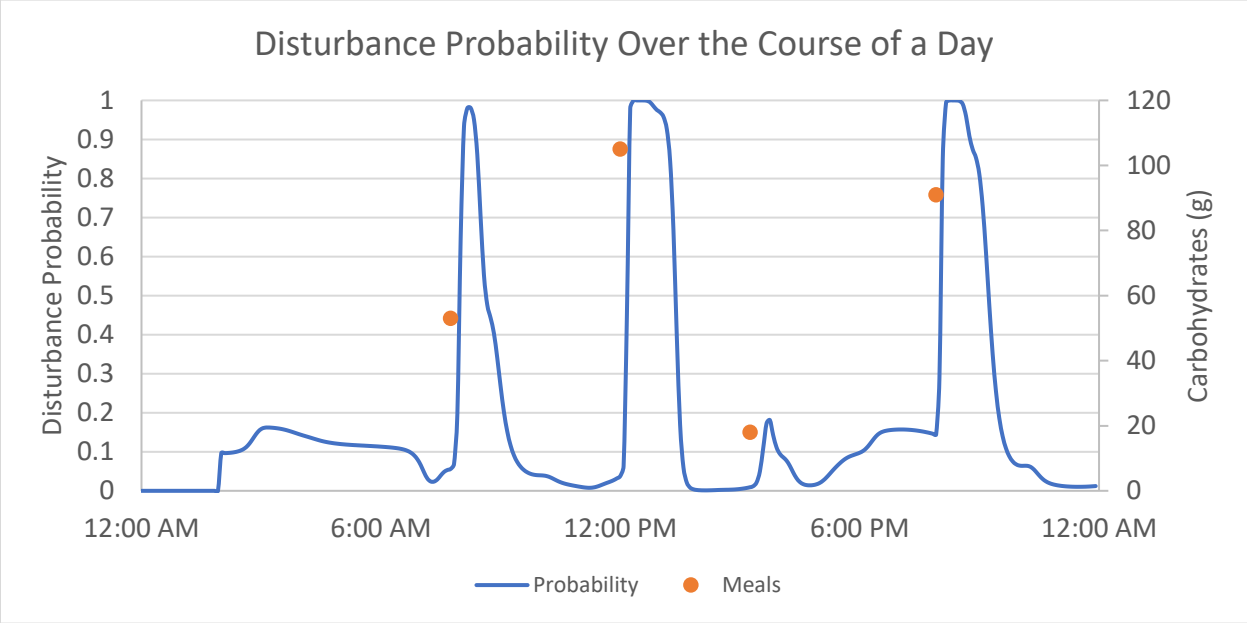

Figure 7 - An example of the disturbance probability detector output for one day of simulated data. The disturbance probability is shown in blue, and recorded meal amounts are displayed with orange markers corresponding to the number of carbohydrates ingested by the patient.

The probability value in this example never exceeded 0.2 for changes in BG not related to large meals that could be caused by normal glucose variability, CGM sensor noise, or snacks. It would not be appropriate to deliver a priming bolus in any of these situations. When the subject ate a small (i.e., approximately 20 gram) snack in the afternoon, the disturbance probably did not rise to a value nearly as high as it did following meals. It should be noted that this example was generated from simulation CGM values which lack much of the noise and variability in BG values found in actual data. The logistic regression-based detection algorithm was trained on simulation data because meals were the only disturbance that changed BG values, but the safety of the BPS system was evaluated with real data to address these concerns that may be present in the context of actual use.

Defining the Feature Generation Window

The window of time selected to generate the features from the CGM data was chosen based on two criteria, the delay associated with the detections and the model's sensitivity to false alarms. The output of the detector was compared using 30 to 120 minutes of past CGM values to determine the appropriate amount of data to use for the polynomial fit. Figure 8 shows an example of how the choice of the window of time used for the features affected the disturbance probability signal. The CGM values over the course of a day are shown in the top subplot, and the disturbance probability values found using 30 to 120 minutes of CGM values for the feature generation are shown in the bottom subplot.

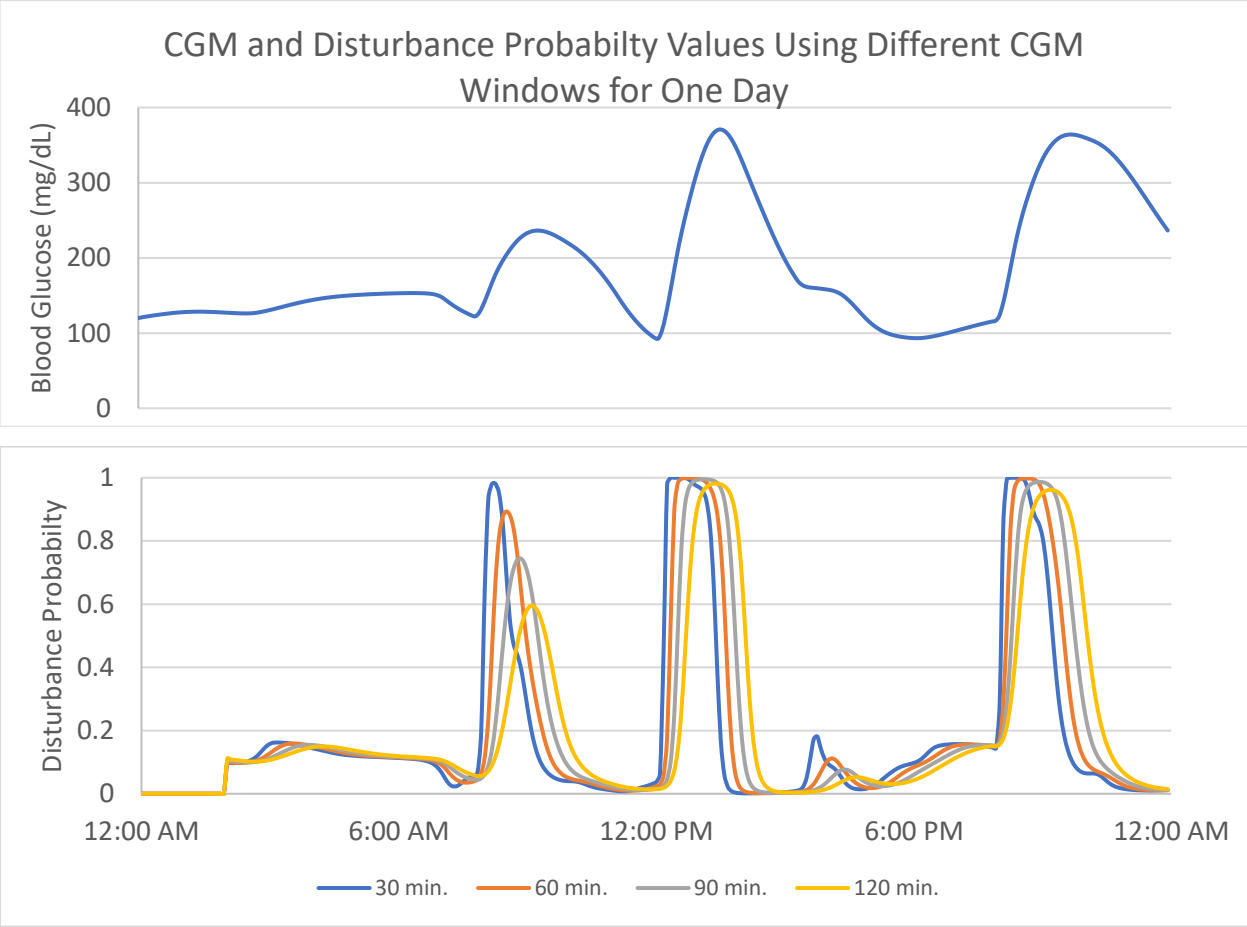

Figure 8 - An example of the disturbance probability output for a CGM trace using different windows of time for the polynomial fitting in the feature generation process. The top subplot shows the CGM values over one day in blue. The bottom subplot shows the different disturbance probability values found using 30 to 120 minutes of CGM data.

The decision to choose 30 minutes as the appropriate amount of time to generate the features was determined by observing the detector's output during periods when glucose rose following eating.

In the example shown in Figure 8, it can be seen that when glucose began to rise following the meal events, each of the detectors using different windows of time for the polynomial fit had increased disturbance probability values. The algorithm using the 30-minute window of CGM values provided a disturbance probability signal that was more responsive to abrupt changes in glucose values. This effect allowed the BPS system to be reactive to rapid changes in BG, which was essential due to the time constants associated with insulin to prevent hyperglycemia. The detector's responsiveness comes at the cost of the potential for false alarms, which was why the strategy employed in the BPS system to determine dose amounts and thresholds was selected based on the system's safety regarding the risk of hypoglycemia.

Model Comparison

Logistic regression is one of the most widely used and also one of the simplest classification algorithms available. The choice to use this approach was selected mainly because its output was a probability value that could be interpreted as the likelihood of a meal occurring in the last 30 minutes. Additionally, because it is a linear combination of coefficients and feature values, each feature's relative weight and importance are apparent.

An experiment was conducted to determine if logistic regression was the appropriate algorithm to select and if more complex approaches would not provide significant value. The same features and methods used to train the logistic regression model were applied to numerous other classification algorithms. The performance of each algorithm was determined based on its classification accuracy and is listed in Table 2.

Table 2 – The accuracy of classification algorithms for the holdout validation portion (25%) of the simulation dataset used for training.

Algorithm	Classification Accuracy
Logistic Regression	**89.8%**
Fine Tree	93.0%
Medium Tree	92.4%
Coarse Tree	91.5%
Fine KNN	89.6%
Medium KNN	93.3%
Coarse KNN	93.4%
Cosine KNN	91.5%
Cosine KNN	93.4%
Weighted KNN	92.6%
Linear Discriminant	89.4%
Boosted Trees	93.0%
Bagged Trees	93.2%
Subspace Discriminant	88.6%
Subspace KNN	90.3%
RUSBoosted Trees	90.6%

The results of this evaluation show that some other classifiers did produce better accuracy than logistic regression, but only to a marginal degree, and none of the classifiers were more than 3.6% more accurate. There are other classifiers available, many not included in this experiment, that perform better than logistic regression. However, this accuracy comes at the cost of interpretability, which is important from a design and safety perspective. Again, the purpose of the classification algorithm was not to determine whether or not each sampling interval was in the postprandial window. The goal was to use a methodology that would provide useful information, like the probability of a meal-like disturbance having occurred, to inform the priming bolus system. For this purpose, logistic regression was determined to be the most straightforward and, therefore, best choice.

Determining the Automatic Bolus Priming System Dosages

Because the BPS was meant to operate without input from the user, meal sizes were unknown to the system. It was determined that the doses should be based on the user's TDI so that the automatic priming insulin boluses were not dependent on carbohydrate amounts and were individualized. TDI provides information regarding the patient's sensitivity to insulin as well as their daily carbohydrate intake. The primary design consideration for this system was safety, so the bolus priming amounts were chosen based on the amount of hypoglycemia that they caused. It was determined that the BPS would be considered acceptably safe if it did not cause more than one additional hypoglycemic event per day. An experiment was conducted using the net effect simulation technique to find the percent of TDI and probability thresholds for the BPS. In the simulation experiment, historical data was compared to new automatic dosing strategies.

The data used was from the data collection period leading up to a clinical study conducted in 2019 at UVA (NCT03859401).[129] The study participants were all adults, age 18 to 65, who had T1D for more than a year, used an insulin pump, and had HbA1c levels of less than or equal to 8.6%. Individuals were excluded if they had diabetic ketoacidosis in the preceding 12 months, were pregnant, or had significant cardiac conditions. In the four weeks leading up to the participants' admission, they were asked to wear an insulin pump, CGM, and activity tracker. During the data collection period, individuals recorded meals using their insulin pump or a smartphone application. Participants were asked to exercise moderately between four and seven in the evening four days a week, achieving heart rates of 110 to 140 beats per minute for at least 30 minutes. Other than the physical activity requirement, they were allowed to live normally during this period of time. All subjects used senor augmented pump therapy during the data collection period. The demographic information for the 14 participants is shown in Table 3.

Table 3 – The clinical trial subjects' demographics for the cohort used in the net effect re-simulation experiment.[129]

Characteristic	Mean ± SD
Age (years)	43.43 ± 13.17
Weight (kg)	82.33 ± 15.16
Height (cm)	168.90 ± 11.76
TDI (u)	41.59 ± 12.67
Baseline HbA1c (%)	6.61 ± 1.06

These historical clinical data were subjected to various new automatic priming dose strategies and evaluated. Single doses equal to percentages of the individuals' TDI amount were delivered at varying disturbance probability thresholds. These values ranged from 3% to 9% of the individual's TDI and probability thresholds from 0.2 to 0.9. Because the primary goal was to determine the safety of this approach in terms of false alarms and subsequent hypoglycemia when there were no meals, data were excluded in the two hours following recorded meals.

When the probability threshold was exceeded, an insulin dose determined from the percent TDI was delivered. After this dose, BG values were simulated for the next two hours, and the number of hypoglycemic events that did not already exist in the record was counted. This procedure was repeated at each five-minute interval and for each disturbance probability and TDI amount pairing. Figure 9 shows the average number of hypoglycemic events per day for each disturbance probability threshold and TDI percent.

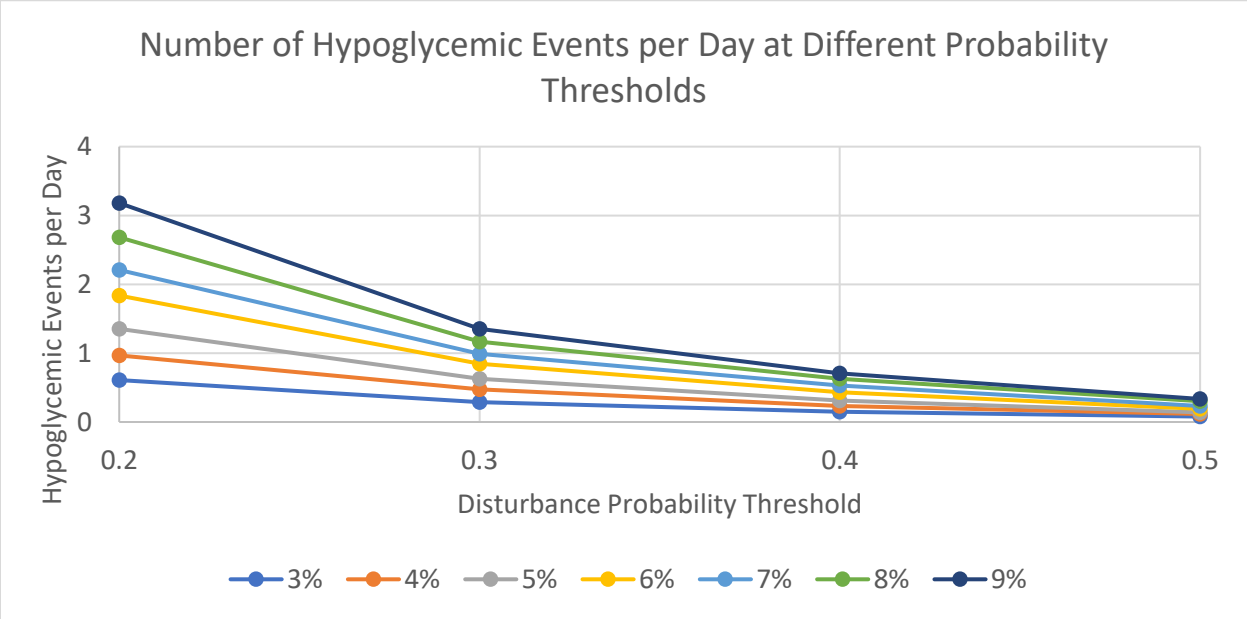

Figure 9 - The mean number of hypoglycemic events per day at each probability threshold and TDI amount.

The thresholds were selected based on the criteria of not allowing more than one additional hypoglycemic event per day. At the escalating thresholds for $\pi_{disturbance}$, the BPS delivers different amounts of the patient's TDI,

$$P_{TDI}(t) = \begin{cases} 0\% \; if \; \pi_{disturbance}(t) < 0.2 \\ 4\% \; if \; 0.2 \leq \pi_{disturbance}(t) < 0.3 \\ 7\% \; if \; 0.3 \leq \pi_{disturbance}(t) < 0.4 \\ 10\% \; if \; \pi_{disturbance}(t) \geq 0.4 \end{cases}.$$

The BPS dose, J_{BPS}, was then determined based on the user's TDI and the amount of insulin that was previously injected by the BPS system, IOB_{BPS}. This equation is,

$$J_{BPS}(t) = P_{TDI}(t) \cdot TDI - IOB_{BPS}(t),$$

where IOB_{BPS} was the amount of insulin on board determined using a six-hour curve from previous BPS boluses.[130] It was essential to include the insulin on board (IOB) from previous injections so that priming doses were not compounded with one another if there was a significant and prolonged glycemic disturbance. The IOB curve used in the BPS is depicted in Figure 10.

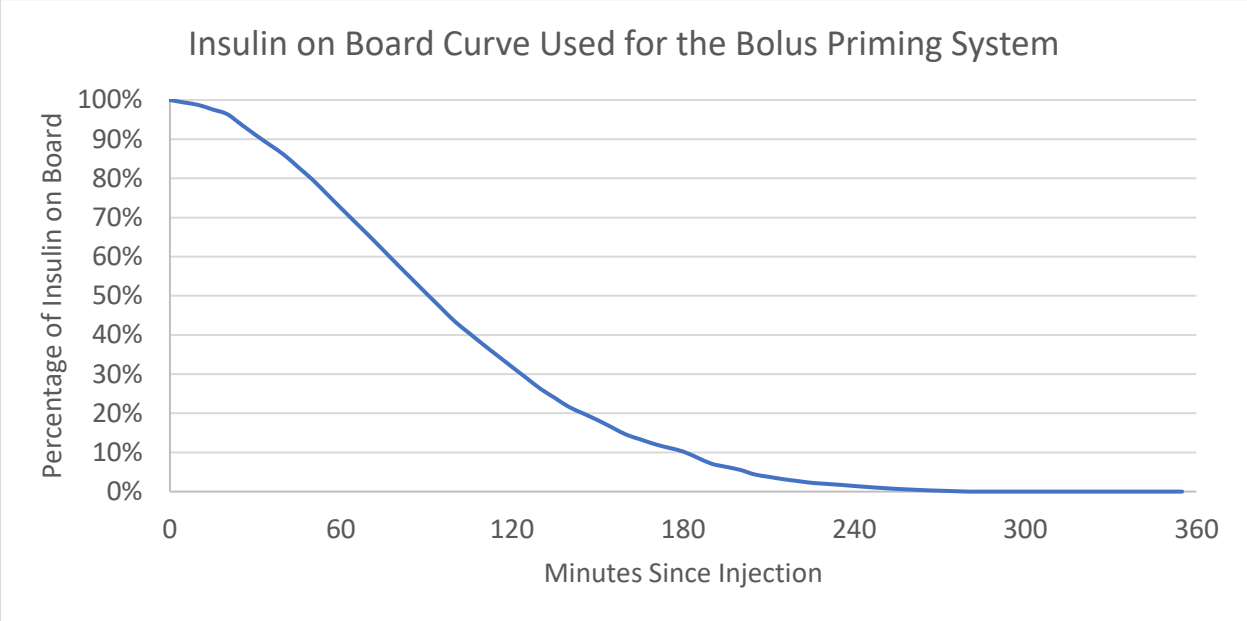

Figure 10 - The insulin on board curve used for the bolus priming system.

Clinical Evaluation

Study Design

A randomized, crossover clinical trial was conducted at UVA in January of 2021. This study was approved by the Institutional Review Board as well as the US FDA and was listed for enrollment on ClinicalTrials.gov (NCT04545567). Because adolescents often have the highest rates of missed or late boluses and the highest average HbA1c, 21 12 to 20-year-olds were recruited for the five-night hotel-based camp study. Participants were eligible if they had T1D and had used an insulin pump for more

than six months. Exclusion criteria included the use of oral glucose-lowering drugs (e.g., metformin) and diabetic ketoacidosis or a severe hypoglycemic event in the last six months.

All individuals involved in the study used the UVA artificial pancreas study platform, the Diabetes Assistant (DiAs), which receives BG values from a Dexcom G6 CGM device and sends commands to a Tandem t: ap insulin pump.[131] The study team monitored participants remotely using a cloud-based web monitoring system, DiAs Web Monitoring.[132] The experimental automatic insulin dosing controller, known as Rocket, was compared to the extensively tested Unified Safety System Virginia (USS Virginia) control algorithm.[133–135] Rocket employed an MPC framework where BG was predicted based on an individualized insulin-glucose model, and a control action was decided (i.e., series of insulin infusions) by optimizing a cost function. This cost function included terms to correct the current BG value to the target, penalties for low BG values, and a regularization term to weight changes in consecutive insulin injections. When running, Rocket determined the basal infusion rate and if a priming bolus should be delivered through BPS based on the current disturbance probability at every five-minute interval. Rocket was also integrated into the Safety System and Hyperglycemia Mitigation System to prevent hypoglycemia and correct hyperglycemia.[136,137] Both study control systems could operate in hybrid closed-loop mode as well as fully closed-loop mode. When meal boluses were commanded in Rocket, 50% of the amount of insulin typically delivered, based on the subject's CR, was given.

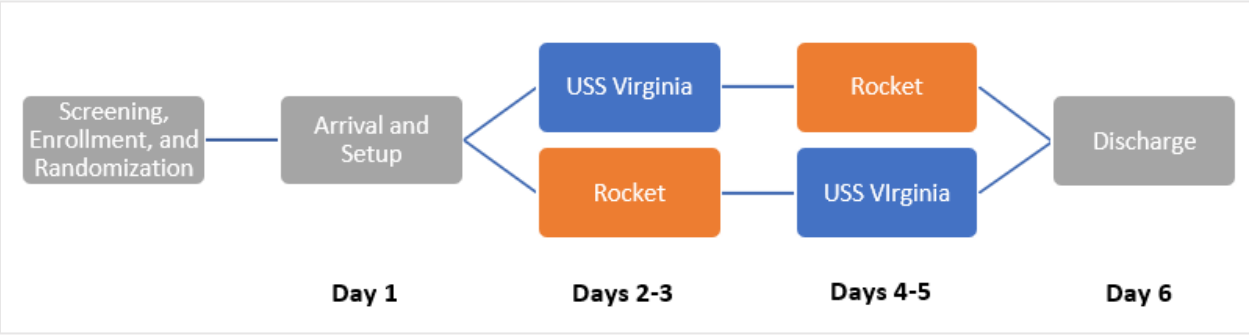

Figure 11 – A diagram of the Rocket camp study design. Screening, enrollment, and randomization were conducted before the admission. The hotel admission lasted for six days, and each participant used the Rocket and USS Virginia control systems.

Figure 11 is a diagram of the study design. Participants were enrolled, screened, and randomized before the beginning of the trial. All participants provided at least 14 days of preliminary data to identify model parameters in the Rocket controller. The setup was completed on the first day after participants arrived. Participants spent days two and three using the controller they were initially randomized to and then crossed over at the begging of day four to the other control system. Breakfast,

lunch, and dinner were eaten on each day of the study. Breakfast and lunch were chosen by each individual based on preference and contained 47 ± 9 grams of carbohydrates. Dinner was not announced on days three and five to observe the postprandial response for each participant under the different control systems in fully closed-loop mode. Dinner was the same each day and consisted of 35 to 42 grams of protein, 27 to 41 grams of fat, and 44 to 62 grams of carbohydrates based on what the subjects chose.

The study's primary outcome was the percent time in the 70 to 180 mg/dL range in the six hours following dinner. Additionally, the percent time in tight time in range (i.e., 80 to 140 mg/dL), hypoglycemia (i.e., <70 mg/dL), hyperglycemia (i.e., >180 mg/dL), and mean BG will be discussed. All metrics are presented as the mean ± standard deviation (SD) or the median [minimum to maximum] if they were not normally distributed. A paired t-test was used to compare the normally distributed results, and a nonparametric Wilcoxon signed-rank test was applied if the data were not normally distributed.

Outcomes

18 participants completed the study out of the 21 initially enrolled. One participant was excluded because of scheduling difficulty, and two participants were excluded because they tested positive for SARS-co-V2. Of those who completed the study, nine were male, and nine were female. The average age was 15.6 ± 1.6 years. Mean height and weight were 166.6 ± 8.9 cm and 65.2 ± 11.5 kg, respectively. The average duration of diabetes was 7.7 ± 3.2 years. Participants had an average baseline HbA1c of 7.4 ± 1.5% and a time in the 70 to 180 mg/dL range of 60.0 ± 17.3%. The mean TDI was 59.6 ± 16.3 units.

The BPS delivered an insulin dose after 15 of the 18 unannounced dinners (83.3%). In the two hours following eating, these insulin deliveries ranged from 1.32 units to 6 units and averaged 2.37 units. The BPS delivered an average of 3.29% of the patient’s TDI ranging from 3% to 7%. The first BPS bolus was delivered an average of 28 minutes 43 seconds ± 10 minutes 26 seconds after the beginning of the meal. Figure 12 shows a picture generated from the data collected during the clinical trial illustrating how BPS performed following the unannounced meal. In this example, it can be seen how roughly 25 minutes after eating, the BPS delivered an automatic priming bolus equal to 3% of the participant's TDI. Even though no manual meal bolus was taken, this individual’s BG level only briefly exceeded 180 mg/dL following eating. The BPS never gave boluses due to fluctuations in glucose at any point other than the six hours after the unannounced dinner.

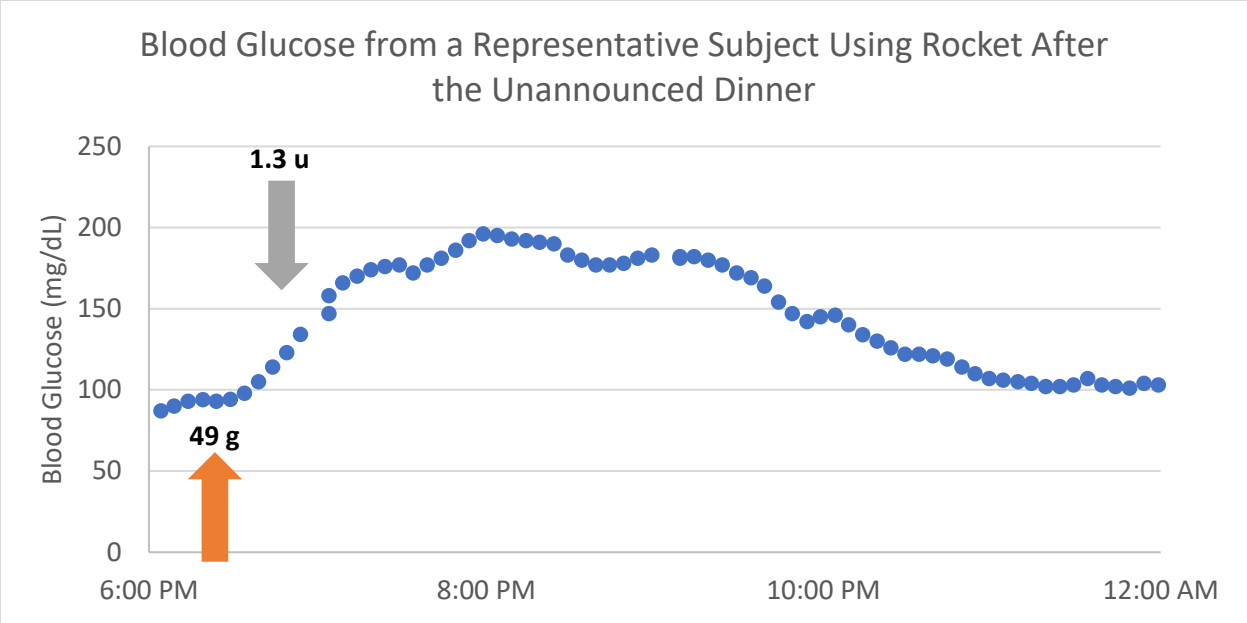

Figure 12 – The blood glucose values from a representative subject using Rocket after the unannounced dinner. The meal consisting of 49 grams of carbohydrates is shown with the orange arrow, and the 1.3 u (3% TDI) BPS bolus is shown with the grey arrow.

Glycemic outcomes in the six hours following the unannounced meal were favorable for the Rocket controller in comparison to USS Virginia. The time in range (i.e., 70 to 180 mg/dL) was 53% [40 to 71%] for USS Virginia and 83% [64 to 93%] for Rocket (p=0.004). The times in tight range (i.e., 80 to 140 mg/dL) was 27% [22 to 36%] and 49% [41 to 59%] for USS Virginia and Rocket, respectively (p=0.002). Mean BG was 166 ± 26 mg/dL for USS Virginia and 141 ± 21 mg/dL for Rocket (p = 0.001). The time above range (i.e., >180 mg/dL) was lower for Rocket (17% [1.3 to 34%] vs. 47% [28 to 60%], p = 0.01). In the six hours following the unannounced dinner, there was no significant difference in the amount of hypoglycemia experienced by either system which was less than 1% for both.

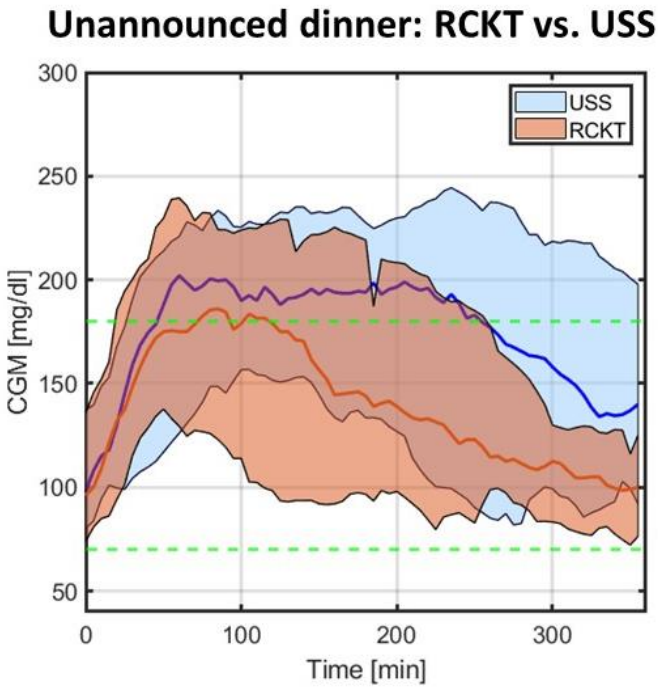

Figure 13 - Cloud plots of CGM values following the unannounced dinner for each control system. Rocket is shown in orange and USS Virginia in blue. The thick lines represent the mean BG, and the edges of the clouds show the 10th to 90th percentile. The green dashed lines show the euglycemic range (i.e., 70 to 180 mg/dL).

Figure 13 shows cloud plots representing the 10th to 90th percentiles of the CGM values for each controller in the six hours following the unannounced dinner under fully closed-loop control. The results from Rocket are shown in orange, and the USS Virginia's results are in blue. The thick lines represent the mean values for each treatment. The target range (i.e., 70 to 180 mg/dL) is shown with the horizontal green dashed lines.

Here it can be seen that BG rose at a similar rate for both control systems, but the mean peak BG was lower for Rocket. Additionally, the amount of time required for BG values to reenter the euglycemic range (i.e., 70 to 180 mg/dL) was less for Rocket than for the USS Virginia. Overall, it is clear that the average amount of time spent euglycemia is greater for the subjects when they used the Rocket controller. Also, it can be seen how the range of values for Rocket was tighter than it was for USS Virginia, indicating less variability among subjects.

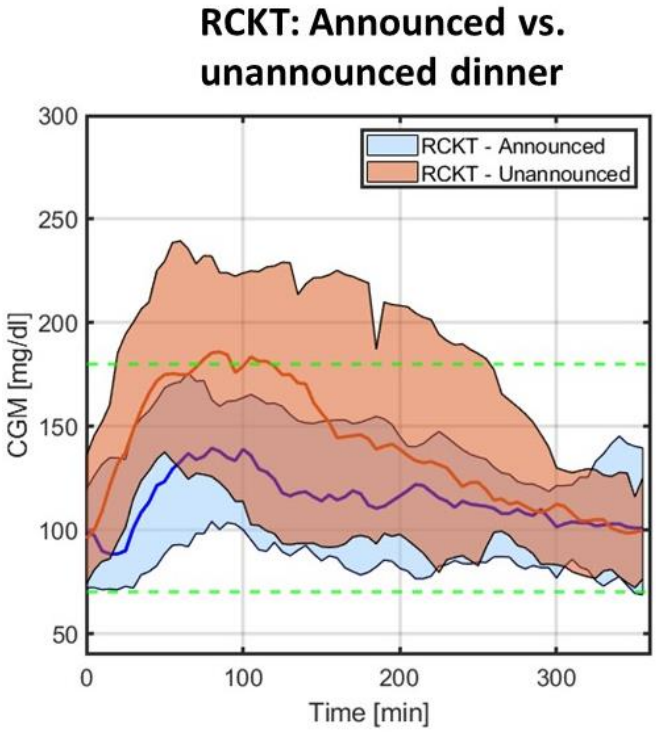

Figure 14 - Cloud plots of CGM values for Rocket after the announced and unannounced dinner. The unannounced meal is in orange and the announced one in blue. The thick lines represent the mean BG, and the edges of the clouds show the 10th to 90th percentile. The green dashed lines show the euglycemic range (i.e., 70 to 180 mg/dL).

Figure 14 **Error! Reference source not found.**compares the postprandial values for Rocket in h ybrid closed-loop mode, in blue, where meals were announced, and fully closed-loop, in orange, where meals were not. When the meal was not announced to the system and no manual bolus was given, BG rose sooner after eating. The peak BG value was also higher in this case. In hybrid closed-loop mode, the 90th percentile of CGM values never exceeded the hyperglycemic threshold. Additionally, the variability of BG values among subjects is less when the meal was announced.

Obviously, BG values will be lower when the meal size is known and insulin is given at the beginning of the meal. What is notable about the fully closed-loop results is that the mean peak BG was barely higher than the upper limit of the euglycemic range (i.e., 180 mg/dL). Additionally, the mean BG value for all subjects was only higher than that threshold for a very short period of time, roughly 30 minutes. Finally, the MPC control system brought the BG level to almost the same value in the target range (approximately 100 mg/dL) after both the unannounced and announced meal.

The BPS embedded in Rocket behaved properly during this clinical trial from the perspective of safety. There were no boluses delivered except for those following eating, and the boluses triggered by

the glycemic disturbances did not lead to any more hypoglycemia than the comparison control system. However, it should be noted that both systems had very little hypoglycemia following the unannounced dinner. The Rocket system had 83% time in range after eating without a meal bolus, which suggests that the BPS could react to eating events where the user of the system did not take insulin and mitigate hyperglycemia. A large-scale test of this system under challenging scenarios (e.g., stress, physical activity, infusion site occlusion) would provide a greater perspective on the system's limitations and safety. It is still unclear if the BPS would be adequate in replacing meal boluses or if it should serve as a safeguard against significant and prolonged hyperglycemia following the occasional missed prandial insulin dose. Overall, the Rocket control system showed to be safe and effective in this clinical evaluation, in some ways outperforming the state-of-the-art publicly available artificial pancreas system.

Aim 2 - Retrospective Glycemic Disturbance Detection

Overview

Data quality is often a concern in retrospective data analysis, especially when information is self-reported. In T1D, the most impactful disturbance on glycemia is consumed carbohydrates. Because of this, individuals with T1D are asked to record meals as precisely and accurately as possible so that insulin levels can be titrated. These self-reported eating records are regularly inaccurate or incomplete. Often records of consumed carbohydrates are logged when a mealtime insulin bolus is administered, which can often lead to inaccuracies. The errors in this data result from numerous factors, including the frequency at which people take insulin after mealtimes or forget altogether.

Additionally, the rate of glucose appearance in plasma depends on the ratio of macronutrients (i.e., carbohydrates, protein, and fat) in the food consumed. People with diabetes rarely record this information, but it can be vital in making informed insulin dosing decisions. The problems associated with these sources of data cause a litany of problems for event reconstruction, model fitting, and the training of machine learning algorithms.

By taking existing records, fixing incorrect event times, and detecting unreported disturbance events, a better understanding of what occurred in the past, which treatments worked well, why they may not have, could be leveraged to create new technologies. Having correct data is especially important for data-driven approaches because models will be incorrectly trained if data records are wrong. Furthermore, in a fully closed-loop insulin dosing system, the timing and magnitude of events (e.g., mealtimes and carbohydrate amounts) would be unknown and absent from the data record because there is no input from the user regarding these disturbances. In this aim, our approach to reconstructing the disturbance record is defined. Again, this approach focused on detecting events where insulin was required (i.e., positive glycemic disturbances) and not necessarily meals. The first detector described in this chapter that was meant to be used when meal boluses were administered is referred to as DSS2, and the second detector that was intended to be used when there were no meal boluses is referred to as RCKT+. These abbreviations are based on the projects that the algorithms were designed for Decision Support System 2 (DSS2) and Rocket Plus (RCKT+).

Retrospective Disturbance Detection Using Bolus Insulin and Glucose Measurements

Introduction

If boluses are taken at mealtimes using functional insulin therapy, like sensor-augmented pump therapy or hybrid closed-loop therapy, insulin doses may be a valuable indicator of when positive glycemic disturbances occurred. Although many people with T1D dose insulin based on an estimation of the carbohydrates in the food they just ate, some people take insulin doses concurrently with eating but do not record carbohydrates. In this case, both the size and timing of meal events are unknown.

Connected insulin pens have a memory of insulin injections and are growing increasingly prevalent. The users of these devices often have a reliable record of insulin but no record of the carbohydrates they consumed. Using insulin bolus and CGM records to reconstruct disturbance events could also be helpful for this population of people with T1D.

A disturbance detection algorithm was developed using bolus insulin and CGM records to leverage the information provided by people with T1D who otherwise may not have quality eating records. This logistic regression-based detection algorithm was trained on a dataset where the participants used sensor-augmented pump therapy. Numerous features were generated at the time of each CGM measurement (i.e., every five minutes) that were indicative of significant glycemic disturbances. The combination of those features and the selected coefficients determined whether a disturbance had occurred close to that time. The ability of this algorithm to classify sampling points as a part of a glycemic disturbance was evaluated. Further analysis of this algorithm and a second algorithm used to detect disturbances will be detailed later in this chapter.

Training Data

The dataset used for training the algorithm was from the same clinical trial as the experiment to determine the priming insulin dose amounts for the BPS (NCT03859401).[129] These data were collected from 14 subjects using sensor-augmented pump therapy at home. The subjects were asked to exercise multiple times per week, but other than that requirement, they behaved normally. A full description of the dataset is in Aim 1 in the section titled “Determining the Bolus Priming System Dosages.”

Meal records were obtained by downloading the insulin pumps used by the participants, but because of the reasons mentioned earlier, it could be assumed that these records contained errors. For this dataset, each five-minute interval of the dataset was labeled based on if there was a rise in BG of greater than 40 mg/dL in the two hours following. The five-minute intervals where this was true were

considered the positive class, and all other data intervals were in the negative class. This labeling method was selected because it was not reliant on patient-reported data and selected five-minute intervals in the positive class that immediately preceded or included rises in glucose, thus indicating a large glycemic disturbance. It should be stressed that in many applications where data reconstruction is useful or necessary, it is less critical to detect eating than to detect events caused by glycemic disturbances and require insulin doses. This characteristic may or may not be accurate for all eating events, such as those where BG does not rise.

Feature Selection

Because the focus of the detector was to determine when it was essential to dose insulin, features were generated that would distinguish those events from all other times. When data cannot be verified, as is often the case, the only reliable records collected are CGM values and insulin records downloaded from the memory stored on an insulin pump or pen. Because these data streams are the only verifiable collected data, they were used to generate the features.

Glycemic disturbances are often characterized by BG values increasing at a rapid rate. The rise in BG results from consumed carbohydrates being processed through the digestive system and appearing in plasma blood as glucose. BG values rise even more quickly when carbohydrates are consumed, and insulin is not taken before the onset of eating. The rate of change of BG values (i.e., slope) and the second-order rate of change (i.e., curvature) could indicate a large glycemic disturbance, and because of this, several features were selected initially to capture this effect.

If the correct insulin dose is taken when eating, there might not be a considerable rise in BG following the meal. Nevertheless, the disturbance detection algorithm needed to capture these events because insulin was required in this particular situation. As described in the introduction, the net effect is a helpful approach for quantifying such glycemic disturbances. If the model is uninformed by ingested carbohydrates and an insulin dose is taken, BG should decrease. If this is not the case, there is a corresponding increase in the net effect to account for the glucose-lowering disturbance (i.e., insulin injection). To generate the net effect signals that encompassed the effect of meals, the model used to determine the disturbance signal was unaware of all recorded meals. When insulin was injected at mealtimes, and there were no large increases in BG, there were resultant positive increases and peaks in the net effect disturbance signal to explain the data in terms of the model. For these reasons, some features in the initial set using the value and rates of change of the net effect were chosen.

The insulin record is an excellent indicator of when people experienced major glycemic disturbances as insulin is one of the only ways other than physical activity to reduce BG in these circumstances. People will often take insulin for meals without recording carbohydrate amounts. This is often the case for people who do not use insulin pumps and instead take manual insulin injections (i.e., multiple daily injection therapy). With the increasing prevalence of connected insulin pens, which automatically store a digital record of injections and dose amounts, it is increasingly popular to have verified insulin records with no recorded meals. Some of the features in the initial set were related to insulin bolus amounts which could be obtained from an insulin pump or connected pen.

From CGM, net effect disturbance signal, and insulin values, an initial set of 39 features were selected. These features included the current value of each metric calculated as well as the maximum and mean in a 30-minute window centered at the current five-minute interval. The features were calculated for each five-minute interval of the training dataset described. Once the initial model was trained, the final set of features was determined based on the effect of each feature in the set on the classification accuracy. Eventually, 26 features were chosen for the final version of the logistic regression classification model, and new coefficients were determined using the training dataset.

Feature Generation

The data used for this disturbance detection algorithm included a vector of BG values, CGM, net effect values, NE, and bolus amounts, i. Each of the features was calculated using the data at each five-minute interval. The net effect values were found using the calculations described by Patek et al.[85] A description of the feature set is listed in Table 4.

Table 4 – A description of features used for the bolus insulin and CGM disturbance detection algorithm. Each feature was calculated at each sampling interval, t.

Description	Formula
First derivative of the CGM values	$x_1(t) = \frac{dCGM(t)}{dt}$
Second derivative of the CGM values	$x_2(t) = \frac{d^2CGM(t)}{dt^2}$
Maximum of the first derivative of the CGM values and zero	$x_3(t) = \max(0, \frac{dCGM(t)}{dt})$
Maximum of the second derivative of the CGM values and zero	$x_4(t) = \max(0, \frac{d^2CGM(t)}{dt^2})$
Maximum of the product of the first and second derivative of the CGM values and zero	$x_5(t) = \max(0, \frac{dCGM(t)}{dt} x \frac{d^2CGM(t)}{dt^2})$
Current insulin bolus amount	$x_6(t) = i(t)$
Current CGM value	$x_7(t) = CGM(t)$
First derivative of the NE values	$x_8(t) = \frac{dNE(t)}{dt}$
Second derivative of the NE values	$x_9(t) = \frac{d^2NE(t)}{dt^2}$
Maximum of the first derivative of the NE values and zero	$x_{10}(t) = \max(0, \frac{dNE(t)}{dt})$
Maximum of the second derivative of the NE values and zero	$x_{11}(t) = \max(0, \frac{d^2NE(t)}{dt^2})$
Maximum of the product of the first and second derivative of the NE values and zero	$x_{12}(t) = \max(0, \frac{dNE(t)}{dt} x \frac{d^2NE(t)}{dt^2})$
The current NE value	$x_{13}(t) = NE(t)$

For every feature calculated, an additional feature was included in the classification algorithm representing the maximum value of that feature for the 15 minutes before and after the current interval. In total, there were 26 features used in the classification algorithm.

From these features, an output from the logistic regression, $y_{detect,1}$, was calculated using the following formula,

$$y_{detect,1}(t) = \beta_0 + \sum_{i=1}^{26} \beta_i \cdot x_i(t),$$

The value of each of the predictor coefficients determined from the training dataset is given in Table 5.

Table 5 - The coefficients used in the bolus insulin and CGM logistic regression disturbance detection algorithm.

Constant	Value	Constant	Value
$\boldsymbol{\beta_0}$	-2.57	$\boldsymbol{\beta_{14}}$	-0.88
$\boldsymbol{\beta_1}$	-13.46	$\boldsymbol{\beta_{15}}$	15.54
$\boldsymbol{\beta_2}$	238.69	$\boldsymbol{\beta_{16}}$	165.06
$\boldsymbol{\beta_3}$	-5.93	$\boldsymbol{\beta_{17}}$	3.96
$\boldsymbol{\beta_4}$	-361.07	$\boldsymbol{\beta_{18}}$	-233.25
$\boldsymbol{\beta_5}$	364.37	$\boldsymbol{\beta_{19}}$	135.57
$\boldsymbol{\beta_6}$	0.03	$\boldsymbol{\beta_{20}}$	0.10
$\boldsymbol{\beta_7}$	-0.09	$\boldsymbol{\beta_{21}}$	0.07
$\boldsymbol{\beta_8}$	1454.94	$\boldsymbol{\beta_{22}}$	-1392.72
$\boldsymbol{\beta_9}$	-22857.12	$\boldsymbol{\beta_{23}}$	1296.29
$\boldsymbol{\beta_{10}}$	109.30	$\boldsymbol{\beta_{24}}$	-94.48
$\boldsymbol{\beta_{11}}$	45407.29	$\boldsymbol{\beta_{25}}$	917.44
$\boldsymbol{\beta_{12}}$	-36996.24	$\boldsymbol{\beta_{25}}$	31527.56
$\boldsymbol{\beta_{13}}$	-2.57	$\boldsymbol{\beta_{26}}$	2.45

The log-odds, $y_{detect,1}$, was then transformed into the probability of a large glycemic disturbance occurring at that particular time denoted as, $\pi_{detect,1}$. This probability was found using the equation,

$$\pi_{detect,1}(t) = \frac{1}{1 + e^{-y_{detect,1}(t)}}.$$

The classification accuracy of the disturbance detection algorithm was evaluated on 25% of the data held out from training. At varying thresholds for the disturbance probability, the algorithm classified each five-minute interval as part of a glycemic disturbance as determined by how the dataset was labeled and evaluated based on its true positive and false positive rates.

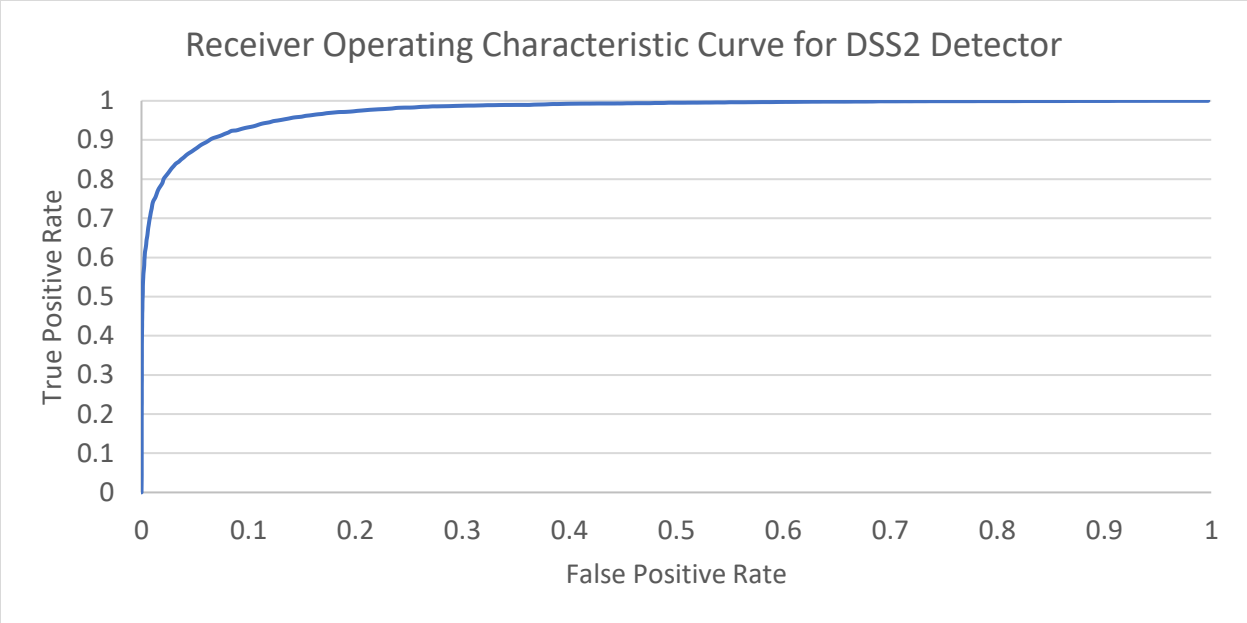

Figure 15 – The ROC curve for the classification results of the retrospective disturbance detector using CGM, the net effect, and bolus amounts on the holdout data.

Figure 15 shows the ROC curve for the detection algorithm. The area under the curve for the detection algorithm is 0.98. An area under the curve of 0.98 demonstrates that the logistic regression algorithm was able to classify many of the labeled five-minute intervals in the holdout dataset with a favorable tradeoff between false positive and true positive detections. It should be noted that this is a very unbalanced dataset, meaning that many more intervals were in the negative class than the positive class, and the evaluation of specific disturbance events described later in this chapter may be more informative in evaluating the algorithm's event detection ability.

Event Time Selection Procedure

Each five-minute interval was either labeled as being in the positive or negative class using the logistic regression classification method. The disturbance classification algorithm selected windows of time where a disturbance was likely to have occurred but did not directly choose the time of the event. The classification vector, $detection_1$, was defined as,

$$detection_1(t) = \begin{cases} 1 \; if \; \pi_{detect,1}(t) > \; \pi_{threshold,1} \\ 0 \end{cases},$$

Figure 16 shows an example of the output of the disturbance detection algorithm for a particular CGM trace. In this example, glucose rose following a suspected eating event. During the period of time where BG was rising, the disturbance probability was greater than the threshold, and

therefore the output of the detector was one, meaning that there was a large glycemic disturbance that occurred during this time frame. Here it can be seen how multiple five-minute intervals could be labeled with the positive class. Therefore, one of the intervals during this period of time needed to be selected as the event time.

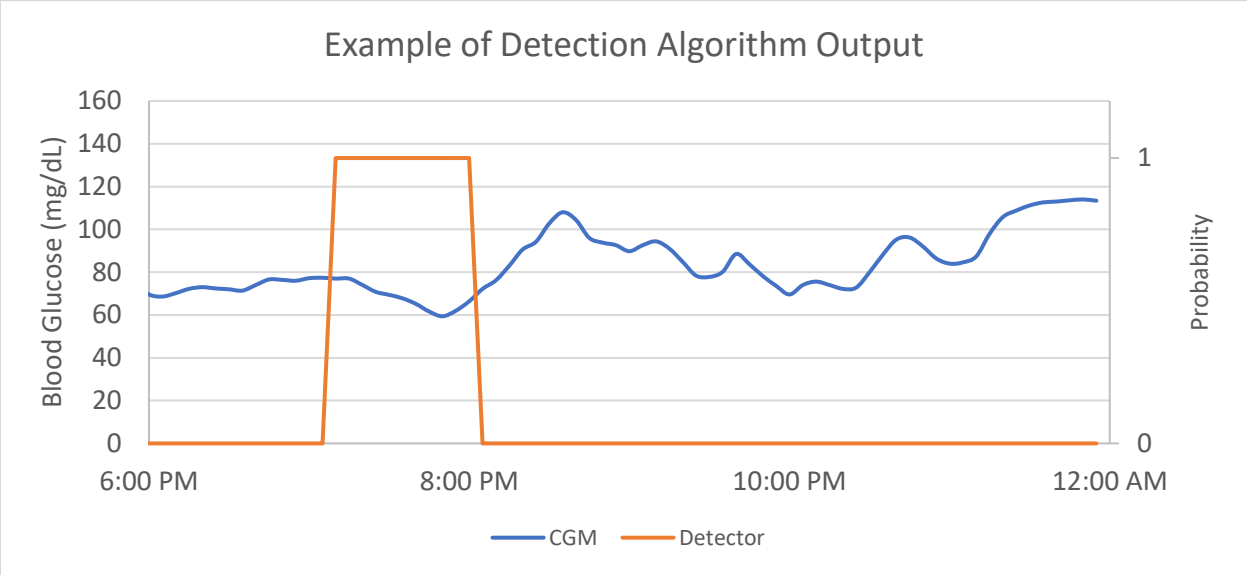

Figure 16 - An example of the disturbance detection output and corresponding BG values. The blue markers indicated CGM values, and the orange markers represent the output of the detector.

The five-minute interval selected to be the time of the disturbance event was chosen based on when the maximum second-order difference of the CGM values (i.e., curvature, $\frac{d^2CGM}{dt^2}$), in that window, was. This time was determined to be the best placement for the detections because it was thought that the maximum curvature would correspond to the beginning of an event, like eating, that would cause BG values to rise. Because the features were non-causal, it was possible for the detection time of an event to be before it occurred. To stop the same event from causing multiple detections, detections that were within one hour were combined. Multiple detections could occur during meals that lasted a long duration and involve multiple rises in glucose and insulin boluses or if an individual has a comorbidity that affects digestions like gastroparesis.

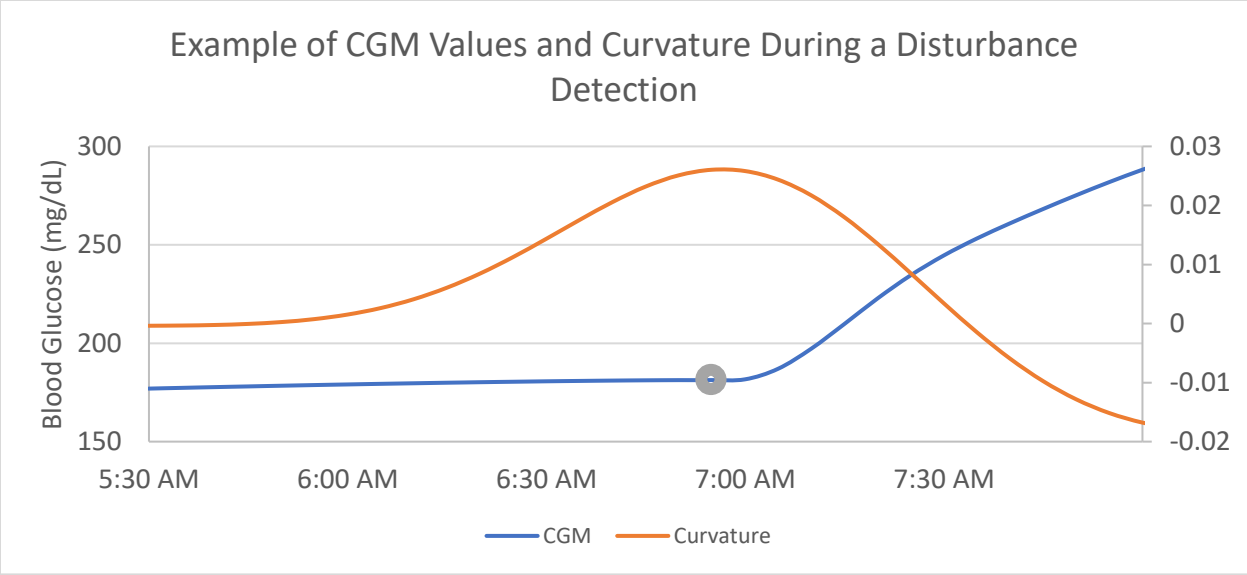

Figure 17 – An example of the CGM values shown in blue and the second derivative of the CGM values shown in orange for a period of time where the disturbance probability was greater than the threshold. The gray marker represents the detection time.

Figure 17 shows an example of the CGM values as well as the corresponding second derivative of the CGM values, $\frac{d^2CGM}{dt^2}$, during a window of time where the disturbance probability was above the threshold. In this example, the maximum CGM curvature (shown with the gray marker) was at 6:55 a.m., which is the beginning of a glucose excursion caused by eating. The meal in this simulation data example occurred at the exact time of the detection.

Retrospective Disturbance Detection Using Basal Insulin and Glucose Measurements

The next generation of automatic insulin dosing systems is likely to be fully closed-loop, meaning that there is no information provided to the system by the patient regarding any major disturbance and no manual meal bolus. In this case, if there are no meal announcements, there would be no record of when the user ate. Thus, meal amounts and the timing of eating events would be completely unknown. Even though the user does not input when large glycemic disturbances occur, it is still necessary to understand the timing of these events to improve treatment. Knowing the timing of glycemic disturbances could allow the system to learn how to better adapt to the user or aid in developing new technologies.

Because of these considerations, only CGM values and automatic doses delivered by the system without user input could be used to reconstruct the meal record and not meal boluses. A disturbance detection algorithm was designed using only CGM and basal insulin records and was agnostic to recorded carbohydrates to meet the requirements of the next generation of insulin dosing systems.

Historical Disturbance Estimation

Because disturbances were not known to the system, a methodology was used to estimate the historical disturbances experienced by the user. These disturbance signals were then used to generate features in the detection algorithm. The method for generating these disturbance signals was developed by a colleague and is in one of our collaborative works that has been submitted for publication.[138]

A model-based approach was used to estimate historical glycemic disturbances for each day of data collected to estimate the disturbances. This signal followed the same sampling time as the other signals used in the detection methodology, every five minutes. The estimation procedure used a Kalman filter with a version of the SOGMM using only insulin and BG information as inputs. The linearization operating point was the average basal insulin infusion rate, average CGM value, and steady-state solution for the model equations. The measurement and process noise covariance matrices were empirically selected so that the daily signatures appropriately represented glycemic disturbances. Figure 18 shows an example of the disturbance signal, meal and insulin records, and BG values for one day of data in the top, middle, and bottom subplots.

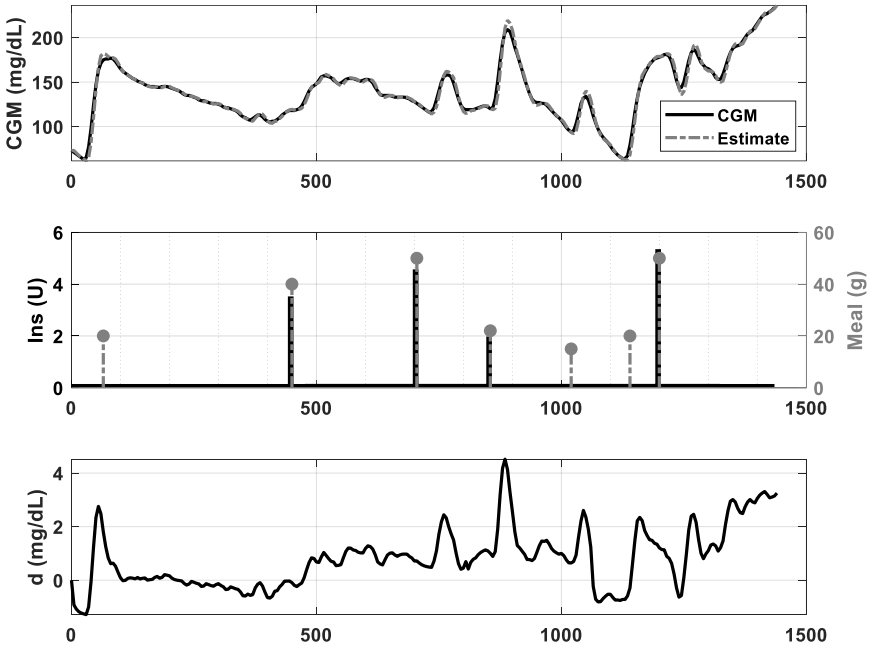

Figure 18 - The top subplot shows the glucose trace over one 24-hour period (1440 min.). The middle subplot shows the insulin boluses and meals recorded by the patients. The bottom subplot shows the estimated disturbance, $\hat{d}$, over a day.[138]

In this example, it can be seen how the disturbance signature rises to a positive value following eating events in a manner that is similar in terms of magnitude and rate of change to CGM values. This signal characterized glycemic disturbances well and provided a valuable tool for estimating disturbances not known to the model. This estimation was instrumental in situations where meal information was not available.

Disturbance Signal Filtering

For some individuals, the disturbance generation process led to the creation of signals that gradually increased over the day. This effect was the result of the slow dynamics of certain aspects of the model. Figure 19 shows an example of how the estimated disturbance signal for a representative subject exhibiting this trend slowly drifted upwards over the 24-hour span. Ideally, the disturbance signal would be centered at zero and only have positive increases immediately following meals. The signal for this day begins slightly below zero and slowly increases. The trendline shows how the average value increases throughout the day.

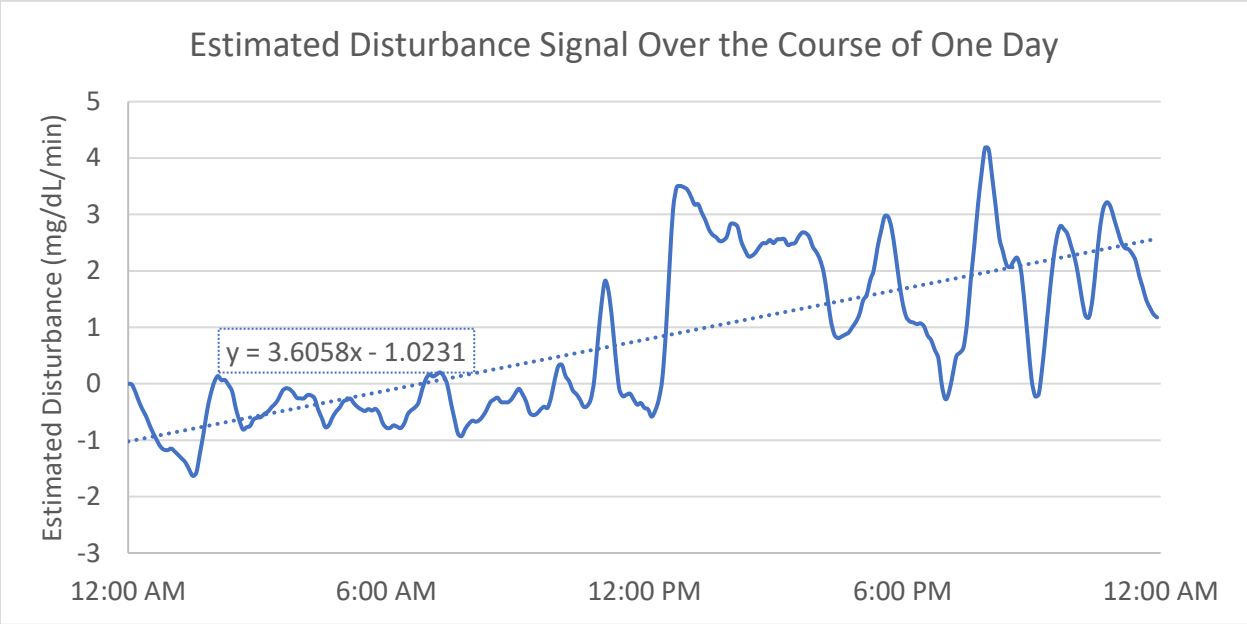

Figure 19 - The estimated disturbance signal for one real subject for a single day. The linear trendline is shown with the dashed line, and the equation is shown on the chart area.

An IIR High Pass filter was applied to the daily disturbance signals to account for this issue in the estimation process. A passband frequency of 0.0028 Hz was used to eliminate any low-frequency changes in the signal with a cycle of greater than six hours. It was determined that six hours was the appropriate amount of time for the filter because anything with a frequency greater than this was likely

to cause more acute changes in glucose and should be considered in the disturbance behavior. This filter was anti-causal and zero-phase to eliminate phase distortion. Figure 20 shows the disturbance signal for the same day of actual patient data as Figure 19 in the filtered and unfiltered form.

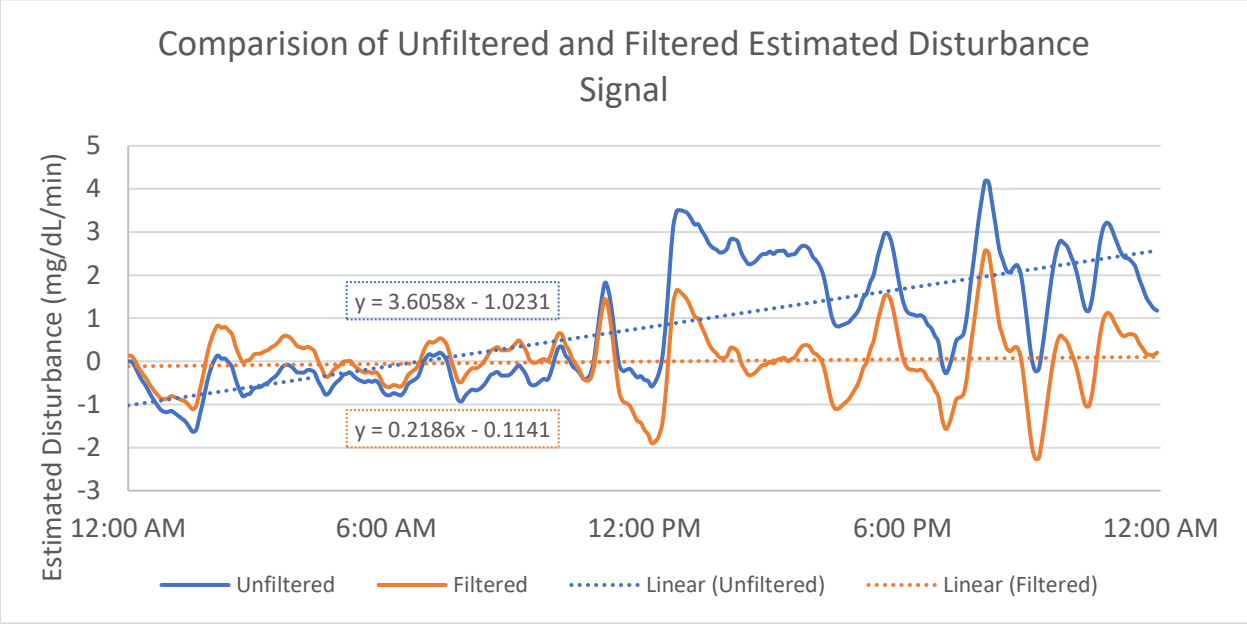

Figure 20 - A comparison of the unfiltered and filtered estimated disturbance signal for one day of actual data. The trendlines shown with the dashed lines represent the signals of the corresponding colors. The equation for the trendline of the unfiltered signal is outlined in blue, and the trendline equation for the filtered signal is outlined in orange.

The unfiltered signal, in blue, has an upward trend throughout the day, causing an offset in values from the zero axis. The filtered orange disturbance signal is much more centered on the axis, and the peaks in the signal around what presumably are meals are extenuated. A comparison of the slopes of the linear trendlines shows that the unfiltered signal has a positive slope of 3.61, thus indicating a positive bias over the day, whereas the slope of the orange signal is 0.22. The difference in the trendlines slopes indicates how well this filter worked to eliminate low-frequency noise in the signal estimation. The new filtered disturbance signals had more pronounced and distinct peaks in the disturbance signal.

Feature Generation

As records of meals and the associated boluses would be absent in a fully closed-loop system, CGM and insulin data are the only sources of information that could be used to detect meal-like glycemic disturbances retrospectively. The disturbance detector was created using features that charactered disturbances using the vector of estimated disturbance values, d, and continuous glucose measurements, CGM, for each day of historical data collected. To account for noisy measurements, the

estimated disturbance values were smoothed before features were generated using a moving average over an hour centered at the current interval. A description of the features which were calculated for each five-minute sample, t, is listed in Table 6. These features involving polynomial fitting were generated using least-squares. These features were chosen based on insights gathered in the design of the DSS2 algorithm.

Table 6 – A description of the features for the CGM and basal insulin-only retrospective disturbance detection algorithm.

Feature	Description
$\boldsymbol{f_1}$	*Intercept term from the second-order polynomial fit on* $c_1 = CGM(t-6), \dots, CGM(t+6)$
$\boldsymbol{f_2}$	*Slope term from the first-order polynomial fit on* $c_2 = CGM(t), \dots, CGM(t+12)$
$\boldsymbol{f_3}$	*Curvature term from the second-order polynomial fit on* $c_1 = CGM(t-6), \dots, CGM(t+6)$
$\boldsymbol{f_4}$	$f_2 \cdot f_3$
$\boldsymbol{f_5}$	*Intercept term from the second-order polynomial fit on* $d_1 = d(t-6), \dots, d(t+6)$
$\boldsymbol{f_6}$	*Slope term from the first-order polynomial fit on* $d_2 = d(t), \dots, d(t+6)$
$\boldsymbol{f_7}$	*Curvature term from the second-order polynomial fit on* $d_1 = d(t-6), \dots, d(t+6)$
$\boldsymbol{f_8}$	$f_6 \cdot f_7$
$\boldsymbol{f_9}$	*Maximum* d *value in the next hour* $d_{max} = max\, d_2$

Disturbance Detection

Once features were generated for each five-minute interval, t, the output of a logistic regression equation, $y_{detect,2}$, was evaluated. The equation for the logistic regression was,

$$y_{detect,2}(t) = \beta_0 + \sum_{i=1}^{9} \beta_{\mathrm{i}} \cdot f_{\mathrm{i}}(\mathrm{t}).$$

The regression coefficients were found by training a logistic regression classifier on the same dataset as was used for the other classification algorithm (NCT03394352).[129] The training dataset was labeled in the same manner as the other detection algorithm by setting intervals where glucose rose at least 40 mg/dL in the next two hours as the positive class and all other times as negative. The values for each of the logistic regression coefficients, β_{0-9}, are given in Table 7.

Table 7 - The coefficients used in the basal insulin and CGM logistic regression disturbance detection algorithm.

Constant	Value
$\boldsymbol{\beta_0}$	*-1.1584*
$\boldsymbol{\beta_1}$	*14.6012*
$\boldsymbol{\beta_2}$	*0.0135*
$\boldsymbol{\beta_3}$	*-0.0111*
$\boldsymbol{\beta_4}$	*-0.4954*
$\boldsymbol{\beta_5}$	*2661.6419*
$\boldsymbol{\beta_6}$	*-0.2154*
$\boldsymbol{\beta_7}$	*-2.4333*
$\boldsymbol{\beta_8}$	*-13551.6432*
$\boldsymbol{\beta_9}$	*2.9627*

The output of the logistic regression equation was then transformed into the disturbance probability value, $\pi_{detect,2}$. The equation for this transformation was,

$$\pi_{detect,2}(t) = \frac{1}{1 + e^{-y_{detect,2}(t)}}.$$

The classification accuracy was evaluated in the same way as the other detector. 25% of the training data was held out, and the classifier was evaluated on its ability to label each five-minute interval as in the positive or negative class. Figure 21 shows the ROC curve for this classification algorithm. The area under the curve for this detector was 0.92, which is 0.06 lower than the other algorithm.

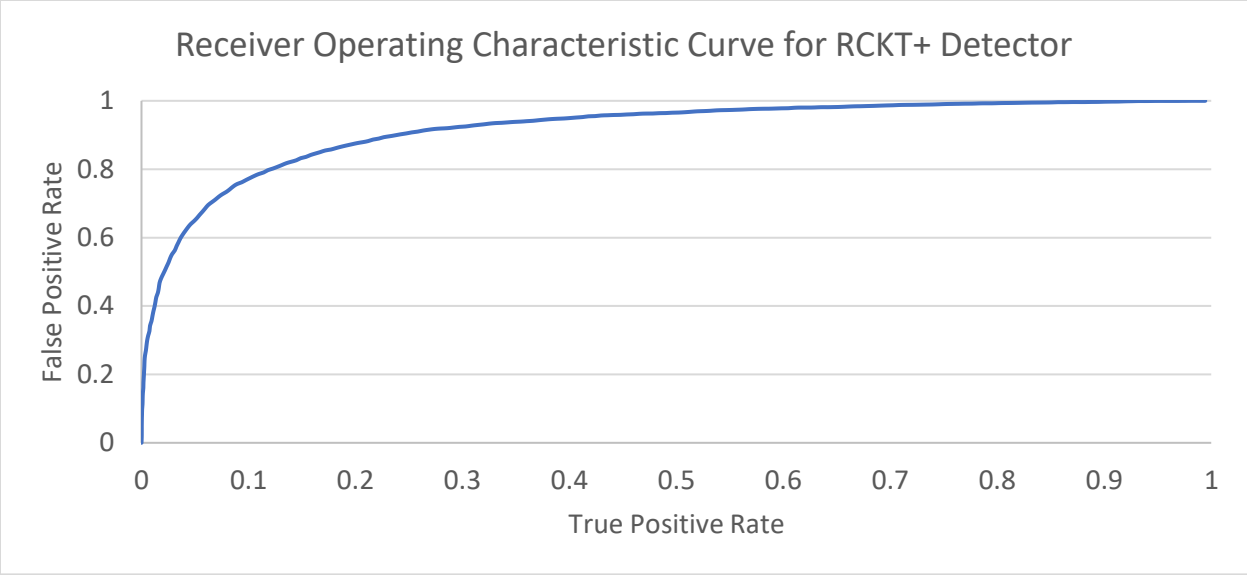

Figure 21 – The ROC curve for the classification rate of the retrospective disturbance detection algorithm evaluated on the holdout training data.

Event Time Selection Procedure

Windows of time where the disturbance probability was above the threshold, $\tau_{threshold,2}$, were then labeled and stored in the detection vector, $detection_2$.

$$detection_2(t) = \begin{cases} 1 \; if \; \pi_{detect,2}(\mathrm{t}) > \tau_{threshold,2} \\ 0 \; otherwise \end{cases}$$

The detection times for RCKT+ were determined by selecting the five-minute interval in the amount of time where the disturbance probability was above the threshold where the curvature of the CGM values was the greatest. Just as was done in the other detector, DSS2, if detection times were within one hour of each other, the first detection time was used, and the subsequent detections in that hour were removed.

Comparison of the Two Detection Approaches

Although both algorithms serve the same ostensive purpose, to detect large positive glycemic disturbances, each requires different data and has a different application. The first described algorithm, DSS2, uses insulin boluses and CGM values and is well suited for data collected from subjects using sensor-augmented pump therapy, multiple daily injections with a connected smart insulin pen, or hybrid closed-loop. The second detection algorithm described, RCKT+, uses only basal insulin delivery amounts, CGM values, and the estimated disturbance found using CGM and basal insulin records.

The intention of the experiments described in the following sections is to determine the performance of the two algorithms on both simulated and real data collected during a clinical trial. The simulation dataset was larger, contained information from more patients, and included some realistic physiological sources of glycemic variability. The actual dataset used was collected during a clinical trial admission where the study team recorded meal events and insulin doses. This dataset, although smaller, contained periods where the participants exercised and sources of glycemic variability and measurement noise that are not present in the simulation dataset. Both evaluations provide information about the performance of the disturbance detection algorithms under different conditions.

Evaluation Using Simulation Data

Experimental Setup

An experiment was designed to compare the accuracy of each detection approach under somewhat ideal conditions using data produced by the UVA/Padova T1D simulator. Simulation data was used because mealtimes were known precisely, and a large amount of data could be generated. Additionally, the variability of the in silico subject population allowed the detection algorithm to be tested under many different combinations of physiology present in real patient populations represented as system parameters.

The features required for each detection algorithm were generated, and the classification algorithms were both evaluated at each five-minute interval of the dataset. A binary vector defining if each interval was above the threshold for the detectors was calculated for a series of values. The algorithm thresholds, $\tau_{threshold,1}$ and $\tau_{threshold,2}$, ranged between zero and one. Then the detection times were determined based on the maximum curvature of the CGM values during the windows of time above the threshold. If a detection was within one hour of another detection, the latter detection was eliminated.

These detections were evaluated against the known mealtimes from the simulation dataset. A detection was considered a true positive detection if it was within one hour of an actual meal. False positives were any detections not within an hour of a meal. Meals could only be detected once, so if there were two detections following a meal, the second would be considered a false alarm. Each detector was evaluated for its true positive rate, false positive rate, and the amount of time that the detection was from the actual mealtimes.

The data was generated from 100 virtual subjects over 12 days. During this period, the simulated subjects used sensor-augmented pump therapy. The virtual participants were administered three meals a day, breakfast, lunch, and dinner. Mealtimes and amounts were randomly selected for each subject. Breakfast occurred from 6:30 a.m. and 7:30 a.m., lunch was between 12:30 p.m. and 1:30 p.m., and dinner was from 6:30 p.m. and 7:30 p.m. All meals ranged in amount from 50 and 70 grams of carbohydrates. This dataset contained 3,600 meals at varying times and sizes. The simulation considered the effect of the dawn phenomenon and intraday variability of the patients' insulin sensitivity.

The detection approaches were evaluated on the true positive and false positive rates at each threshold. Additionally, the average amount of time between the detection, t_{detect}, and the event, t_{event}, was calculated for each true and false positive rate.

$$time\ to\ detect = t_{detect} - t_{event}$$

Appropriate thresholds were selected for each algorithm using the true and false positive results. To get a sense of how the detection algorithms would perform were they to be implemented, the detection performance was evaluated as well as the distribution of detection times. These distributions gave a sense of the skewness of the algorithms concerning the tendency to detect events either before or after the time of occurrence.

Results

The ROC curves for both the DSS2 algorithm, shown in blue and the RCKT+ algorithm, shown in orange. These curves, relating the true and false positive rates, show that in the simulation data experience, both algorithms had high rates of true detections while maintaining low rates of false alarms. Both algorithms quickly attained true detection rates of greater than 90% while maintaining false positive rates of less than 0.001. It appears that, in general, the RCKT+ algorithm was able to achieve higher true positive rates at lower false positive rates than the DSS2 algorithm. Both algorithms quickly converged to a true positive rate of more than 90% and stayed consistently at that detection rate as the average false positive rate increased.

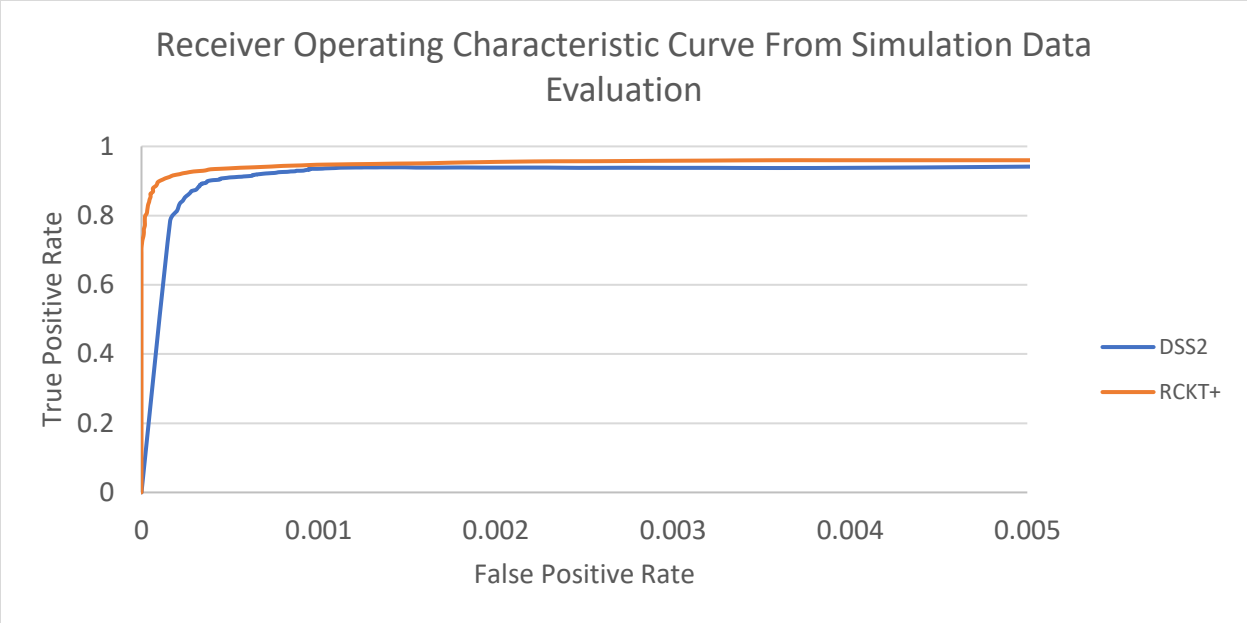

Figure 22 – The ROC curve for the simulation experiment based on the rate at which meals were detected within one hour of the actual time. DSS2 is shown in blue, and RCKT+ is shown in orange.

A threshold was selected for both detectors of 0.1, based on when each detector achieved high true positive rates. With the nominal threshold, the average true positive rate for the DSS2 disturbance detector was 96.87 ± 13.22%, and the mean false positive rate was 0.21 ± 0.22%. The average true positive rate for the RCKT+ detector was 98.79 ± 10.14%, and the false positive rate was 0.70 ± 0.22%. The mean time difference between the true detection times and the recorded meal events was 0.04 ± 6.02 minutes and 0.04 ± 5.94 minutes for the DSS2 and RCKT+ detectors. Figure 23 shows histograms of the amount of time between detections and the actual mealtimes. The top subplot shows the distribution of the DSS2 detections, and the bottom subplot shows the distribution for RCKT+.

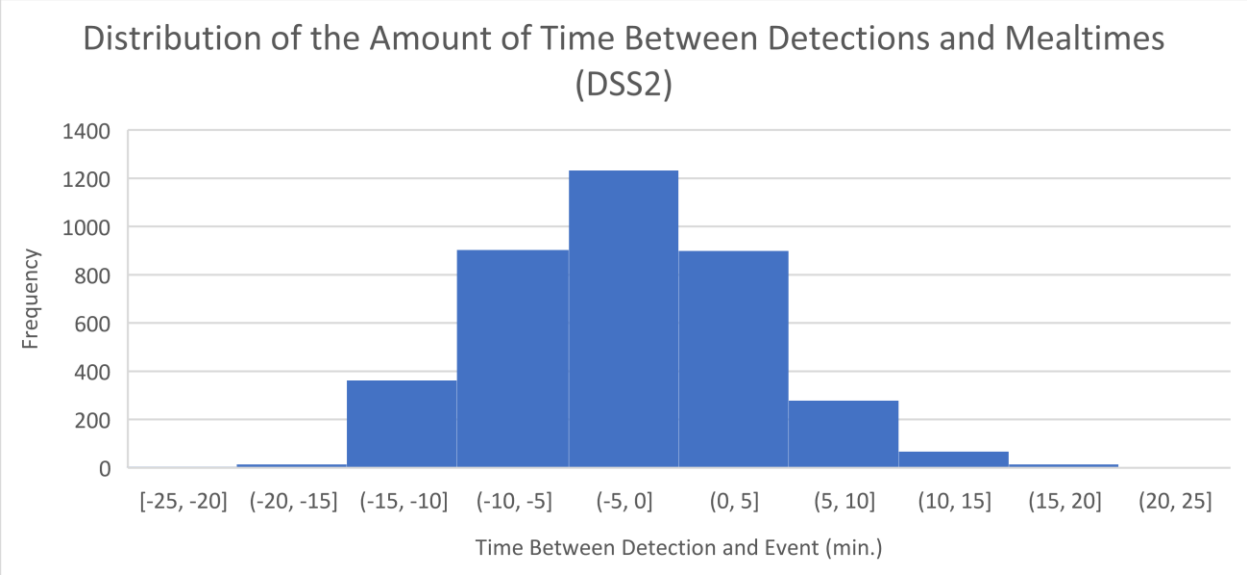

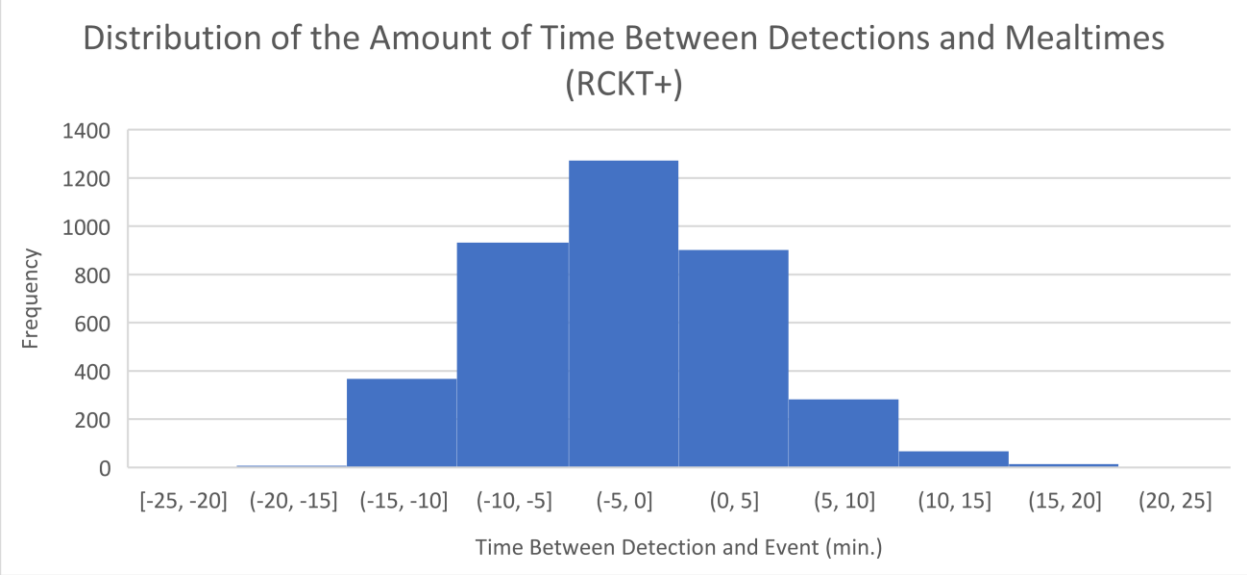

Figure 23 – The histogram of meal detection times compared to the actual mealtimes for each detector on the simulation dataset. DSS2 is shown in the top subplot, and the distribution of the RCKT+ detections is shown on the bottom.

Both disturbance detection algorithms correctly detected more than 96% of meals in the simulation dataset with less than a 1% false positive rate, and the amount of time between the detections and the actual mealtimes was less than one minute on average. The distributions of the time between the detections and the mealtimes show that each algorithm distribution was centered at roughly zero and approximated a normal shape. In this distribution, there is no strong bias from either detector towards detecting meals before or after their occurrence, which is favorable. A major caveat of these results is that the data used was generated using a simulation platform and therefore may not include some sources of glycemic variability present in real life. The experimental setup included sources

of low-frequency variability (e.g., diurnal insulin sensitivity variation, dawn phenomenon), but the only major abrupt disturbances to BG were related to meals.

Overall, the results of this experiment showed the accuracy of both detection algorithms. The DSS2 algorithm performed slightly worse in terms of the true detection rates but had a lower false positive rate than RCKT+ at the nominal threshold. This algorithm did require many more features and for there to be information collected from the patient regarding manual meal boluses. Although it required more features, the DSS2 algorithm could be used on data collected from patients not on insulin pump therapy (i.e., multiple daily injections). The RCKT+ algorithm in its current form would not work unless a full record of basal insulin was known. Overall, both detection algorithms had exceptionally high true positive rates and very low false positive rates when applied to a simulated dataset.

Ultimately, it is tough to evaluate detection algorithms. There is no true record of when events happened in actual data, or the datasets are very small and limited, and in simulation, there is far less glycemic variability than what is true in real life. The next section describes the results of an experiment conducted on a limited real-life dataset.

Evaluation Using Clinical Data

Experimental Setup

The same experiment that was conducted with the simulation data was repeated with a real dataset. This evaluation was performed because simulation data have much less variability, noise, and other sources of entropy that would make it difficult to determine when disturbance events like meals occurred. This experiment also provided an opportunity to evaluate how the detection algorithms would perform in real life.

Any data related to meal and insulin events collected outside of a strictly controlled clinical environment are likely flawed. For this reason, the data used to evaluate the proposed method were actual patient data collected during part A of the Glucose Variability study (GV2a) at UVA, where participants meal and insulin information was recorded meticulously under the supervision of the study team.[139] During this admission study participants were exposed to meal challenges of various sizes and daily physical activity. This study was funded through a grant awarded to UVA from the National Institutes of Health and was approved by the Institutional Review Board. These data include physiological measures such as height and body weight, which affect parameters in the insulin-glucose model, and diabetes management-related information such as delivered insulin, meals, basal profiles,

CGM measurements, SMBG measurements, carbohydrate to insulin ratios, and BG correction factors. Because this was collected in the Clinical Research Unit of the UVA Hospital under a strict protocol, it is known that meals and insulin happened precisely when they were recorded.

This rare high-quality dataset provides the opportunity to use it as a testbed, which is unique considering many recent clinical trials have been at home, and mealtimes cannot be verified. The admission portion of the GV2a study was conducted in the Fall of 2015 through the Winter of 2016 at UVA. During the two-day admission, participants were monitored by the study team as they managed their T1D using a decision support system. A subset of 11 patients was selected from the GV2a data because they were pump users and had complete data for the admission. The patient demographics for this dataset are shown in Table 8.

Table 8 – The participant demographics for the GV2a dataset.

Characteristic	Mean ± SD
Age (years)	40.91 ± 11.39
Weight (kg)	78.19 ± 16.54
Height (cm)	169.19 ± 10.69
TDI (u)	45.96 ± 17.85
Baseline HbA1c (%)	7.71 ± 0.80

Results

Figure 24 shows the ROC curve for the two detectors, DSS2 and RCKT+, evaluated on the clinical dataset. The results for DSS2 are shown in blue, and RCKT+ is shown in orange.

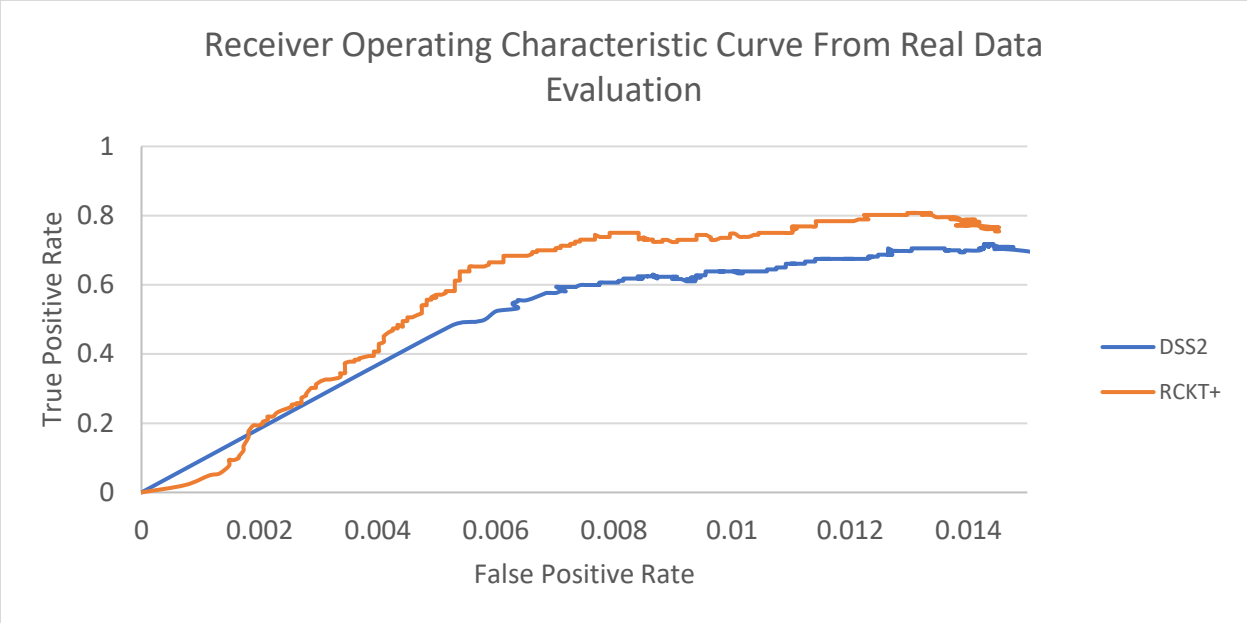

Figure 24 - The ROC curve for clinical data experiment based on the rate at which meals were detected within one hour of the actual time. DSS2 is shown in blue, and RCKT+ is shown in orange.

From these results, it is clear that once again, the RCKT+ algorithm outperforms the DSS2 algorithm at most combinations of true positive and false positive rates.

When the same threshold used in the was simulation dataset was used in this experiment, the DSS2 algorithm correctly detected 70.13 ± 19.95% of eating events on average, whereas RCKT+ detected 78.47 ± 18.43%. The false positive rate for the DSS2 algorithm was 1.26 ± 0.56%, and the false positive rate for the RCKT+ algorithm was 1.40 ± 0.61%. The mean amount of time between detections from the DSS2 and RCKT+ algorithms was -10.62 ± 27.05 minutes and -10.70 ± 27.69 minutes.

The distributions of the amount of time between detections and the actual events are shown in Figure 25. The results for the DSS2 detector at the nominal threshold value are shown in the top plot, and the results from the RCKT+ detector are shown in the bottom plot.

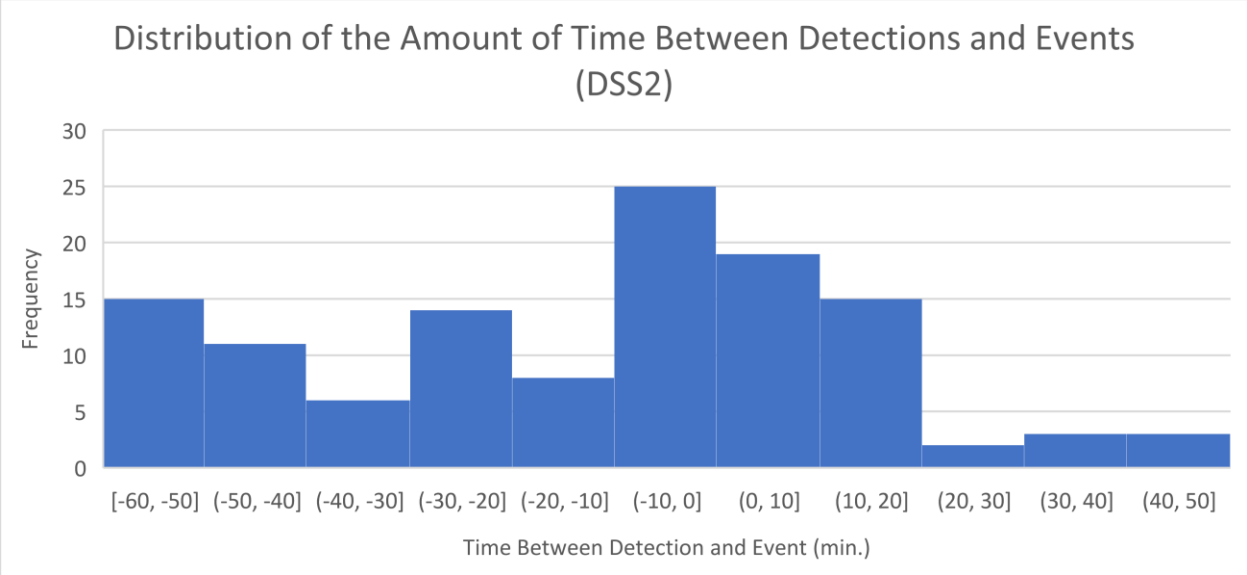

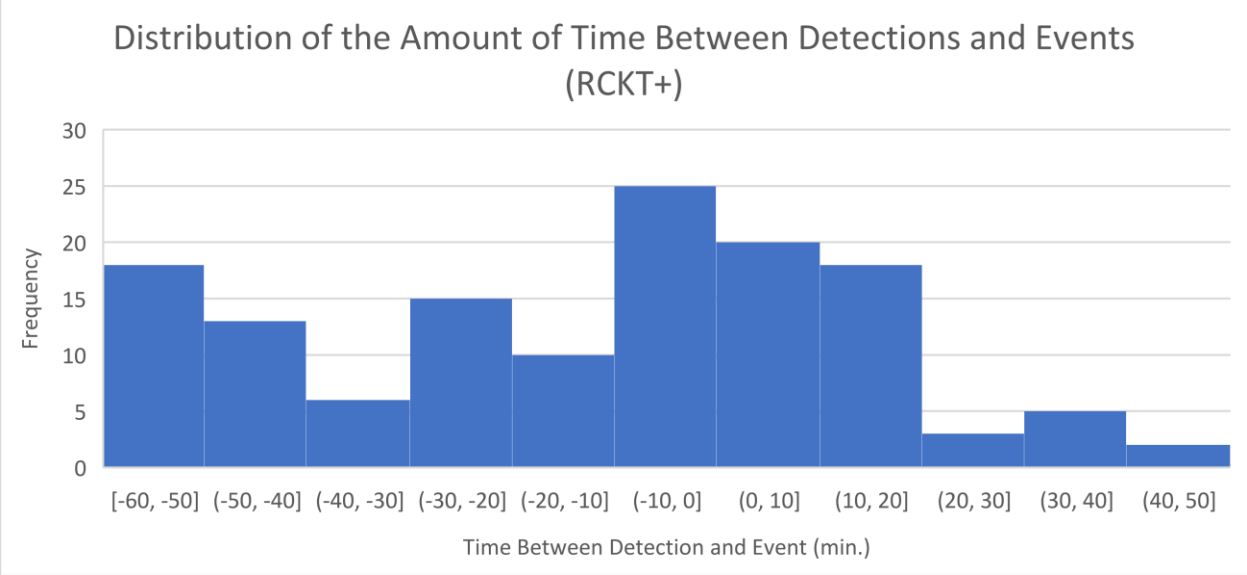

Figure 25 – The histogram of meal detection times compared to the actual mealtimes for each detector on the clinical dataset. DSS2 is shown in the top subplot, and the distribution of the RCKT+ detections is shown on the bottom.

The evaluation of the performance of the detection capability on actual data of the two algorithms was noticeably different from the experiment using simulation data. It could easily be seen in the ROC curves that both detection algorithms had lower true positive detection rates at the corresponding false positive rates when applied to the real data. When the nominal detection threshold was chosen for each algorithm, the true positive rates were lower, and the false positive rates were higher than in the simulation experiment. The true positive rate for the DSS2 algorithm was 26.74% lower in the experiment using the real data than the experiment using the simulation data. For the RCKT+ algorithm, the true positive rate was 20.32% lower in the real data experiment.

Furthermore, in the clinical experiment, the events were often detected roughly ten minutes before the actual time of occurrence. In the simulation experiment, events were almost always detected within five minutes of the correct time. For each of the metrics discussed, the SD of the values was higher during the real data experiment, indicating greater variation between subjects in terms of algorithm performance.

There is a striking difference between the results of the two experiments, but there are also numerous plausible explanations as to why it might be so different. In the simulation experiment, there are low-frequency glycemic disturbances such as changes in the insulin sensitivity of the in silico individual and also physiologic factors like the dawn effect. There are no other factors that change BG values dramatically other than meals. The lack of variability caused by this effect of the simulation platform makes it acutely evident from BG values when meals occurred. When the subjects were administered food, their BG values rose abruptly, leading to pronounced glycemic excursions. Following relatively short postprandial glucose excursions, BG values usually returned to the basal value.

In the clinical data, the effect of glycemic disturbances is not always as evident. Many factors affect how BG changes following meals present in real life, but not in the UVA/Padova simulation platform. The participants of the GV2a clinical trial that the actual data were collected from exercised in the admission. Physical activity was not integrated into the version of the simulation platform used to create the in silico data. The changes in insulin sensitivity associated with physical activity likely affected BG levels in the participants during and after the event. This perturbation may have contributed to more glycemic variability leading to false alarms or false negatives and increased insulin sensitivity which caused less pronounced glycemic excursions.

Interestingly, the timing of disturbance detections was different in the results of the two experiments. When applied to the simulation data, the algorithms detected disturbances on average at around the time that these events occurred. The time between the time selected for the detections and the actual disturbance times was approximately normal. This distribution is ideal for this application because there was little bias in the detection times.

When applied to real data, the algorithms selected times for the detected events that were often before the actual event. This offset is probably the result of the chosen features. When these two algorithms were being designed, it was assumed that individuals would frequently give insulin after or during meals and not before. Because of this consideration, both algorithms use features that include

the maximum value in the window of time that spans into the future. In this particular clinical dataset, the study team ensured that all insulin boluses were administered at the beginning of meals. Based on surveys of people with T1D, this is unlikely to be the case in an unsupervised environment.

Ultimately, the performance of a detection algorithm is most important when it is applied to actual data. The simulation experiment provides an excellent tool for determining the effectiveness of a method in ideal conditions but often lacks the variability experienced in real life. Furthermore, it should be noted that the detectors were evaluated on recorded meals and not glycemic disturbances. It is likely that many of the meals that were not detected did not cause a large change in glucose values. Because there was physical activity during the clinical admission, it is possible that there were no significant rises in BG after some meals due to increased insulin sensitivity.

Aim 3 – Determination and Implementation of Patterns of Glycemic Disturbances in a Fully Closed-Loop Insulin Dosing System

Introduction

Due to the nature of the time dynamics of insulin, feedforward control is necessary to prevent unwanted deviations from target glucose, specifically hyperglycemia, following large positive glycemic disturbances like ingested carbohydrates. Fully closed-loop artificial pancreas systems thus far have not been able to handle the challenges with postprandial glucose excursions with feedback control alone. This is due to the time constants associated with insulin and ingested carbohydrates which have caused feedback-only controllers to inadequately compensate for rises in BG caused by eating carbohydrates. For this reason, mealtime insulin has traditionally been taken proactively (i.e., feedforward control), and it is currently recommended that people with T1D use functional insulin therapy, which is a manual form of feedforward control, to deliver insulin before eating.

This chapter discusses how regular patterns of behavior derived using data mining were leveraged to anticipate glycemic disturbances in a fully closed-loop artificial pancreas system. The data-driven techniques used allowed for personalized, dynamic accounts of behavior and could be updated as behavior changes. Daily disturbance signatures were clustered using unsupervised learning, and these regular patterns were transformed into glycemic disturbance profiles weighted based on the probability of each and implemented in an MS-MPC. This probability value was updated in real-time using current estimates for the disturbance experienced by the individual using the system. The effectiveness of the disturbance patterns, derived from actual patient data and the BPS, was evaluated in a large-scale simulation experiment using the UVA/Padova T1D simulator. Additionally, the utility of this methodology in preventing postprandial hyperglycemia was evaluated and discussed.

Model Predictive Control

MPC is a control strategy that is informed by predictions made from a model of the dynamic process that is being modulated. MPC differs from some other control strategies (e.g., proportional–integral–derivative control) because current measurements and future values are considered in the cost function that is being minimized. In T1D, MPC has been used to predict future BG using a physiological model and titrate insulin appropriately.[140] In artificial pancreas systems that use MPC, insulin injections are decided at each sampling time based on a series of constraints and what control action would be optimal in terms of the cost function.

MS-MPC is a control strategy that considers predictions from an ensemble of N parallel MPC controllers. The MS-MPC methodology was first described by Lucia et al. in 2012 and has been expanded in subsequent work.[141,142] Each model in the ensemble uses a different disturbance signal as an input. The control action is decided from a consensus of the MPC controllers. Figure 26 shows a graphical depiction of the MS-MPC strategy.

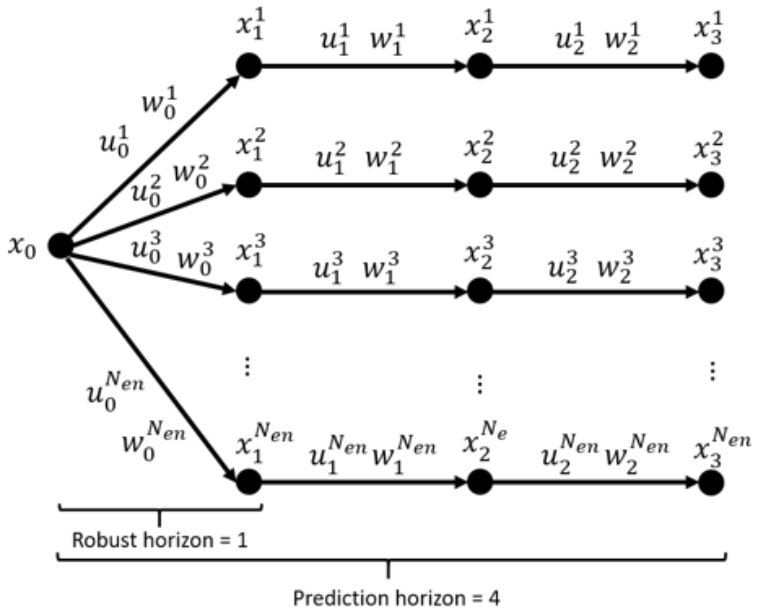

Figure 26 – A depiction of the multistage model predictive control strategy. [143]

In this example, a control action is chosen at x_0 based on the predictions made from the N MPC models and the associated inputs u and disturbances w. This control strategy allows for the consideration of multiple possible disturbances that the system might experience.

Our group's simulation and clinical experiments have shown how anticipatory profiles integrated into automatic insulin dosing systems can reduce the unwanted effects of glycemic disturbances. Simulation experiments have demonstrated that MS-MPC controllers informed by disturbance profiles to anticipate moderate exercise's effects can reduce hypoglycemia.[143–145] These results were later confirmed in a randomized crossover clinical trial with 15 adult participants.[129] There were fewer hypoglycemic events (9 vs. 33), and the percent time where BG was less than 70 mg/dL was 1.3% lower while the participants used the MS-MPC system compared to a well-tuned standard MPC. The overall reduction in hypoglycemia resulted in no significant increase in the amount of time where BG was greater than 180 mg/dL.

It was also demonstrated in silico that the capacity of the MS-MPC framework to anticipate glycemic disturbances caused by meals.[146] In that work, disturbance profiles were generated from a representative real subject and then used to perform closed-loop experiments using the 100 adult cohort of the University of Virginia/Padova T1D simulator. The results showed an average increase in the amount of time in euglycemia (i.e., 70 to 180 mg/dL) of 1.6% when using a hybrid closed-loop approach and 16.4% when using a fully closed-loop approach.

Other research groups have also used a multiple model approach to mitigate disturbances in a fully closed-loop insulin dosing system. Cameron's 2012 manuscript describes a methodology for an automated insulin dosing system that uses multiple BG prediction models, each informed by different disturbances.[147] When the system determined that one disturbance was more likely, additional weight was given to that model's predictions. Additionally, information was included regarding the likely timing of meal disturbances based on normal mealtimes, the time of the last meal, and sleep schedule. Using this approach, Cameron et al. were able to reduce the two-hour prediction error by 45% without meal detection and 18% with meal detection. The three-hour prediction error was reduced by 60% without meal detection and 30% with it.

Cameron et al. extended these findings in a 2014 clinical trial.[148] The multiple model probabilistic controller (MMPC) was used by ten patients in an inpatient study where they consumed five unannounced meals. For the six patients who used the final version of the controller, the mean CGM TIR was 78%. During the admission, there was only one controller-induced hypoglycemia.

The MMPC was evaluated on ten patients in an inpatient clinical study where the mean TIR was 142 mg/dL overall and 125 mg/dL overnight.[149] A different version of the algorithm that was tested in a hotel-based study with 15 subjects achieved an overall mean BG of 152 mg/dL and a mean overnight BG of 139 mg/dL.

An MS-MPC structure was chosen as the closed-loop system controller for this application because it allowed for insulin dosing decisions to be made based on the predictions of multiple models, each perturbed by a different disturbance signal. These disturbance signals represented the average disturbance experienced by the individual on days that were grouped. Elements of the cost function were determined from each prediction and were weighted based on an online estimation of the profile’s posterior probability.

Indicator Signals

The first step in the process of generating the behavioral patterns was to calculate the historical disturbance signals for each day of historical data. The historical disturbance generation procedure was done in the same way that is described previously. Once the daily disturbance signals were generated, large disturbance events were detected using the RCKT+ detector described in Aim 2. The detection procedure was carried out to create a reconstructed record of the disturbance events experienced by the individual over the data collection period. Then binary signals, referred to as indicator signals in this text, were generated from the disturbance record. These indicator signals were zero at all times except for the period following disturbances. Figure 27 shows an example of the indicator signal. In this case, the disturbance was at time t, and the post-disturbance window is of length n_{window}.

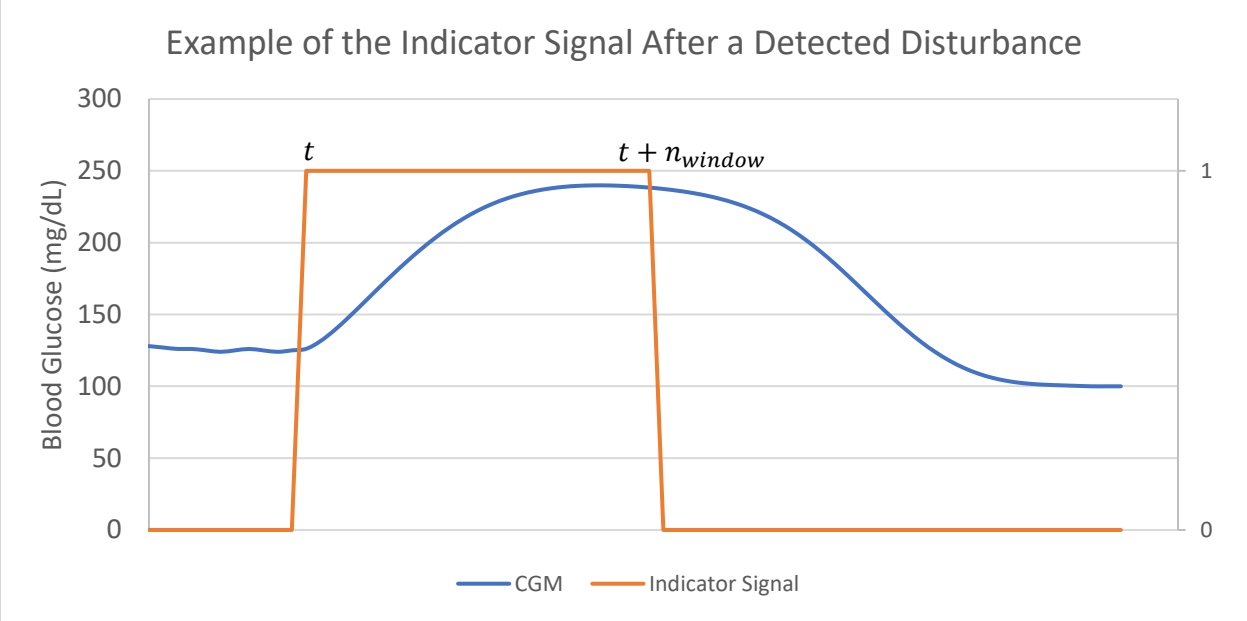

Figure 27 – An example of an indicator signal. t shows the time of the disturbance event, and the post-disturbance window is of length n_{window}.

The indicator signals were generated solely for the clustering process used to create the disturbance profiles for each individual. It should be noted that these signals notably only include information regarding the timing of disturbances and not any information about the magnitude of these events. It was decided that it was more important from the perspective of the intended application, a fully closed-loop insulin dosing system, to aggregate information related to the timing rather than the magnitude of perturbations. This design choice was due to the goal of this approach being to anticipate disturbance events. Grouping signals that include the magnitude of the historical disturbances, like the

disturbance signature, d, may cause events that occurred at different times but had overlapping effects to be combined. How the length of the post-disturbance windows was determined will be discussed in a later section.

Profile Generation

Clustering Algorithm

K-means clustering is one of the most widely used unsupervised learning methods. The algorithm originated in a paper authored by Hugo Steinhaus in 1956.[150] The standard algorithm used today was proposed by Stuart Lloyd in 1957 as a part of his work at Bell Labs, although he did not publish this work until 1982.[151] Edward W. Forgy published a similar method in 1965. Because both researchers were developing the idea simultaneously, it is sometimes referred to as the Lloyd-Forgy algorithm. The first know use of the phrase k-means was in a manuscript by James McQueen in 1967.[152]

The number of clusters used, k, is predefined, and the algorithm begins by randomly picking k objects to be the initial cluster centroids. Iteratively pieces of data are assigned to a cluster based on which centroid is closest. Then, the cluster centroids are recomputed. This process is repeated until the cluster centers stabilize or the max number of iterations is reached.

The k-means algorithm can be formally described as beginning by defining the set of n observations as, $x_1, \dots, x_n$. Each of these observations is of length, l, and is made up of the different features for that observation. K-means then divides the observations into k sets, $S = S_1, \dots, S_n$ by minimizing the within-cluster sum of squares. This objective is described as,

$$\arg\min_{S} \sum_{i=1}^{k} \sum_{x \in S_i} \|x - \mu_i\|,$$

where μ_i is the centroid of S_i.

K-means was selected as the algorithm to group the data for numerous reasons. This choice was made because the concept behind the algorithm is relatively simple to understand, and it was a goal to have as much transparency integrated into the black box methods used as possible. K-means is one of the most widely employed unsupervised learning algorithms, and there is a multitude of built-in functions that were accessible and easy to adapt to the application at hand. The structure of the algorithm and the packages normally provided in prebuilt functions made it easy to interchange distance measures which was an advantage from the perspective of design flexibility. Although this choice was

debated, it was ultimately decided that having a centroid-based clustering algorithm was favorable to a density-based clustering algorithm because each piece of information (i.e., day of data) would be explicitly assigned to a cluster. To appropriately determine the closeness of the different signals, a distance measure was chosen.

Distance Measure

The Hamming distance is a measure to evaluate the difference in two binary vectors of information of the same length. Richard Hamming initially developed it in 1950.[153] Often, the Hamming distance is used in information theory to determine the difference between two strings of the same size, but it can and has been used for many other applications. The Hamming distance, h, is found using the following formula,

$$h = \sum_{i=1}^{n} \|a_i - b_i\|$$

where a and b are binary vectors of length n. Because the indicator signals could only have two values, zero and one, this was chosen as the appropriate distance measure to use for the clustering procedure.

A handful of other clustering approaches were explored before it was determined that the indicator signals and the Hamming distance should be used. Initially, the disturbance signals themselves were clustered. A few different distance measures were tested (e.g., dynamic time warping), and ultimately none of them produced results as good as using the indicator signals. The profiles were judged based on visual inspection of the disturbance profiles. It was intended to have profiles near zero at all points of the day except for the time following disturbances where they rose abruptly, roughly mimicking the shape of the glucose rate of appearance curve. The unideal nature of the profiles, generated using other distance measures and signals, results from the high dimensionality of the signals. Additionally, days with disturbance signals of similar average magnitude were being grouped using the other approaches. It was favorable for the intended application (i.e., use in an MS-MPC controller) that days, where disturbances coincided, were grouped instead of clustering days with similar average disturbance magnitudes.

Cluster Evaluation Metric

Clustering is an unsupervised learning task, meaning that the data being grouped is unlabeled. Therefore the proper classification for each datum is unknown. Additionally, the number of clusters that accurately represent the inherent classes of the data is also not known. Each person with T1D has a

different number of distinct patterns in the glycemic disturbances he or she experiences. These distinct patterns could result from many different factors that affect everyday life, such as work, sleep, school, hormones, physical activity, and eating habits. Because it was important for each individual's data correctly, a clustering metric was needed to determine the appropriate number of groups, k, for each individual.

Several metrics evaluate the intracluster and intercluster variability that are widely used and can be useful. Intracluster variability or cohesion is a measure of how different an object is from the other objects in its assigned cluster. Intercluster variability or separation represents how different an object is from other clusters. Ideally, the cohesion of clustered data would be minimized, and separation would be maximized. Metrics that evaluate clusterings, such as the silhouette score, Calinski-Harabasz index, and Davies-Bouldin, quantify the intracluster and intercluster variability of data grouped using unsupervised learning.[154–156]

The silhouette score, s, is calculated using the formula,

$$s = \frac{b - a}{\max(a, b)},$$

where a is the mean distance between some datum and all other points in the same class and b is the mean distance between a sample and all other data points in the next nearest cluster. An advantage of the silhouette score is that it is bounded between negative and positive one making it easy to interpret. A score of negative one represents poorly clustered data, and a score of one indicates that the data is clustered very densely. A score near zero indicates that there are overlapping or uninformative clusters. A disadvantage of this metric is that the silhouette score is generally higher for convex clustering than density-based clustering methods (e.g., DBSCAN). An additional disadvantage is the high computation complexity of determining the silhouette score.

The Calinski-Harabasz index can be found for a set of data, E, of size, n_E, which has been split into k clusters by determining, CH. CH is the ratio of the between and within-cluster dispersion and is defined as,

$$CH = \frac{trace(B_k)}{trace(W_k)} x \frac{n_E - k}{k - 1}$$

where $trace(B_k)$ is the trace of the between-group dispersion matrix and $trace(W_k)$ is the trace of the within-cluster dispersion matrix defined by,

$$W_k = \sum_{q=1}^{k} \sum_{x\ set\ C_q} (x - c_q)(x - c_q)^T,$$

and

$$B_k = \sum_{q=1}^{k} n_q (c_q - c_E)(c_q - c_E)^T,$$

where C_q is the set of points in a given cluster q. c_q is the center of cluster q. c_E is the center of E, and n_q is the number of points in cluster q.

Advantages of the Calinski-Harbasz index are that the score is higher, although unbounded, when the clustering is more separate and cohesive, and the metric is fast to compute. This index tends to be higher for convex clusters than for density-based clustering methods like the silhouette score. The Calinski-Harabasz index also penalizes clustering with more groups. This aspect of the metric can be advantageous or not, depending on the application.

The Davies-Bouldin index is the average similarity between a given cluster C_i and its most similar cluster, C_j. It is found using the equations,

$$DB = \frac{1}{k} \sum_{i=1}^{k} \max_{i \neq j} R_{i,j},$$

and

$$R_{i,j} = \frac{s_i + s_j}{d_{i,j}},$$

where k is the number of clusters. s_i and s_j are the average distances between the center of the respective clusters, each object in that cluster and $d_{i,j}$ is the distance between the center of clusters i and j.

The advantage of the Davis-Bouldin index is that it is relatively easy to compute. A disadvantage is that this metric can only be computed using Euclidean distance. Similar to the other metrics discussed, the Davis-Bouldin index is also lower for density-based methods. This metric also maximizes cluster cohesion, which may be appropriate for some applications, but not all.

An experiment was conducted to determine how the different metrics changed the number of clusters chosen. The data used for this experiment was collected during a six-month-long at-home clinical trial (NCT03563313).[133] The only inclusion criteria were a diagnosis of T1D, using insulin therapy for at least one year, and being over 14 years old. The 124 participants used a hybrid closed-loop automatic insulin dosing device during this time and otherwise behaved as they usually would. The demographics for this study are shown in Table 9.

Table 9 – A description of the demographics from the large dataset used collected during the Diabetes Closed-Loop Protocol 3 pivotal trial.

Characteristic	**Mean ± SD**
Age (years)	33.09 ± 16.14
Weight (kg)	76.61 ± 16.44
Height (cm)	172.42 ± 8.92
TDI (u)	45.90 ± 24.36
Baseline HbA1c (%)	7.44 ± 0.96

In this experiment, each patient from a large dataset had their data clustered into $k = 1, \dots, 10$ clusters. The number of clusters chosen for that subject was based on what value of k produced the best value. The distribution of k based on which metric was used is shown in Figure 28.

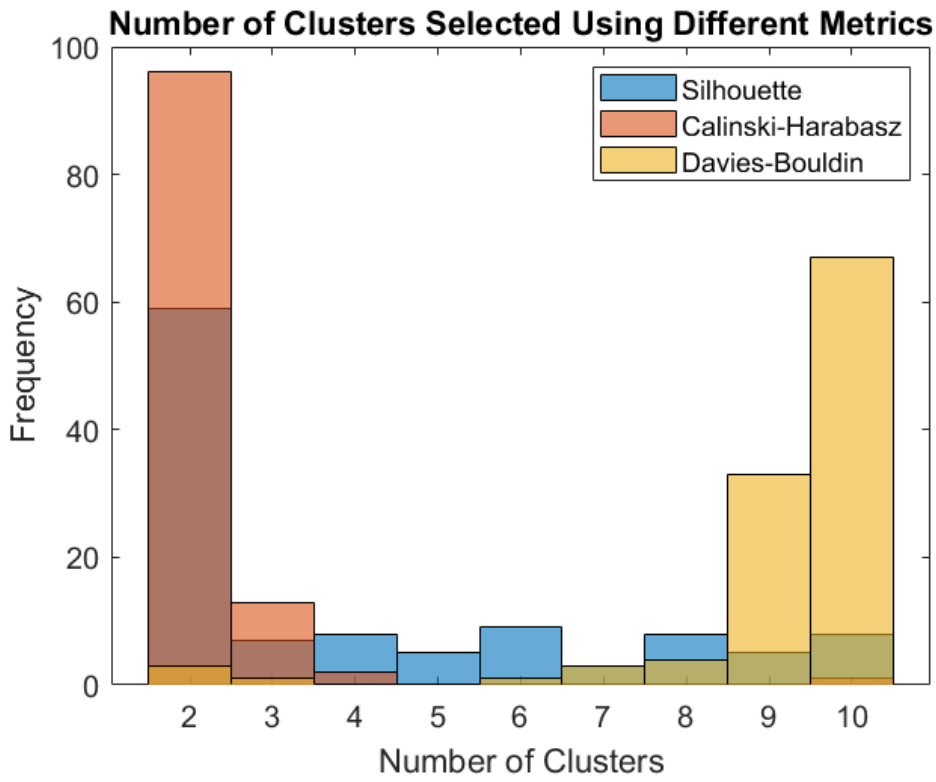

Figure 28 – The histogram of the number of clusters selected for the sample population based on the clustering metric chosen.

The metrics produced different distributions of the number of clusters selected for each subject. Because the Calinski-Harabasz index penalizes the number of clusters used to separate the data, most subject's data was split into two, three, or four groups. The Davies-Bouldin index strongly penalizes intracluster variability, and thus the subjects' data were grouped into more clusters. The silhouette score produced a more distributed selection of clusters across the subjects.

Ultimately, it was decided that the Calinski-Harbasz index was the most appropriate metric for this application. This decision was a subjective design choice but was determined by the criterion that the disturbance profiles should be easy to implement in a mobile platform. For this purpose, it was easier to have fewer clusters than more.

Postprandial Length

After deciding that the indicator signals were to be used for the clustering process, the amount of time used for the post-disturbance window was determined. Windows of one, two, and three hours were evaluated. An experiment was conducted to select the proper window length where the subjects from a large-scale clinical trial had their data reconstructed and indicator signals generated using the different window lengths for each of the days in the six-month data collection period. These signals

were then clustered, and the Calinski-Harabasz score was determined for each subjects' groupings. Higher Calinski-Harabasz scores indicate that the clustering more accurately represents the variability inherent to the dataset than lower values.

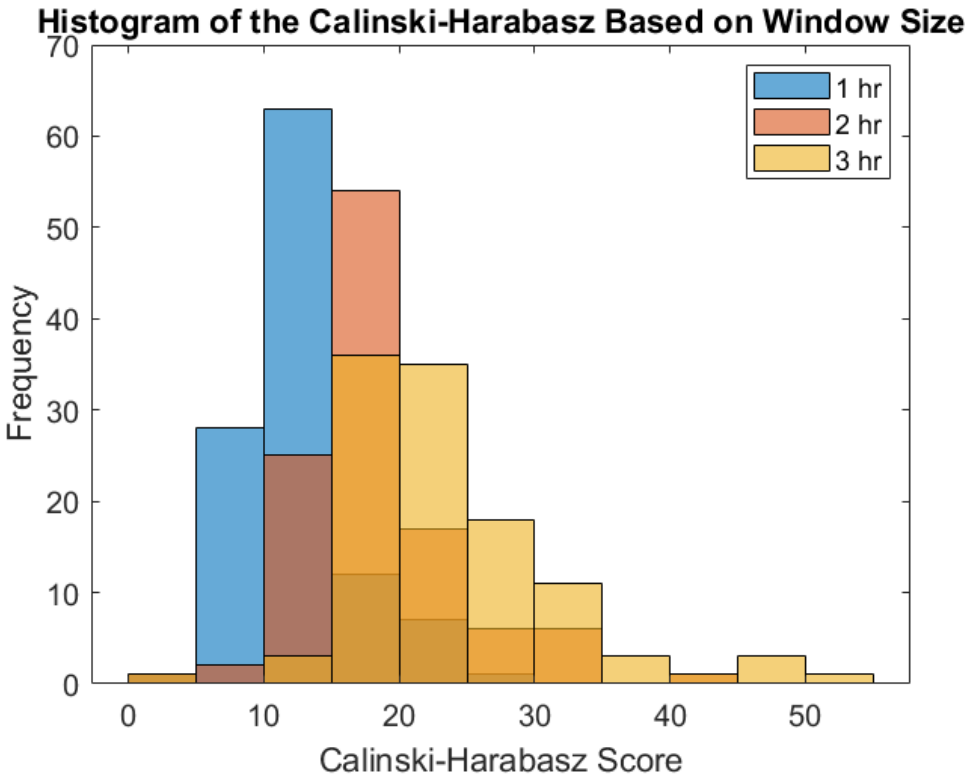

Figure 29 – The distribution of the Calinski-Harabasz scores for the dataset using the different disturbance windows.

In this distribution, it can be seen that there is a positive relationship between the length of the disturbance window and the Calinski-Harabasz scores. This is explained because if the disturbance windows are longer, there will be many more similarities between signals grouped together, even if the disturbance events happened at different times on those days. It was determined that a two-hour window would most appropriately capture the events while separating disturbances that happen at disparate times.

Generation of Disturbance Profiles

Once major glycemic disturbances were detected, daily indicator signals were defined to group similar days into clusters (equal to one in the two hours following disturbance detections and zero otherwise). Using k-means with the hamming distance measure, these signals were clustered with $k = 1, \dots, 5$.[151,153] The number of clusters, k, for each individual was based on which produced the highest Calinski-Harabasz score, maximizing cluster separation and cohesion. Once days of data were grouped,

the profile trace, ω, for each cluster, i, at each five-minute interval of the day, j, was determined from the average of each day in the cluster's disturbance signal in that five-minute interval, $d_{m,j}$.

$$\omega_{i,j} = \frac{1}{n_{days,i}} \cdot \sum_{m=1}^{n_{days,i}} d_{m,j} \; for \; i = 1, \dots, n_{clusters} \; and \; j = 1, \dots, 288$$

with $n_{days,i}$ as the number of days grouped into cluster i. These profiles were then smoothed using a centered moving average over an hour. This represented the average disturbance experienced by that individual on the days in that cluster at each point of the day. The profiles were saturated at zero so that only positive disturbances were considered.

The values were then multiplied by a weighting function shown in Figure 30 to deemphasize profiles overnight, allowing for the profile probabilities to return to their prior value at the beginning of each day.

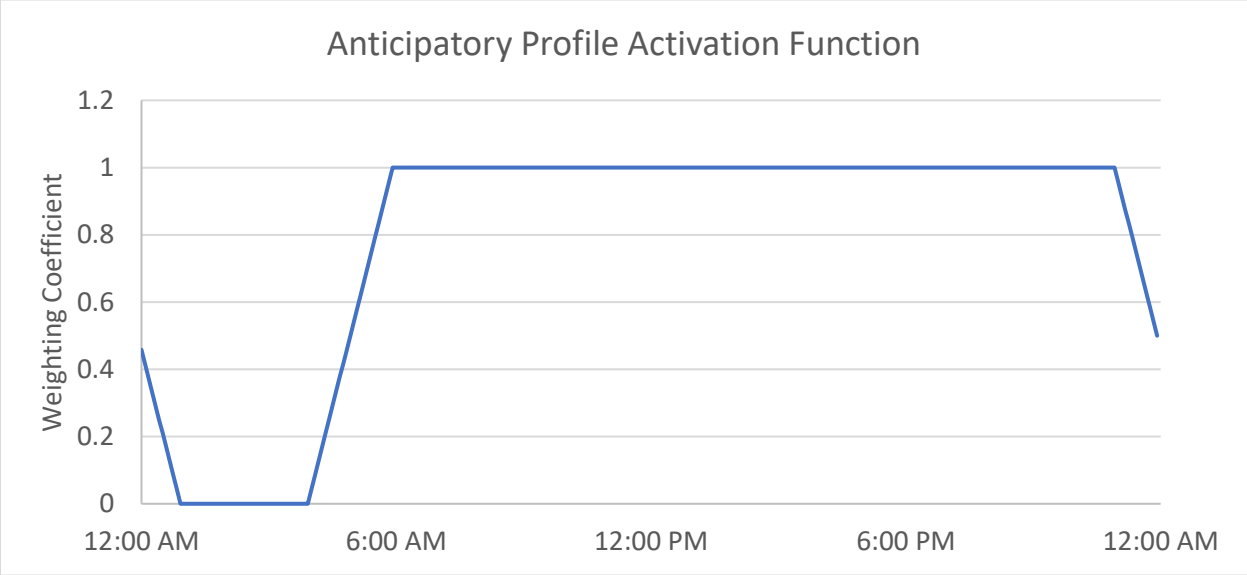

Figure 30 – The activation function for anticipatory disturbance profiles.

The prior probability of each cluster, $\pi_{prior,i}$, was found by taking the proportion of days of data that were assigned to that given cluster.

$$\pi_{prior,i} = \frac{n_{days,i}}{n_{days,total}}$$

where $n_{days,i}$ was the number of days of data in cluster i and $n_{days,total}$ represented the total number of days considered. These prior probability values serve as a starting point so that the initial weight of each profile in the MS-MPC is related to historical data.

Figure 31 shows an example of one subject's profiles. Here it can be seen that this individual's disturbance profiles are elevated following typical times for breakfast (6 a.m. to 8 a.m.), lunch (12 p.m. to 2 p.m.), and dinner (6 p.m. to 8 p.m.). The associated prior probabilities for the profiles indicate that this person eats earlier on 31% of days, and on 46% of the days of data used, the subject ate later. On 23% of days, he or she had less of a discernable pattern of eating determined from the detected disturbances.

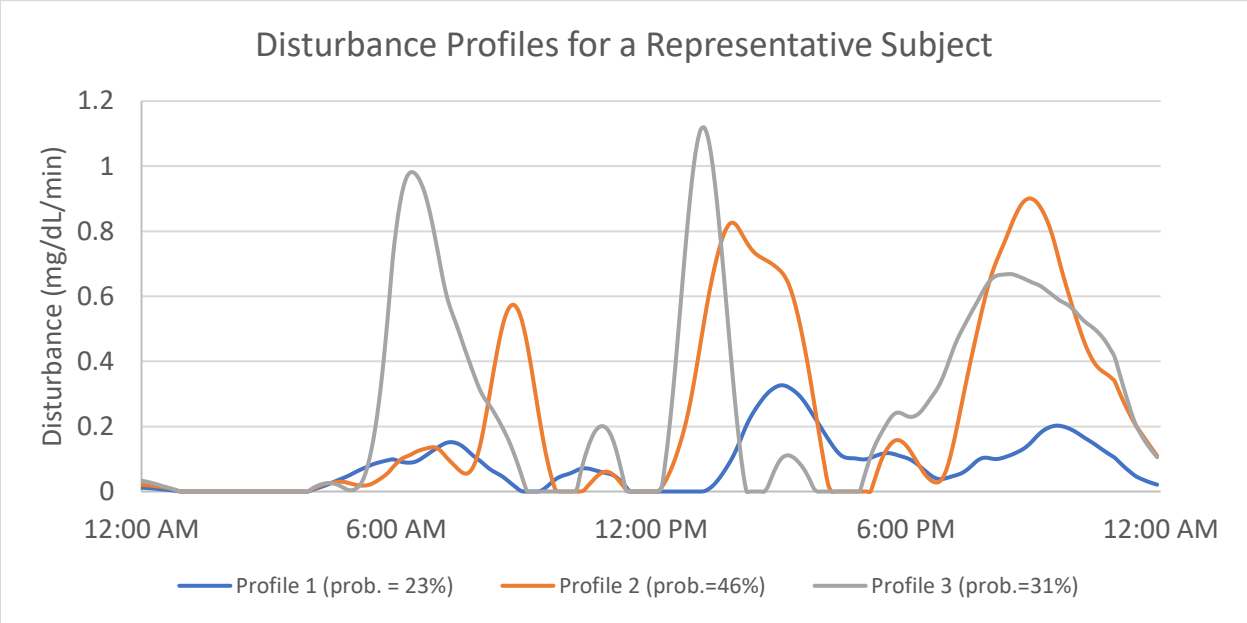

Figure 31 - A representative subject's disturbance profiles. The prior probabilities for each profile are in the legend.

Online Update of Profile Probabilities

In the MS-MPC cost function, the probability value of each profile, π_i, was updated in real-time based on the current disturbance estimate, $\hat{d}$, which was found using the same technique that was applied to the retrospective data. This probability was updated in the system using the current value for the estimated disturbance using a methodology defined by Patek.[157] This process allowed each profile's probabilities to be shifted dynamically following the disturbance currently being experienced by the user. By updating the probability of each profile based on current estimates of the disturbance being experienced by the user of the system, the weight of each model's predictions could be modulated to more accurately reflect what was currently occurring and what disturbances should be anticipated. The

online update process better allowed the controller to respond in both a reactive and anticipatory manner.

A series of calculations were computed at each five-minute interval to update the profile posterior probabilities. The matrices used to update the probability values were defined or initialized to begin the process. These matrices were,

$$A_{update} = \begin{bmatrix} 1 & 5 \\ 0 & 1 \end{bmatrix}, C_{update} = [1 \quad 0],\ G_{update} = \begin{bmatrix} 0 \\ 0 \end{bmatrix}, and\ P_{update} = \begin{bmatrix} 1000 & 0 \\ 0 & 1000 \end{bmatrix}.$$

The measurement noise, V, for the disturbance estimation was determined to be 17.3061 mg/dL/min based on the variance of the estimated disturbance signal when there are no meals in the large clinical dataset described above, and W was heuristically set to 1000. At each iteration, t, the posterior probability of each profile, π_i, was updated based on current measurements of the disturbance, $\hat{d}$, and the estimated variance. The process of updating the matrix was calculated as follows,

$$\breve{P} = A_{update} \cdot P_{update} \cdot A_{update}^T + G_{update} \cdot W \cdot G_{update}^T,$$

$$S = C_{update} \cdot \breve{P} \cdot C_{update}^T + V,$$

$$L = \breve{P}vC_{update}^T \cdot S^{-1},$$

$$P_{update} = \left(I - L \cdot C_{update}\right) \cdot \breve{P}.$$

Once these matrices were updated, the state estimations, $\hat{x}_i$, and probability values, π_i, for each profile could be computed. The state estimate, $\hat{x}_i(t)$, was found using,

$$\hat{x}_i(t) = d_{profile,i}(t) + L \cdot \left(\hat{d}(t) - C \cdot d_{profile,i}(t)\right),$$

where $d_{profile,i}$ was the value of profile, i, at the current five-minute interval of the day, t. Then the measurement estimate for the current profile, $\hat{y}_i(t)$, was calculated as,

$$\hat{y}_i(t) = C \cdot \hat{x}_i(t).$$

The estimated SD for a given profile, σ_i, was then determined using,

$$\sigma_i(t) = \sqrt{C \cdot \breve{P} \cdot C^T + V}.$$

The posterior probability value of each profile, $\pi_i(t)$, was then found using an application of Bayes' Rule.

$$\pi_i(t) = \frac{N(\hat{d}(t); \hat{y}_i(t), \sigma_i(t))\pi_i(t-1)}{\sum_{a=1}^{n_{profiles}} N(\hat{d}(t); \hat{y}_a(t), \sigma_a(t))\pi_a(t-1)}$$

where $N(\hat{d}(t); \hat{y}_i(t), \sigma_i(t))$ was the conditional density of the current estimate, $\hat{y}_i$.

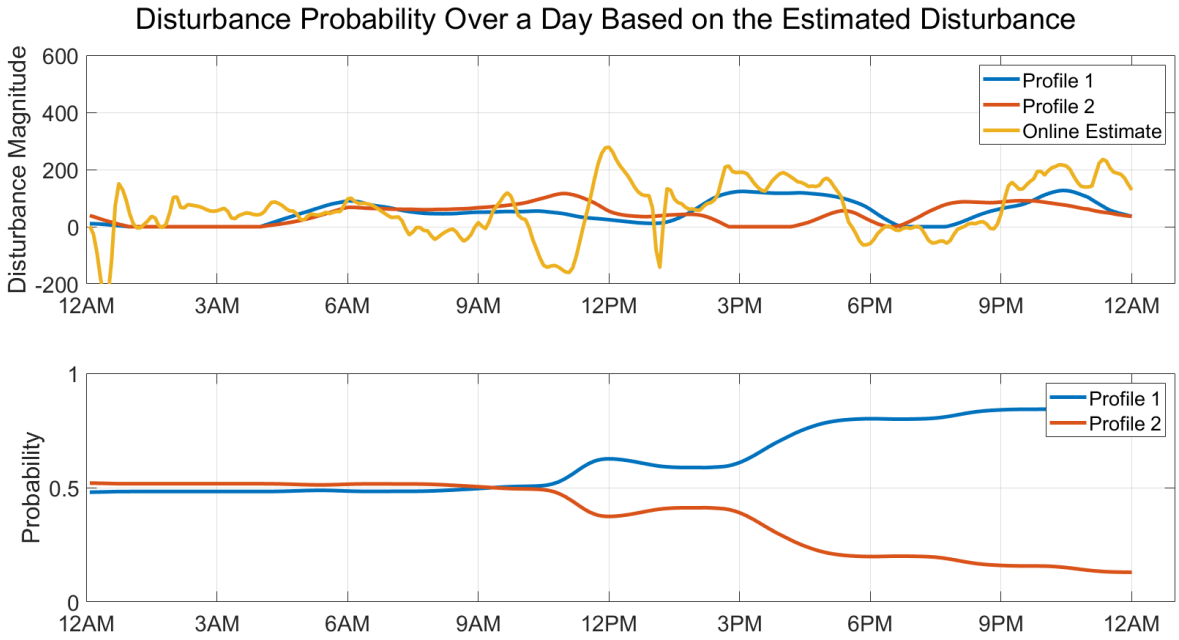

Figure 32 – An example of how the posterior probability values changed for a single day. The top subplot shows the estimated disturbance in yellow compared to the disturbance profiles in orange and blue. The bottom subplot shows the posterior probability of each profile in the respective colors.

Figure 32 shows an example of how the posterior probability values for the profiles changed over the course of a representative day. In the top subplot, the yellow trace represents a series of disturbance estimates that would be determined online in actual use. The orange and blue traces are the values of the disturbance profiles for this particular subject. The bottom subplot shows the posterior probability values of each profile. The posterior probabilities for each are shown in the same color as the profiles above.

In this example, it can be seen that overnight the profile probabilities remain at their prior value because each profile has the same value, zero. The probability of the blue profile begins to supplant the orange profile's probability value around mid-morning. Then as the day goes on and the estimated disturbance begins to match the blue profile more closely, the probability for the blue profile increases.

This example was created by clustering the indicator signals for a subject and then picking a day's disturbance signal at random. Because this was done after the profiles were generated, it was known what profile this particular day should have been associated with. In this case, the correct profile was the blue profile, which ultimately has a higher probability. The average probability value for the blue profile during this day was 62.5%.

Overnight Probability Adjustment

An overnight mode for the online estimation of the disturbance profile probabilities reset the posterior probability back to the prior value. The purpose of overnight mode was to adjust the posterior probabilities of the profiles based on the disturbance estimates collected only during the current day and were not influenced by previous estimates. From 11 p.m. to 1 a.m., the probabilities devolved linearly from the value before the beginning of night mode, π_{night}, to the prior. A line equation was calculated from the current probability to the prior for each of the profiles over the subsequent 24 intervals (i.e., two hours).

$$l_{d,i}(n) = \frac{\pi_{prior,i} - \pi_{night}}{24} \cdot n + \pi_{night} \; for \; n = 1, \dots, 24$$

For the, n, intervals after the beginning of night mode,

$$\pi_i(t) = l_{d,i}(n).$$

This adjustment forced the posterior probabilities of each profile, π_i, to return to the prior value, $\pi_{prior,p}$, two hours after the beginning of overnight mode.

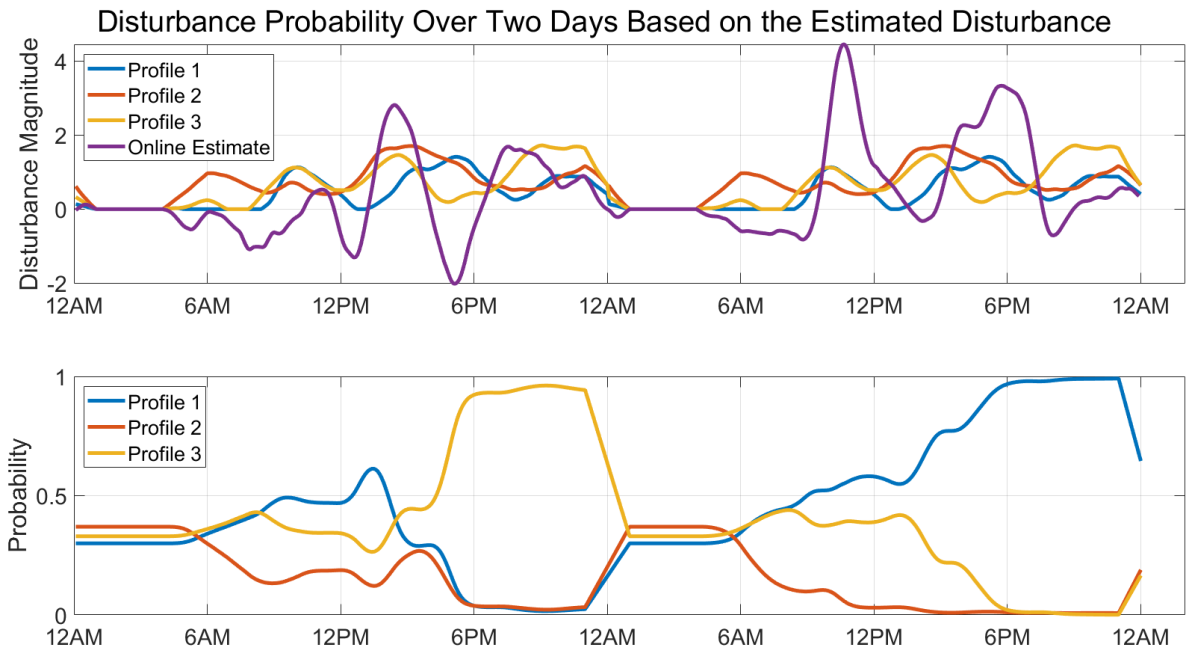

Figure 33 - An example of how the overnight mode resets the profile probabilities back to their prior value. The top subplot shows the disturbance estimate in purple and the profiles in orange, yellow, and blue. The bottom subplot shows the profile posterior probabilities in the respective colors.

Figure 33 shows an example of how the overnight mode works. In this figure, the top subplot shows the disturbance profiles in orange, yellow, and blue and the estimated disturbance in purple over two days. The bottom subplot shows the posterior probability values for the profiles in the respective colors.

Here it can be seen that between 11 p.m. and 1 a.m., each of the profiles' probability values goes from what it was to the prior value of each. This allows for the posterior probabilities to reset overnight instead of changing based on information that may not be relevant for the current day. In this example, the disturbance signal was rightfully assigned to the yellow cluster in the first 24 hours and then to the blue profile in the second 24 hours.

Controller Tuning and Detuning

It was important for the design of the control system that the disturbance currently being experienced by the user was prioritized over the anticipatory profiles. The controller tuning and detuning procedure is fully described in Corbett et al.[138] The goal of this framework was to anticipate future perturbations and respond to what is occurring in the present. All the profile probabilities were

scaled using the probability of the current disturbance estimate, ρ_0 to allow for the control system to react to disturbances in real-time. This value was calculated by,

$$\gamma_1 = \frac{\ln 81}{dh_{max} - dh_{min}}, \quad \gamma_2 = \frac{\ln 81}{\pi_{max} - \pi_{min}},$$

$$a_1 = \frac{1}{8}\left(e^{-\gamma_1 \cdot dh_{min}} - 9e^{-\gamma_1 \cdot dh_{max}}\right),$$

$$a_2 = \frac{1}{8}\left(e^{-\gamma_2 \cdot \pi_{min}} - 9e^{-\gamma_2 \cdot \pi_{max}}\right),$$

$$\rho_0(\mathrm{t}) = \min\left(\frac{a_1}{a_1 + e^{-\gamma_1 \cdot \widehat{d}(t)}} + \frac{a_2}{a_2 + e^{-\gamma_2 \cdot \pi_{disturbance}(t)}}, 0.99\right),$$

where,

$$[dh_{min}, dh_{max}] \subset [0, 10], [\pi_{min}, \pi_{max}] \subset [0, 10],$$

$$\gamma_1 = \frac{\log(81)}{dh_{max} - dh_{min}}, \gamma_2 = \frac{\log(81)}{\pi_{max} - \pi_{min}},$$

The adjusted probabilities, $\pi_{adjusted,i}$, were found by multiplying the profile probabilities by $1 - \rho_0$.

$$\pi_{adjusted,i}(t) = \pi_i(t) \cdot (1 - \rho_0(\mathrm{t}))$$

Simulation Experiment

Both the BPS described in Aim Two and the disturbance profiles representing patterns in behavior were designed to be implemented in a fully closed-loop automatic insulin dosing system using an MS-MPC framework. An experiment was designed using both actual data and the UVA/Padova T1D simulator to determine the effect of each separately and in combination with one another. The design of this experiment and its results are described in the following sections.

Experimental Setup

Data

Data collected during the unsupervised at-home portion of a large-scale pivotal trial conducted at UVA (NCT03563313) was used to evaluate this method.[133] This data is from 124 adult and adolescent participants with T1D over six months, during which they used a hybrid closed-loop automatic insulin

dosing system with meal announcements. 100 clinical subjects' data were randomly selected and paired to an in silico subject in the UVA/Padova T1D simulator platform. The first five months of the collected data from the real subjects were used to create meal profile clusters. These profiles were multiplied by five to evoke a noticeable difference between treatments. Seven days with at least one recorded meal were randomly selected from the remaining month of collected data. This week of meal records was scaled by the body weight of a matched subject in the simulation cohort and then used as the meal protocol of the simulation experiment. The simulation setup included intraday insulin sensitivity variability and the real eating records allowed for more realistic behaviors in the simulation which represented actual patterns of eating behavior.

Control Strategy

This experimental configuration was then tested with the four configurations of the control system: MPC, MS-MPC, MPC+BPS, MS-MPC+BPS. The modular control strategy is depicted in Figure 34 below. These four configurations included different elements of what was described in the previous sections related to the BPS and the MS-MPC using the disturbance profiles. The MPC used was a standard well-tuned controller. This controller setup also included modules native to the University of Virginia mobile platform used for clinical trials, DiAs. These modules included a safety system, an autocorrection system, and a state estimation system.

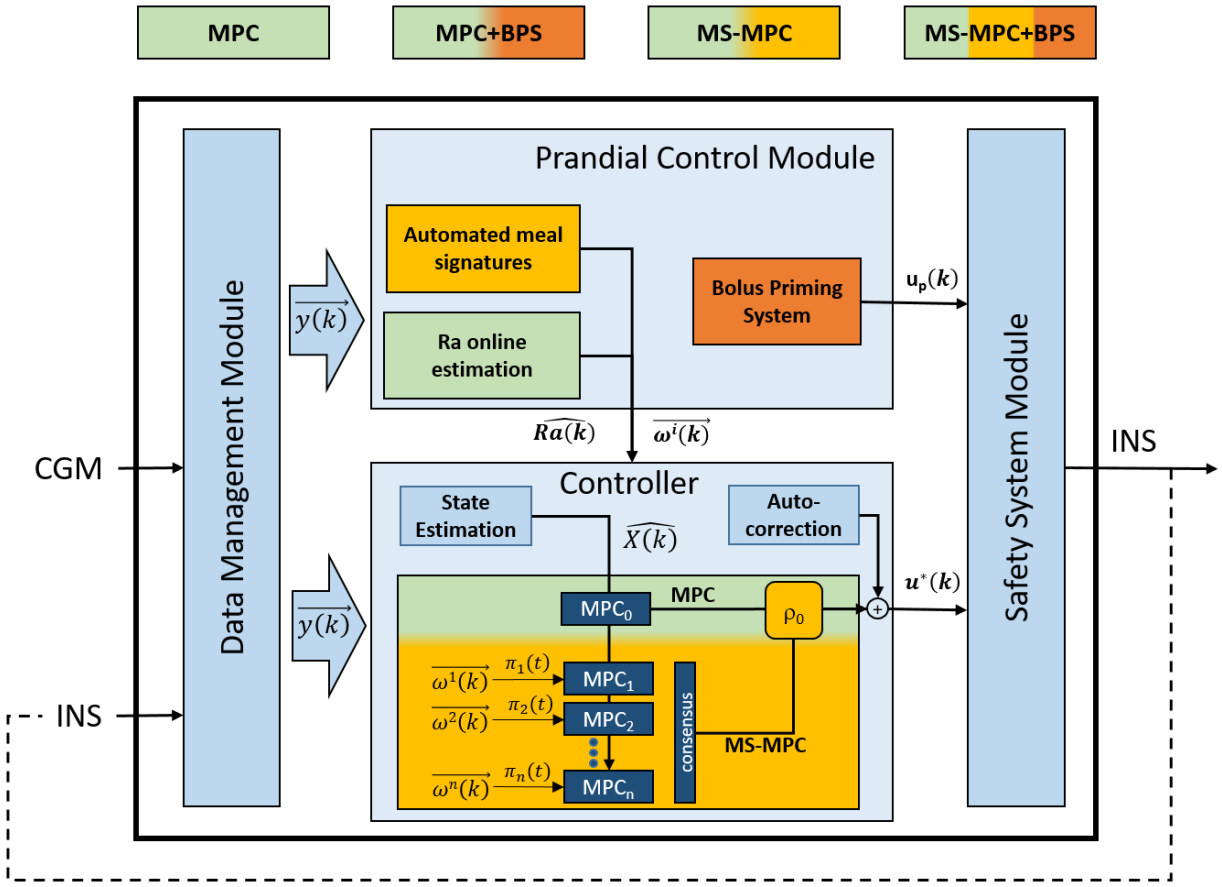

Figure 34 – A schematic of the control strategies tested which are the meal naive approach (MPC in green) to the meal anticipating with priming boluses (MS-MPC+BPS in a combination of green, yellow, and orange). BG readings are shown as $y(k)$, disturbance profile values as ω^n, profile posterior probabilities as π_n, online disturbance estimate as $\widehat{R_a}$, and u as the commanded insulin injections.

Treatment Comparison

Treatments were compared overall and during the four hours after meals using the relevant metrics described by Maahs et al.'s criteria for evaluating automatic insulin dosing systems.[158] Statistical significance was not reported because the assumptions of such tests are not particularly informative in a simulation environment.[159] The simulation experiment results suggest that using the anticipatory profiles in the MS-MPC and the BPS reduced BG values overall.

On average, when delivered, the BPS boluses were 27.64 ± 29.70 minutes after the actual mealtime. 4% of the patients' TDI was delivered after 64.11% of meals, 7% was delivered after 36.72%, and 10% was delivered after 22.18%. The timing of BPS doses was similar in this experiment to when it was evaluated in the clinical experiment, with boluses being delivered on average approximately 30 minutes after the meal began. Unlike the clinical experiment, roughly 35% of meals did not have an

automatic bolus in the two hours afterward. This may be attributed to the dynamics of the simulator and how the in silico subjects responded to unannounced ingested carbohydrates.

The primary outcome, the time when BG was between 70 to 180 mg/dL (i.e., time in range) over the course of the whole experiment, improved from 72 ± 17.7% with MPC only to 73.4 ± 17.4% with anticipation and 75.5 ± 17.1% with the BPS. The maximum effect was seen with the combination of priming bolus and anticipation with time in range reaching 77.2 ± 16.7%, or 5.2% greater than MPC alone (see Figure 35).

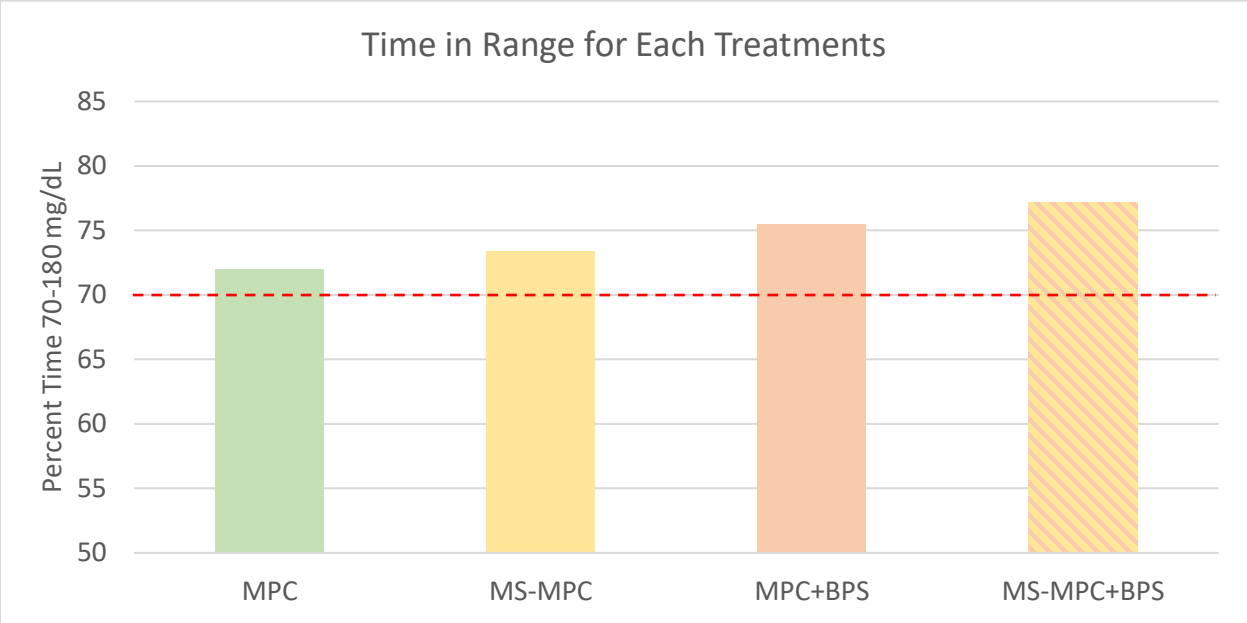

Figure 35 – The time in range values for each prandial control module: While MPC achieves time in range above the consensus target (i.e., 70%) shown with the red dashed line, the disturbance patterns, in yellow, and the BPS, in orange, both improve glycemic control, the effect is further improved when combined which is shown in striped yellow and orange.

The mean BG for the MS-MPC+BPS was the lowest (155.14 ± 31.88 mg/dL). The other controller configurations had higher mean BG values of 165.49 ± 33.49, 161.61 ± 33.60, and 159.65 ± 33.20 mg/dL for the MPC, MS-MPC, and MPC+BPS, respectively. This trend in lower BG values was represented similarly in the time below ranges (i.e., <50, <60, and <70 mg/dL), time in tight range (i.e., 70 to 140 mg/dL), and time above ranges (i.e., >180, >250, and >300 mg/dL). The BPS and anticipatory profiles also reduced the SD of BG values and caused the system to deliver more insulin overall. The overall results of the experiment are listed in Table 10.

Table 10 – The artificial pancreas evaluation metric mean ± standard deviation values from simulation experiments overall.

Controller	MPC	MS-MPC	MPC+BPS	MS-MPC+BPS
<50 mg/dL (%)	0.03 ± 0.21	0.07 ± 0.40	0.02 ± 0.15	0.14 ± 0.54
<60 mg/dL (%)	0.06 ± 0.41	0.23 ± 0.85	0.10 ± 0.45	0.33 ± 1.01
<70 mg/dL (%)	0.14 ± 0.64	0.47 ± 1.37	0.24 ± 0.81	0.65 ± 1.58
70-140 mg/dL (%)	49.16 ± 17.94	50.35 ± 19.25	51.92 ± 17.61	53.81 ± 18.89
70-180 mg/dL (%)	72.02 ± 17.67	73.37 ± 17.38	75.50 ± 17.07	77.17 ± 16.73
>180 mg/dL (%)	27.85 ± 17.47	26.16 ± 17.25	24.27 ± 16.84	22.18 ±16.45
>250 mg/dL (%)	9.92 ± 11.51	9.31 ± 11.25	7.66 ± 10.71	7.02 ± 10.28
>300 mg/dL (%)	4.81 ± 8.29	4.52 ± 8.03	3.74 ± 7.86	3.43 ± 7.36
Mean (mg/dL)	165.49 ± 33.49	161.61 ± 33.60	159.65 ± 33.20	155.14 ± 31.88
Standard Deviation (mg/dL)	53.90 ± 33.49	53.62 ± 32.72	49.51 ± 34.32	48.91 ± 32.82
CV (%)	30.46 ± 12.09	31.12 ± 11.89	28.85 ± 12.01	29.44 ± 11.88
Total Daily insulin (u)	36.72 ± 17.33	37.65 ± 17.57	38.09 ± 18.04	39.20 ± 18.34

In the four hours following meals, the effect of the anticipatory profiles and BPS was more evident. During this period, the time in range was 60.73 ± 25.39% for the MS-MPC+BPS. The mean time between 70 to 180 mg/dL was 3.78%, 5.9%, and 8.94% less for the MPC+BPS, MS-MPC, and MPC configurations. Postprandial mean BG was also 4.51 to 10.35 mg/dL lower for the MS-MPC+BPS than for the other controller setups. The amount of time where BG was less than 70 mg/dL for all of the controller setups was less than 1% during this timeframe. Table 11 lists the results during the postprandial period.

Table 11 – The artificial pancreas evaluation metric means and standard deviation values from simulation experiments during the four hours after meals.

Controller	MPC	MS-MPC	MPC+BPS	MS-MPC+BPS
<50 mg/dL (%)	0.00 ± 0.02	0.00 ± 0.02	0.00 ± 0.01	0.03 ± 0.15
<60 mg/dL (%)	0.01 ± 0.08	0.03 ± 0.16	0.01 ± 0.06	0.08 ± 0.33
<70 mg/dL (%)	0.03 ± 0.17	0.08 ± 0.33	0.06 ± 0.32	0.17 ± 0.53
70-140 mg/dL (%)	23.02 ± 18.78	27.79 ± 22.09	25.67 ± 18.92	31.24 ± 22.28
70-180 mg/dL (%)	51.79 ± 26.12	54.83 ± 26.00	56.95 ± 25.83	60.73 ± 25.39
>180 mg/dL (%)	48.18 ± 26.09	45.09 ± 25.96	42.99 ± 25.81	39.10 ± 25.32
>250 mg/dL (%)	17.87 ± 19.85	16.61 ± 19.28	13.77 ± 18.46	12.46 ± 17.91
>300 mg/dL (%)	8.68 ± 14.73	8.13 ± 14.34	6.69 ± 13.77	6.19 ± 13.16
Mean (mg/dL)	197.20 ± 54.44	191.11 ± 54.17	188.59 ± 54.36	181.72 ± 52.27
Standard Deviation (mg/dL)	53.87 ± 30.73	54.59 ± 30.37	49.67 ± 32.03	50.00 ± 30.96
CV (%)	25.69 ± 9.09	26.97 ± 8.95	24.61 ± 8.96	25.83 ± 8.76
Insulin Delivered (u)	3.52 ± 1.92	3.61 ± 1.98	3.67 ± 2.07	3.79 ± 2.13

Discussion

This simulation, which encompasses realistic eating behaviors in T1D, indicates that mean BG values were lowest for the MS-MPC+BPS, followed by the MPC+BPS, the MS-MPC, and the MPC overall and after eating. This relationship was maintained in terms of the percent time where BG was in the euglycemic ranges (i.e., 70 to 140 mg/dL and 70 to 180 mg/dL) and the hypoglycemic ranges (i.e., <50, <60, and <70 mg/dL). It was reversed in the amount of time where BG was in the hyperglycemic ranges (i.e., >180, >250, and >300 mg/dL). This relationship shows that both the anticipatory profiles and the BPS had the effect of lowering BG values over the course of the study. Overall, the MPC+BPS had a 5.84 mg/dL lower mean BG and a percent time where BG was between 70 and 180 mg/dL that was 3.38% higher than the MPC. The MS-MPC case resulted in a 1.35% greater amount of time where BG was between 70 and 180 mg/dL compared to the MPC, where no disturbance profiles were used. The MPC+BPS and MS-MPC+BPS cases had a difference of 1.67% in the amount of time where BG was 70 to 180 mg/dL. This difference indicates a synergetic interaction between BPS and the anticipatory disturbance profiles.

Across the four configurations, there was no meaningful change in the amount of hypoglycemia overall. Comparing the MPC and MS-MPC+BPS shows that the modules may be responsible for increasing the time when the user was in the hypoglycemic range by less than ten minutes while increasing the time in euglycemia by 5% overall, which is clinically relevant.

The most insulin was used when both the BPS and profiles were active (i.e., MS-MPC+BPS). This amount was less when only BPS was used (i.e., MPC+BPS), then even less when just the profiles were used (i.e., MS-MPC), and the least when the standard MPC. Interestingly, the MS-MPC case had the highest average CV, followed by MPC, MS-MPC+BPS, and MPC+BPS.

The postprandial time when BG was between 70 to 180 mg/dL was increased by nearly 10% when the anticipatory profiles and BPS were used compared to the standard MPC. Additionally, there was an increase in the 70 to 140 mg/dL range, but this amount was slightly smaller. This difference resulted from a reduction in the amount of time in hyperglycemia (i.e., >180 mg/dL) and a reduction in the mean BG of roughly 16 mg/dL. Combining the MS-MPC structure and BPS had its greatest effect during the postprandial period by lowering BG values without increasing hypoglycemia.

A limitation of this work is that this is a simulation study and does not include some variability inherent in free-living conditions (e.g., stress, hormonal changes). An additional and significant limitation is that there was no physical activity which could cause both a risk for hypoglycemia and hyperglycemia in the simulation. Because the system does not know future actions like a person might, physical activity could be dangerous if increased automatic insulin delivery preceded it. This issue should be addressed in future versions by incorporating our past methodologies that consider inputs related to negative disturbances in the prediction model. Other improvements could involve using activity sensors to detect eating and exercise events. Model personalization could also improve the generation of the disturbance estimation procedure.

This experiment showed that in a simulation environment, both the BPS and the disturbance profiles positively impacted the amount of time that BG values are in the euglycemic range while also decreasing hyperglycemia. The modules were the most impactful during the four hours following eating. Both modules improved the amount of time when BG was in the euglycemic range and did even better in combination. The reduction in mean BG values attributed to the BPS and disturbances profiles increased hypoglycemia, but only to a degree that is not clinically meaningful. The BPS and disturbance profiles seem to impact the variability of glucose, although the cause of this is unclear. Future work

should determine how this system is impacted by situations that may create risk for hypoglycemia and hyperglycemia.

Determining the Signature Factor

Once it was decided that the disturbance profiles combined with the BPS and MS-MPC control system effectively lowered BG values overall and especially following meals, another design consideration had to be determined. The magnitude of the profiles was primarily a result of the filtering procedure and how the clusters were formed and was not wholly representative of the values in the daily disturbance signatures.

The magnitude of the disturbances was largely dampened by the filtering and averaging. The filtering lowered the magnitude by eliminating all of the increases or decreases related to low-frequency changes in the disturbance. Figure 36 shows an example of the disturbance profiles for a representative subject generated using the unfiltered disturbance signatures, shown in the top plot, and the filtered signatures are shown in the bottom subplot.

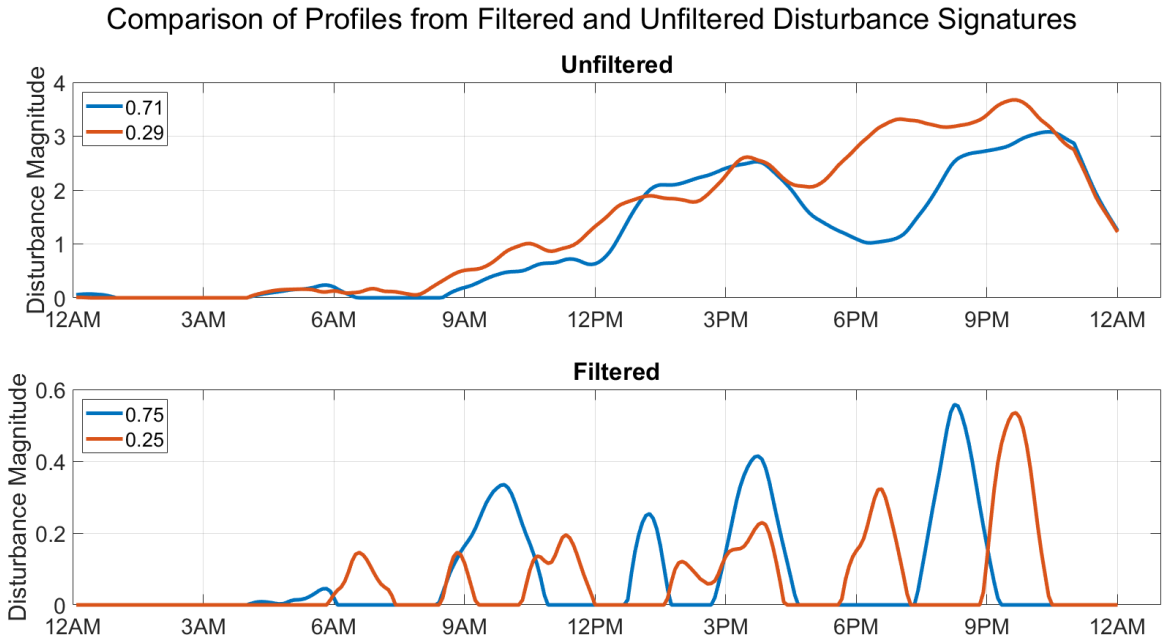

Figure 36 - A comparison between the profiles generated with the unfiltered and filtered disturbance signals.

It can be seen that in this example, the unfiltered signatures produce profiles that have a magnitude that is at the peaks four times greater than the profiles made with the filtered signals. Additionally, there is a slow increase of the profile values over the course of the day when the profiles

were generated using the unfiltered signals. The disturbance profiles created with the filtered signals have no noticeable increase over the course of the day and have much more distinct peaks that are roughly at the same time as less distinct bumps in the unfiltered profiles. The process of finding the profile trace also decreased the value of the signals in comparison to what the estimates would be because the average was found across the value of each day's signals in the cluster.

Because the signature magnitude was a concern, it was decided that the profiles should be modified by multiplying them by a factor to produce signatures that were of a similar value to the daily disturbance estimate signatures. To determine the "signature factor," the experiment described in the previous section was repeated, this time with the profiles multiplied by a factor. Once the new profiles were generated, the week of simulation data from the original experiment was evaluated using the MS-MPC+BPS setup. Table 12 shows the results for the experiment using signature factors of one, three, five, ten, and twenty on the profiles generated using the filtered disturbance signals. Table 13 shows the results for the profiles generated using the unfiltered signals multiplied by one, three, and five. All of the results for time in range are presented as a percent. Mean, SD, coefficient of variation (CV) are in mg/dL, and TDI is in units.

Table 12 - The artificial pancreas evaluation metric mean ± standard deviation values from simulation experiments redone with different signature factors applied to the filtered signals overall.

Factor	**1**	**3**	**5**	**10**	**20**
<50	0.04 ± 0.23	0.05 ± 0.23	0.06 ± 0.25	0.14 ± 0.46	0.3 ± 0.92
<60	0.12 ± 0.44	0.13 ± 0.45	0.16 ± 0.5	0.31 ± 0.8	0.62 ± 0.62
<70	0.25 ± 0.74	0.27 ± 0.76	0.33 ± 0.89	0.65 ± 1.42	1.24 ± 2.14
70-140	49.13 ± 15.52	50.31 ± 15.88	51.37 ± 16.06	53.1 ± 16.54	55.26 ± 55.26
70-180	76.28 ± 15.75	76.88 ± 15.69	77.36 ± 15.66	78.04 ± 15.72	78.63 ± 15.84
>180	23.47 ± 15.4	22.86 ± 15.31	22.31 ± 15.22	21.31 ± 15.12	20.13 ± 14.99
>250	6.97 ± 9.78	6.85 ± 9.7	6.73 ± 9.62	6.47 ± 9.39	6.17 ± 9.21
>300	3.19 ± 6.94	3.17 ± 6.88	3.11 ± 6.83	3 ± 6.67	2.9 ± 6.56
Mean	159.79 ± 27.13	158.59 ± 27.02	157.41 ± 26.96	154.97 ± 26.85	151.69 ± 26.94
SD	46.65 ± 31.24	46.6 ± 31.28	46.59 ± 31.26	46.73 ± 31.09	47.23 ± 30.32
CV	27.4 ± 12.12	27.56 ± 12.19	27.77 ± 12.25	28.32 ± 12.33	29.32 ± 12.23
TDI	37.47 ± 18.05	37.84 ± 18.17	38.19 ± 18.28	38.91 ± 18.52	39.92 ± 18.86

Table 13 - The artificial pancreas evaluation metric mean ± standard deviation values from simulation experiments redone with different signature factors applied to the unfiltered signals overall.

Factor	**1**	**3**	**5**
<50	0.1 ± 0.41	0.55 ± 1.48	0.89 ± 2
<60	0.22 ± 0.22	1.05 ± 1.05	1.68 ± 1.68
<70	0.45 ± 1.18	1.84 ± 2.97	2.85 ± 3.61
70-140	53.36 ± 53.36	56.99 ± 56.99	57.98 ± 57.98
70-180	78.07 ± 15.73	79.02 ± 15.72	78.93 ± 15.53
>180	21.48 ± 15.21	19.14 ± 14.94	18.21 ± 14.81
>250	6.42 ± 9.47	5.81 ± 9	5.61 ± 8.93
>300	3.02 ± 6.67	2.77 ± 6.36	2.71 ± 6.38
Mean	154.95 ± 27.15	148.23 ± 27.87	145.13 ± 28.65
SD	46.64 ± 30.88	47.66 ± 29.82	48.57 ± 29.83
CV	28.25 ± 12.14	30.35 ± 11.84	31.64 ± 11.7
TDI	38.84 ± 18.41	40.88 ± 19.05	41.93 ± 19.31

As the signature factor increased, there was an increase in insulin injected, variability in terms of SD and CV, the amount of percent time spent in range (i.e., 70 to 140 mg/dL and 70 to 180 mg/dL), and the percent time where the participants were hypoglycemic (i.e., <50, <60, and <70 mg/dL) for both the filtered and unfiltered profiles, overall. The amount of hypoglycemia that occurred was of primary concern. A signature factor of twenty for the filtered profiles resulted in a smaller amount of time where BG was less than 70 mg/dL than a factor of five for the unfiltered profiles, which was used in the original experiment. For the unfiltered profiles, it seems that a factor of three produced the best results in terms of the tradeoff between time in euglycemia and time in hypoglycemia.

Table 14 - The artificial pancreas evaluation metric means and standard deviation values from simulation experiments redone with different signature factors applied to the filtered signals during the four hours after meals.

Factor	**1**	**3**	**5**	**10**	**20**
<50	0 ± 0.03	0 ± 0.03	0.01 ± 0.05	0.02 ± 0.08	0.05 ± 0.2
<60	0.01 ± 0.01	0.02 ± 0.02	0.02 ± 0.02	0.05 ± 0.05	0.15 ± 0.15
<70	0.05 ± 0.24	0.06 ± 0.24	0.07 ± 0.27	0.16 ± 0.49	0.42 ± 0.93
70-140	22.72 ± 22.72	24.25 ± 24.25	25.76 ± 25.76	28.43 ± 28.43	32.04 ± 32.04
70-180	57.12 ± 24.43	58.29 ± 24.36	59.32 ± 24.28	61.24 ± 24.08	63.29 ± 24.07
>180	42.83 ± 24.39	41.66 ± 24.32	40.61 ± 24.24	38.6 ± 23.99	36.29 ± 23.95
>250	12.66 ± 17.18	12.43 ± 17.08	12.18 ± 16.96	11.69 ± 16.56	11.13 ± 16.29
>300	5.88 ± 12.66	5.84 ± 12.58	5.72 ± 12.5	5.55 ± 12.25	5.37 ± 12.12
Mean	187.62 ± 46.45	186.05 ± 46.34	184.5 ± 46.28	181.42 ± 45.94	177.53 ± 45.85
SD	47.27 ± 29.29	47.4 ± 29.47	47.55 ± 29.49	47.98 ± 29.64	48.61 ± 28.73
CV	23.63 ± 8.92	23.89 ± 8.96	24.17 ± 9	24.82 ± 9.09	25.82 ± 9.02
TDI	3.55 ± 2.01	3.61 ± 2.03	3.66 ± 2.05	3.77 ± 2.09	3.91 ± 2.17

Table 15 - The artificial pancreas evaluation metric means and standard deviation values from simulation experiments redone with different signature factors applied to the unfiltered signals during the four hours after meals.

Factor	1	3	5
<50	0.02 ± 0.1	0.13 ± 0.51	0.26 ± 0.79
<60	0.04 ± 0.04	0.33 ± 0.33	0.7 ± 0.7
<70	0.13 ± 0.45	0.77 ± 1.64	1.34 ± 2.22
70-140	28.89 ± 28.89	35.35 ± 35.35	37.39 ± 37.39
70-180	60.91 ± 24.15	64.97 ± 23.73	66.22 ± 23.35
>180	38.96 ± 24.05	34.27 ± 23.71	32.44 ± 23.51
>250	11.6 ± 16.78	10.47 ± 16.08	10.08 ± 15.85
>300	5.58 ± 12.29	5.11 ± 11.72	4.99 ± 11.69
Mean	181.32 ± 46.36	173.1 ± 46.89	169.62 ± 47.92
SD	47.82 ± 29.27	49.14 ± 28.35	50.14 ± 28.45
CV	24.76 ± 8.93	26.88 ± 8.75	28.08 ± 8.67
TDI	3.72 ± 2.07	3.94 ± 2.15	4.05 ± 2.19

Table 14 shows the results for the filtered signals during the four hours following meals. Table 15 includes the same information but for the profiles generated using the unfiltered signals. It can be seen how when the signature factor was increased, the amount of hypoglycemia, euglycemia, total insulin delivered, and glycemic variability for the filtered signals also increased. This increase resulted in a decrease in hyperglycemia. Again, when the signature factor increased beyond three for the unfiltered profiles, the amount of time in euglycemia actually decreased as the percent time where the subjects were in the hypoglycemic range increased.

Comparing the two profiling techniques indicates that the profiles generated using the filtered signals may need to be multiplied by a factor of 10 to 20 to produce an acceptable level of glycemic control in terms of the tradeoff between hypoglycemia, euglycemia, and hyperglycemia. The unfiltered signatures produced an amount of euglycemia (roughly 79%) overall and during the postprandial window (approximately 65%), which is excellent considering that there were no mealtime insulin doses. It is apparent that the filtering process is necessary to eliminate the tendency for some subjects to have profiles that increased steadily throughout the day. The filtered disturbance profiles had much better

characteristics regarding how they were close to zero for most of the day and peaked rapidly following disturbance events. This attribute is ideal from a control perspective because it allows the control system to be informed by the disturbances in a way similar to how glucose appears in plasma after eating.

Conclusion

Summary of Findings

The primary goal of this dissertation research was to reconstruct a historical record of disturbances and determine an appropriate way of dosing insulin to mitigate hyperglycemia without input from the user of the system with T1D. People with T1D currently spend a considerable amount of time trying to determine how to titrate insulin. The work involved in this process is both time-consuming and a physical and mental burden, which has consequences in terms of quality of life, time management, mental health, and the development of diabetes-related complications. Mitigating positive glycemic disturbances, often caused by ingested carbohydrates, is challenging due to the pharmacodynamics of insulin and how glucose appears in plasma blood. The three aims of this dissertation summarized below serve to achieve tasks that would help mitigate these disturbances and achieve better glycemic control overall for people with T1D.

Aim 1 - Real-time Disturbance Detection and Mitigation

In Aim 1, a methodology was developed to detect disturbances in real-time and deliver automatic insulin boluses based on the TDI of the individual. This approach for mitigating hyperglycemia was designed to focus on safety, specifically with an emphasis on hypoglycemia. The results of an analysis where historical data was re-simulated using the net effect showed that at each TDI amount and its paired disturbance probability threshold, no more than one hypoglycemic event was caused per day due to the automatic bolusing system.

If sufficiently effective, this automatic method of dosing insulin could potentially eliminate the need for manual mealtime insulin doses. The results of a pilot study conducted at UVA in January 2021 where this system, the BPS, was used in an MPC-based artificial pancreas demonstrated how this approach performed when real people were using it. During the study, the BPS administered automatic boluses for more than 80% of meals. Additionally, there were no automatic boluses that occurred at any point other than the two hours after a meal, and there were no hypoglycemic events caused by the BPS. The BPS boluses were delivered roughly 30 minutes on average after the beginning of the meal. The use of the BPS integrated into an MPC resulted in a time in range that was 30% higher than the state-of-the-art USS Virginia control system. Despite this increase in euglycemia compared to the legacy artificial pancreas system, there was no significant increase in the amount of hypoglycemia experienced by the

participants. Both systems had a percent time where BG was less than 70 mg/dL of less than 1%, which equates to less than 15 minutes per day.

Although not observed in the clinical trial, a weakness of the BPS is that it can be sensitive to noisy CGM measurements because of how the disturbance probability is being determined. The disturbance probability used to determine the insulin doses was found using only the last 30 minutes of CGM data. Artifacts in the CGM data could lead to errant BPS boluses when it is not necessary. This issue is a serious safety concern considering that up to 10% of the system user's TDI can be delivered through the BPS. An insulin dose of this quantity could result in severe hypoglycemia.

Future research should be conducted to determine how the process of estimating the disturbance probability could be made more robust. A particular concern is the frequency of which these artifacts occur at night due to the wearer of the CGM compressing the sensor in their sleep. This artifact causes CGM readings to be artificially lower as the sensor is compressed and then rise as the pressure is released. This effect can happen anytime but often occurs when people are asleep and lying on the CGM sensor. Because BG values go down and then abruptly rise, the BPS disturbance probability value can exceed the threshold for an insulin dose if this effect is pronounced enough. A profile could be constructed that modulates how much insulin should be given at different points in the day to address this concern. This profile could be designed so that the percentage of TDI delivered is more during the daytime when disturbances (e.g., meals) are more likely to occur, and reduced at night when acute positive disturbances are less likely.

The profiles could potentially be determined using the historical disturbance profiles that are described in Aim 3. These inferred signals would provide a good representation of when the disturbances occurred in the past and could be utilized to determine a weighting function for the amount of TDI that the BPS can deliver. At the very least, the disturbance information could provide a sense of when the person is unlikely to eat, like when they are normally asleep. Alternatively, the user could input his or her sleep schedule manually.

Aim 2 - Retrospective Glycemic Disturbance Detection

Aim 2 describes the design and performance of two glycemic disturbance detection algorithms. The first algorithm, DSS2, was designed to be used on data that includes mealtime insulin doses. These data could be collected from people who use sensor-augmented pump therapy, multiple daily injection therapy with a connected insulin pen, or hybrid closed-loop therapy. The DSS2 algorithm used features

derived from historical CGM and insulin records as well as the calculated net effect values. This logistic regression-based algorithm was trained to classify windows of time as part of a glycemic disturbance.

The second disturbance detection algorithm, RCKT+, was explicitly designed to be used for data collected from users of a fully closed-loop insulin dosing system, where mealtime insulin boluses are not present. This algorithm used features determined from past CGM data as well as information from historical daily disturbance signals. Like the first algorithm, RCKT+ was trained to determine whether or not each sampling interval was a part of positive glycemic disturbance or not.

The two algorithms were compared in terms of false positives, true positives, and the amount of time between disturbances (i.e., meals) and detections using simulation-generated and actual clinical trial data. On both the clinical and simulation data, RCKT+ outperformed DSS2 in terms of the true positive rate achieved at each respective false positive rate. When a set threshold was chosen, both algorithms had detection times within one minute of the mealtime for the simulation data. There was a negligible difference in the SD between detection times and the actual event times for this dataset. When applied to the real dataset, both algorithms detected events at an average of roughly ten minutes before the real-time and at considerably lower true positive rates. This distribution was left-skewed and indicated that the design of the features which are non-causal might cause events to be detected before when they occurred.

Another factor that may cause this effect is how each algorithm was trained. The data used to determine the logistic regression coefficients was labeled based on if a 40 mg/dL rise in glucose occurred in the two hours after that point in time. It was assumed that due to the time constants of glucose appearing in blood plasma, there would be a delay between rises in glucose and ingested carbohydrates. Additionally, the timing of detection events was based on when the maximum curvature of CGM values occurred in the period of time where the probability of the retrospective disturbance detection algorithms was above a threshold. These assumptions impacted how the start time of disturbance events was chosen and may have led to events being detected earlier than the actual time.

Both detection algorithms performed well on the simulation dataset and less so when applied to the real dataset. The decrease in performance was likely due to the increase in the sources of variability that affect glucose values in the actual dataset. During the admission where the data was collected, the participants ate frequently and exercised, which provided a challenging context for both detection algorithms. Additionally, both algorithms were trained to detect large positive glycemic disturbances

rather than meals and were evaluated on the meal record. It is likely that some if not many of the meals that were not detected had no significant rise in BG following them due to increased insulin sensitivity after exercise. The DSS2 algorithm required more features than the RCKT+ algorithm and had a worse tradeoff between false positives and true positives but served a different purpose. This algorithm was meant to be conservative in terms of false alarms and is the only one that could be applied to data collected from people undergoing multiple daily injection therapy. Conversely, the DSS2 algorithm could not be applied in its current form to fully closed-loop data where mealtime insulin boluses are not present.

Aim 3 - Determination and Implementation of Patterns of Glycemic Disturbances in a Fully Closed-Loop Insulin Dosing System

Aim 3 describes how behavioral patterns were quantified, grouped, translated into profiles representing patterns of glycemic disturbances, and implemented in a fully closed-loop automatic insulin dosing system. This process used information gleaned from historical data to anticipate large positive glycemic disturbances and mitigate hyperglycemia. The patterns were derived using data-driven methods to reflect the perturbations regularly experienced by a particular individual. Ultimately, these profiles were designed to be integrated into an automatic insulin dosing system that does not require meal announcements from the user to help minimize hyperglycemia.

The first step in generating the profiles was to recreate the historical disturbance record from passively collected data (i.e., records from downloaded CGM and insulin pumps). Disturbances were detected from the data using the RCKT+ algorithm described in Aim 2. Once the disturbance record was reconstructed, binary signals were generated for clustering. These signals were zero at all times except for the two hours following detected disturbances, where they were equal to one. The indicator signals were then clustered using k-means. Each cluster's profile trace was found using the historical disturbance signals for each day of data in the cluster. The prior probability of each profile was based on the proportion of days that were included in the cluster.

The profiles were integrated into an MS-MPC framework so that a consensus control action could be made reflecting the potential impact of each perturbation described in the profiles on BG. The posterior probability of each profile and its respective weight in the controller cost function was determined based on current estimates of the disturbance experienced by the individual. The profiles were reset back to their prior values overnight to allow each day to be treated independently.

The results of an experiment comparing different elements of the control system were also presented in Aim 3. In this experiment, five consecutive months of data collected from actual patients using a hybrid closed-loop system was used to create personalized disturbance profiles. The 100 subjects in the UVA/Padova T1D simulator cohort were paired to the real subjects' profiles. Then, seven days with recorded meals from the remaining one month of collected data were used as the meal protocol for a simulation. The meal record for the real subjects was scaled based on the body weight of their paired virtual subject. This scenario was run for each subject using four different controller configurations: MPC, MS-MPC, MPC+BPS, MS-MPC+BPS. The experiment showed that both the BPS and the anticipatory profiles integrated into the MS-MPC increased time in range, decreased hyperglycemia, and minimally increased hypoglycemia. Between the standard MPC and the MS-MPC+BPS, there was a 5.15% increase in time in the euglycemic range and a 5.67% reduction in the amount of time in hyperglycemia. This effect indicates that the anticipatory disturbance profiles combined with the BPS impacted glycemic control in a clinically meaningful way.

The experiment that was conducted demonstrated that both the BPS and the anticipatory disturbance profile lowered mean glucose and reduced hyperglycemia in a simulation environment. This effect was especially evident when both were combined in the MS-MPC+BPS setup. In the four controller setups tested, there was no meaningful increase in hypoglycemia; each only led to an amount of hypoglycemia of fewer than 15 minutes per day, and the controller that delivered the most insulin (i.e., MS-MPC) led to an increase in the time range of 5%. Although, it is unclear how protective the MS-MPC+BPC system would be towards physical activity. The effect of physical activity on the MS-MPC and BPS system components is untested because it is not currently integrated into the simulation platform.

Additional exploration is needed to verify a number of design choices made related to the disturbance profiles. How the patterns are characterized is of particular interest. The dataset used was not labeled, and therefore it is not clear when the disturbance events, often meals, occurred. Further analysis with a large dataset including verified meal data would provide insight into how effective and accurate the disturbance detection and profile generation process is. Because the process that defines the profiles is unsupervised and unlabeled, data with distinct patterns like that collected from shift workers or those with regular schedules would be informative to determine if the patterns in the disturbance signals could be differentiated from each other.

There are also questions regarding the implementation of the disturbance profiles into the MS-MPC framework that need to be explored. It is unclear if the magnitude of the signals is appropriate for

the internal models used in the controller. The signals are dampened because they are taken from the aggregate value of the disturbances experienced by the individual whom they are meant to model and filtered. Some exploration was conducted to determine the multiplicative signature factor, but more research should be done to determine the correct multiplier.

Aspects of the procedure to update the profiles' posterior probabilities were also chosen subjectively. The process and measurement noise covariance values were chosen based on experiments using data that may not represent the population as a whole. A further exploration into the values of the disturbance signal at times when the perturbation is influenced by noise and not an actual disturbance could be fruitful. In its current form, changing the profiles' posterior probabilities requires a considerable amount of information and can be slow to respond when the current disturbance signal represents one profile and then changes to match the value of another profile more closely.

Finally, more research should be conducted about how this approach would be adapted over time as behavior evolves. There is a need to allow this process to be dynamic and robust, allowing for the profiles and the respective noise-related variables to change as more information related to behavior is learned and behavior changes. The data-driven nature of the process that recognizes patterns in behavior allows it to adapt and become more tailored to the individual over time. This aspect is a strength because it creates the opportunity for the method to have a large impact on the control action being taken by the automatic insulin dosing system if there is consistent behavior and a more tentative approach if the user of the system is less consistent in his or her actions.

Discussion

Each of the components described in the aims is distinct but can work together in a meaningful and beneficial manner. The BPS described in Aim 1 could be integrated into any closed-loop system that was tuned to accommodate the priming boluses. A worry is that if a control system were too aggressive to rapidly changing BG values caused by meals where insulin was not taken proactively, actions taken by the BPS could result in hypoglycemia. This concern would have to be accounted for, but otherwise, the BPS does not rely on a specific control framework to operate safely.

The glycemic disturbance detection algorithms were designed specifically to create the disturbance profiles but could also be used for other applications. Often, meal records are incomplete and incorrect. A disturbance detection algorithm could help to augment records collected by patients for numerous purposes. One such example is model personalization. There is a growing interest in

personalized medicine, and an example of that in the field of diabetes technology is personalizing the internal insulin-glucose model used to make predictions in the artificial pancreas control system. To personalize the model, parameters need to be identified. Some of these parameters include time constants related to meals, so knowing the timing of meals and identifying postprandial glycemic excursions is critical. A disturbance detection algorithm, like the ones described, would improve this process by adding events to the meal record that were not recorded or recorded incorrectly by the patient.

An additional component of this process that would be incredibly useful is a disturbance size estimation algorithm. The algorithms provided did not include any disturbance or meal size estimation, which is a critical part of the information necessary to improve the model fitting process. For the application presented, creating disturbance profiles, it was unnecessary to place an exact value on the disturbances, but if a discrete record of events were being reconstructed, this would be. Further work on these algorithms could use the estimated disturbance signals to estimate the perturbation size in an understandable way, like through an estimate of the equivalent amount of carbohydrates.

It would be possible to create the disturbance profiles without the meal reconstruction record. The disturbance detection algorithm was used to create the indicator signals used for the clustering procedure. If a meal record were adequately complete, it would be possible to generate these signals using that account. Additionally, it may be helpful and potentially better to extract features from the disturbance signals themselves and use those to group the signatures. This approach may create a more direct way of grouping days of data where the timing and magnitude of disturbances are similar.

An interesting interplay could be leveraged between the disturbance profiles and the real-time and retrospective disturbance detection algorithms. If established patterns of glycemic disturbances were determined, this information could potentially inform the disturbance detection algorithms in a meaningful and valuable way. During periods where a disturbance was more likely, determined by the profiles, the BPS' disturbance probability threshold could be lower. At other times, when disturbances were less likely (i.e., overnight), the detection threshold could be raised. The modulation of the thresholds would make the detection of disturbances correctly more likely and reduce the risk for false alarms, especially when false alarms would be dangerous, like overnight.

The retrospective algorithms could also benefit the information engrained in the disturbance profiles, similar to how this could be used in the causal algorithm. The retrospective algorithms could be

altered to include features that characterize if a disturbance is likely or unlikely at that time based on the established patterns of behavior for that individual.

It is possible that information from the causal (i.e., real-time) and non-causal (i.e., retrospective) algorithms could be used to help improve both. Per the application of the BPS, the system delivers insulin boluses when it is necessary. Because both algorithms aim to detect these events, information could be learned from these particular instances to better characterize when insulin deliveries are necessary. The retrospective algorithms could be retrained or reimagined to detect these events from this information better.

Although the BPS can work independently, it is unclear if that aspect of the control system alone can provide adequate glucose control following unannounced meals. The addition of the anticipatory profiles would further improve overall glucose control. These modules together may sufficiently mitigate hyperglycemia in a fully closed-loop system.

It seems like the disturbance profiles are best utilized in the MS-MPC framework, but it is feasible that this information could be utilized in a control structure that is not using multiple models. The MS-MPC framework allows for multiple BG predictions, each based on a different perturbance, to be considered in the cost function of the algorithm. This control framework very easily takes the information encompassed in the disturbance profiles into consideration. A possible way that the disturbance profiles could be used in another type of control system is to tune the controller aggressivity. By monitoring the current disturbance and relating that information to the patterns of known behavior encompassed in the profiles, the controller's sensitivity could be modulated during periods of time where a disturbance was likely to be occurring or occur in the immediate future. This change in aggressivity could be helpful for numerous control algorithms and allow the system to react to disturbances better.

Future Work

Each of the processes defined in the aims needs to be evaluated in a real-life context where there are greater sources of error and variability than what is included in the simulation environment. The retrospective disturbance reconstruction appears to have a low false positive rate and acceptable true positive rate when applied to real data, but it is unclear if the consequence of not detecting roughly 20% of eating events will have on the intended applications. The BPS worked very well in the clinical experiment where it was evaluated, but it is unknown if issues with CGM sensors or physical activity,

both of which are present and frequent in real life, will cause the users to experience an unacceptable amount of hypoglycemia. The simulation experiment demonstrated that the disturbance profiles increased the amount of time BG values were in the euglycemic range without increasing hypoglycemia to a large degree, but the effects of exercise and changes of behavior are untested.

A large-scale clinical trial would have to be conducted to determine all of the effects of what is described above and other factors that would impact the system that are unanticipated. Because the BPS and anticipatory profiles both increase the amount of insulin being delivered without knowing the situation that the user is currently or about to be in, both have an element of risk associated with them. Furthermore, it is unclear how the profiles would be adapted over time and for whom this approach would work well or not. A clinical trial lasting over an extended period of time could highlight both the strengths and the weaknesses of these methods.

Another possible approach is to expose the system to these challenges in a controlled environment to elucidate the effects. By conducting multiple smaller pilot studies, the effect of different types of disturbances, such as physical activity, on the system as a whole could be individually studied. Isolating individual challenges to the system could provide more insight into how the algorithm could be improved but still would artificially impose a protocol on the participants, unlike a large-scale free-living trial.

Other Applications

The techniques described below are developed towards rejecting the glycemic disturbances caused by eating, but there are other applications where these techniques could be applied. A logical extension of this method would be to apply this technique, not to meal-related disturbances but those caused by various forms of physical activity. Some aspects of this work have been applied to exercise and have successfully prevented hypoglycemia.[144] Additionally, there are applications in the world of finance where disturbance detection and pattern recognition could be valuable. For instance, if a time series of an individual stock's price is considered, it would be useful to recognize past events, the respective effect on that equity's valuation, and determine which course of action (i.e., buy or sell) will result in the highest profit or mitigate the most loss.

Conclusion

A complete account of the disturbances to the insulin-glucose system, such as meals, is important for managing BG in people with T1D and developing new technology. Records provided by

patients are often fraught with errors due to either misestimations of disturbance magnitudes (i.e., carbohydrate counts), delayed announcements, or unacknowledged events. Additionally, there are many real-time glycemic management issues related to having people titrate insulin manually.

To aid in the management of glycemia automatically and in real-time, a strategy was developed to detect glycemic disturbances and mitigate their unwanted effects by dosing insulin without input from the user of the system. To address the issue of erroneous disturbance records, often reported as meals, two algorithms were developed to detect significant positive disturbances retrospectively. These algorithms could be used for data collected under numerous therapies, including multiple daily injections, sensor-augmented pump therapy, hybrid closed-loop, and fully closed-loop.

Furthermore, historical meal records were reconstructed to recognize patterns in eating behavior. Those patterns were then utilized to anticipate meal disturbances in an artificial pancreas framework. When combined, these techniques reduced hyperglycemia and increased the amount of time the individuals' BG values were in the euglycemic range significantly while not leading to a large number of hypoglycemic events.

The process of managing glucose excursions caused by large disturbances like meals is time-consuming, affects the quality of life, can result in an increased risk of complications, and is overall not ideal for glycemic management. If a system successfully managed the challenges associated with disturbances without input from the user, this could greatly increase the quality of life and management for people with T1D. The work presented in this dissertation made steps towards that goal, but there is more work to be done before a fully closed-loop system is safe and efficacious.

References

1. Röder P V, Wu B, Liu Y, Han W. Pancreatic regulation of glucose homeostasis. *Exp Mol Med*. 2016;48(3):e219. doi:10.1038/emm.2016.6

2. Göke B. Islet cell function: α and β cells - partners towards normoglycaemia. *Int J Clin Pract*. 2008;62(159):2-7. doi:10.1111/j.1742-1241.2007.01686.x

3. Triplitt CL. Understanding the kidneys' role in blood glucose regulation. *Am J Manag Care*. 2012;18(1 Suppl):S11-6. Accessed March 26, 2019. http://www.ncbi.nlm.nih.gov/pubmed/22559853

4. Nordlie RC, Foster JD, Lange AJ. REGULATION OF GLUCOSE PRODUCTION BY THE LIVER. *Annu Rev Nutr*. 1999;19(1):379-406. doi:10.1146/annurev.nutr.19.1.379

5. Han H-S, Kang G, Kim JS, Choi BH, Koo S-H. Regulation of glucose metabolism from a liver-centric perspective. *Exp Mol Med*. 2016;48(3):e218. doi:10.1038/emm.2015.122

6. Gerich JE, Meyer C, Woerle HJ, Stumvoll M. Renal Gluconeogenesis. *Diabetes Care*. 2001;24(2):382-391. doi:10.2337/DIACARE.24.2.382

7. Yang J. Enhanced Skeletal Muscle for Effective Glucose Homeostasis. *Prog Mol Biol Transl Sci*. 2014;121:133-163. doi:10.1016/B978-0-12-800101-1.00005-3

8. Mergenthaler P, Lindauer U, Dienel GA, Meisel A. Sugar for the brain: the role of glucose in physiological and pathological brain function. *Trends Neurosci*. 2013;36(10):587-597. doi:10.1016/j.tins.2013.07.001

9. Deem JD, Muta K, Scarlett JM, Morton GJ, Schwartz MW. How Should We Think About the Role of the Brain in Glucose Homeostasis and Diabetes? *Diabetes*. 2017;66(7):1758-1765. doi:10.2337/DBI16-0067

10. Rosen ED, Spiegelman BM. Adipocytes as regulators of energy balance and glucose homeostasis. *Nature*. 2006;444(7121):847-853. doi:10.1038/nature05483

11. Richardson SJ, Morgan NG, Foulis AK. Pancreatic Pathology in Type 1 Diabetes Mellitus. *Endocr Pathol*. 2014;25(1):80-92. doi:10.1007/s12022-014-9297-8

12. Ferrannini E. Physiology of Glucose Homeostasis and Insulin Therapy in Type 1 and Type 2

Diabetes. *Endocrinol Metab Clin North Am*. 2012;41(1):25-39. doi:10.1016/j.ecl.2012.01.003

13. Saeedi P, Petersohn I, Salpea P, et al. Global and regional diabetes prevalence estimates for 2019 and projections for 2030 and 2045: Results from the International Diabetes Federation Diabetes Atlas, 9th edition. *Diabetes Res Clin Pract*. 2019;157:107843. doi:10.1016/j.diabres.2019.107843

14. Thibault V, Bélanger M, LeBlanc E, et al. Factors that could explain the increasing prevalence of type 2 diabetes among adults in a Canadian province: a critical review and analysis. *Diabetol Metab Syndr*. 2016;8(1):1-10. doi:10.1186/s13098-016-0186-9

15. Egro FM. Why is type 1 diabetes increasing? *J Mol Endocrinol*. 2013;51(1):R1-R13. doi:10.1530/JME-13-0067

16. CDC. *National Diabetes Statistics Report 2020. Estimates of Diabetes and Its Burden in the United States.*; 2020.

17. Bragg F, Holmes M V., Iona A, et al. Association between diabetes and cause-specific mortality in rural and urban areas of China. *JAMA - J Am Med Assoc*. 2017;317(3):280-289. doi:10.1001/jama.2016.19720

18. Yang JJ, Yu D, Wen W, et al. Association of Diabetes With All-Cause and Cause-Specific Mortality in Asia: A Pooled Analysis of More Than 1 Million Participants. *JAMA Netw open*. 2019;2(4):e192696. doi:10.1001/jamanetworkopen.2019.2696

19. Saeedi P, Salpea P, Karuranga S, et al. Mortality attributable to diabetes in 20–79 years old adults, 2019 estimates: Results from the International Diabetes Federation Diabetes Atlas, 9th edition. *Diabetes Res Clin Pract*. 2020;162:108086. doi:10.1016/j.diabres.2020.108086

20. A1C test - Mayo Clinic. Accessed March 24, 2021. https://www.mayoclinic.org/tests-procedures/a1c-test/about/pac-20384643

21. Hemoglobin A1C (HbA1c) Test: MedlinePlus Medical Test. Accessed March 24, 2021. https://medlineplus.gov/lab-tests/hemoglobin-a1c-hba1c-test/

22. The A1C Test & Diabetes | NIDDK. Accessed March 24, 2021. https://www.niddk.nih.gov/health-information/diagnostic-tests/a1c-test

23. DM N, S G, J L, et al. The Effect of Intensive Treatment of Diabetes on the Development and Progression of Long-Term Complications in Insulin-Dependent Diabetes Mellitus. *N Engl J Med*.

1993;329(14):977-986. doi:10.1056/NEJM199309303291401

24. Orchard TJ, Nathan DM, Zinman B, et al. Association between 7 years of intensive treatment of type 1 diabetes and long-Term mortality. *JAMA - J Am Med Assoc*. 2015;313(1):45-53. doi:10.1001/jama.2014.16107

25. Holman RR, Paul SK, Bethel MA, Matthews DR, Neil HAW. 10-Year Follow-up of Intensive Glucose Control in Type 2 Diabetes. *N Engl J Med*. 2008;359(15):1577-1589. doi:10.1056/nejmoa0806470

26. Casagrande SS, Fradkin JE, Saydah SH, Rust KF, Cowie CC. The prevalence of meeting A1C, blood pressure, and LDL goals among people with diabetes, 1988-2010. *Diabetes Care*. 2013;36(8):2271-2279. doi:10.2337/dc12-2258

27. Foster NC, Beck RW, Miller KM, et al. State of Type 1 Diabetes Management and Outcomes from the T1D Exchange in 2016–2018. *Diabetes Technol Ther*. 2019;21(2):66-72. doi:10.1089/dia.2018.0384

28. Harding JL, Pavkov ME, Magliano DJ, Shaw JE, Gregg EW. Global trends in diabetes complications: a review of current evidence. *Diabetologia*. 2019;62(1):3-16. doi:10.1007/s00125-018-4711-2

29. Kalra S, Mukherjee J, Ramachandran A, et al. Hypoglycemia: The neglected complication. *Indian J Endocrinol Metab*. 2013;17(5):819. doi:10.4103/2230-8210.117219

30. Reno CM, Skinner A, Bayles J, Chen YS, Daphna-Iken D, Fisher SJ. Severe hypoglycemia-induced sudden death is mediated by both cardiac arrhythmias and seizures. *Am J Physiol Metab*. 2018;315(2):E240-E249. doi:10.1152/ajpendo.00442.2017

31. Rubin RR, Peyrot M. Psychological issues and treatments for people with diabetes. *J Clin Psychol*. 2001;57(4):457-478. doi:10.1002/jclp.1041

32. Buchberger B, Huppertz H, Krabbe L, Lux B, Mattivi JT, Siafarikas A. Symptoms of depression and anxiety in youth with type 1 diabetes: A systematic review and meta-analysis. *Psychoneuroendocrinology*. 2016;70:70-84. doi:10.1016/j.psyneuen.2016.04.019

33. Rewers A, Peter Chase H, Mackenzie T, et al. Predictors of acute complications in children with type 1 diabetes. *J Am Med Assoc*. 2002;287(19):2511-2518. doi:10.1001/jama.287.19.2511

34. Grey M, Whittemore R, Tamborlane W. Depression in Type 1 diabetes in children natural history and correlates. In: *Journal of Psychosomatic Research*. Vol 53. J Psychosom Res; 2002:907-911.

doi:10.1016/S0022-3999(02)00312-4

35. Merikangas KR, He JP, Burstein M, et al. Lifetime Prevalence of Mental Disorders in U.S. Adolescents: Results from the National Comorbidity Survey Replication–Adolescent Supplement (NCS-A). *J Am Acad Child Adolesc Psychiatry*. 2010;49(10):980-989. doi:10.1016/J.JAAC.2010.05.017

36. Jones JM, Lawson ML, Daneman D, Olmsted MP, Rodin G. Eating disorders in adolescent females with and without type 1 diabetes: Cross sectional study. *Br Med J*. 2000;320(7249):1563-1566. doi:10.1136/bmj.320.7249.1563

37. Colton P, Olmsted M, Daneman D, Rydall A, Rodin G. Disturbed eating behavior and eating disorders in preteen and early teenage girls with type 1 diabetes: A case-controlled study. *Diabetes Care*. 2004;27(7):1654-1659. doi:10.2337/diacare.27.7.1654

38. Striegel Weissman R, Bulik C. Risk Factors for Eating Disorders Open Trial of UCAN View project CBT4BN View project. Published online 2007. doi:10.1037/0003-066X.62.3.181

39. Goebel-Fabbri AE, Fikkan J, Franko DL, Pearson K, Anderson BJ, Weinger K. Insulin restriction and associated morbidity and mortality in women with type 1 diabetes. *Diabetes Care*. 2008;31(3):415-419. doi:10.2337/dc07-2026

40. Goebel-Fabbri AE. Disturbed Eating Behaviors and Eating Disorders in Type 1 Diabetes: Clinical Signifi cance and Treatment Recommendations. *Curr Diab Rep*. 2009;9(2):133-139. doi:10.1007/s11892-009-0023-8

41. Pinhas-Hamiel O. Eating disorders in adolescents with type 1 diabetes: Challenges in diagnosis and treatment. *World J Diabetes*. 2015;6(3):517. doi:10.4239/wjd.v6.i3.517

42. Hanlan ME, Griffith J, Patel N, Jaser SS. Eating disorders and disordered eating in type 1 diabetes: Prevalence, screening, and treatment options. *Curr Diab Rep*. 2013;13(6):909-916. doi:10.1007/s11892-013-0418-4

43. Continuous Subcutaneous Insulin Infusion at 25 Years. *Diabetes Care*. 2002;25:593-598. Accessed March 22, 2018. http://care.diabetesjournals.org/content/25/3/593.full-text.pdf

44. Chaudhry T, Klonoff DC. SMBG Out of Control: The Need for Educating Patients About Control Solution. *Diabetes Educ*. 2013;39(5):689-695. doi:10.1177/0145721713495791

45. Benjamin EM. Self-Monitoring of Blood Glucose: The Basics. *Clin Diabetes*. 2002;20(1):45-47. doi:10.2337/diaclin.20.1.45

46. Evans JMM, Newton RW, Ruta DA, MacDonald TM, Stevenson RJ, Morris AD. Frequency of blood glucose monitoring in relation to glycaemic control: Observational study with diabetes database. *Br Med J*. 1999;318(7202):83-86. doi:10.1136/bmj.319.7202.83

47. Association AD. Diabetes technology: Standards of medical care in diabetes−2021. *Diabetes Care*. 2021;44(Supplement 1):S85-S99. doi:10.2337/dc21-S007

48. Beck RW, Weinzimer S, Miller K, et al. Effectiveness of continuous glucose monitoring in a clinical care environment: Evidence from the Juvenile Diabetes Research Foundation Continuous Glucose Monitoring (JDRF-CGM) trial. *Diabetes Care*. 2010;33(1):17-22. doi:10.2337/dc09-1502

49. Hermanides J, Nørgaard K, Bruttomesso D, et al. Sensor-augmented pump therapy lowers HbA 1c in suboptimally controlled Type1 diabetes; a randomized controlled trial. *Diabet Med*. 2011;28(10):1158-1167. doi:10.1111/j.1464-5491.2011.03256.x

50. Battelino T, Conget I, Olsen B, et al. The use and efficacy of continuous glucose monitoring in type 1 diabetes treated with insulin pump therapy: a randomised controlled trial. *Diabetologia*. 2012;55(12):3155-3162. doi:10.1007/s00125-012-2708-9

51. New JP, Ajjan R, Pfeiffer AFH, Freckmann G. Continuous glucose monitoring in people with diabetes: The randomized controlled Glucose Level Awareness in Diabetes Study (GLADIS). *Diabet Med*. 2015;32(5):609-617. doi:10.1111/dme.12713

52. Wong JC, Foster NC, Maahs DM, et al. Real-time continuous glucose monitoring among participants in the T1D exchange clinic registry. *Diabetes Care*. 2014;37(10):2702-2709. doi:10.2337/dc14-0303

53. Riveline JP, Schaepelynck P, Chaillous L, et al. Assessment of patient-led or physician-driven continuous glucose monitoring in patients with poorly controlled type 1 diabetes using basal-bolus insulin regimens: A 1-year multicenter study. *Diabetes Care*. 2012;35(5):965-971. doi:10.2337/dc11-2021

54. Rachmiel M, Landau Z, Boaz M, et al. The use of continuous glucose monitoring systems in a pediatric population with type 1 diabetes mellitus in real-life settings: the AWeSoMe Study

Group experience. *Acta Diabetol*. 2015;52(2):323-329. doi:10.1007/s00592-014-0643-6

55. Bergenstal RM, Klonoff DC, Garg SK, et al. Threshold-Based Insulin-Pump Interruption for Reduction of Hypoglycemia. *N Engl J Med*. 2013;369(3):224-232. doi:10.1056/nejmoa1303576

56. Weinstock RS, Xing D, Maahs DM, et al. Severe hypoglycemia and diabetic ketoacidosis in adults with type 1 diabetes: Results from the T1D exchange clinic registry. *J Clin Endocrinol Metab*. 2013;98(8):3411-3419. doi:10.1210/jc.2013-1589

57. Pickup JC, Freeman SC, Sutton AJ. Glycaemic control in type 1 diabetes during real time continuous glucose monitoring compared with self monitoring of blood glucose: Meta-analysis of randomised controlled trials using individual patient data. *BMJ*. 2011;343(7815). doi:10.1136/bmj.d3805

58. Garg SK, Voelmle MK, Beatson CR, et al. Use of continuous glucose monitoring in subjects with type 1 diabetes on multiple daily injections versus continuous subcutaneous insulin infusion therapy: A prospective 6-month study. *Diabetes Care*. 2011;34(3):574-579. doi:10.2337/dc10-1852

59. Beck RW, Riddlesworth T, Ruedy K, et al. Effect of continuous glucose monitoring on glycemic control in adults with type 1 diabetes using insulin injections the diamond randomized clinical trial. In: *JAMA - Journal of the American Medical Association*. Vol 317. American Medical Association; 2017:371-378. doi:10.1001/jama.2016.19975

60. Huang ES, O'Grady M, Basu A, et al. The cost-effectiveness of continuous glucose monitoring in type 1 diabetes. *Diabetes Care*. 2010;33(6):1269-1274. doi:10.2337/dc09-2042

61. McQueen RB, Ellis SL, Campbell JD, Nair K V., Sullivan PW. Cost-effectiveness of continuous glucose monitoring and intensive insulin therapy for type 1 diabetes. *Cost Eff Resour Alloc*. 2011;9. doi:10.1186/1478-7547-9-13

62. Walsh J, Roberts R, Bailey T. Guidelines for insulin dosing in continuous subcutaneous insulin infusion using new formulas from a retrospective study of individuals with optimal glucose levels. *J Diabetes Sci Technol*. 2010;4(5):1174-1181. doi:10.1177/193229681000400516

63. Walsh J, Roberts R. *Pumping Insulin: Everything You Need For Success On A Smart Insulin Pump CLICK HERE FOR DOWNLOAD*.; 2006.

64. Davidson PC, Hebblewhite HR, Steed RD, Bode BW. Analysis of guidelines for basal-bolus insulin dosing: Basal insulin, correction factor, and carbohydrate-to-insulin ratio. *Endocr Pract*. 2008;14(9):1095-1101. doi:10.4158/EP.14.9.1095

65. King AB, Kuroda A, Matsuhisa M, Hobbs T. A Review of Insulin-Dosing Formulas for Continuous Subcutaneous Insulin Infusion (CSII) for Adults with Type 1 Diabetes. *Curr Diab Rep*. 2016;16(9). doi:10.1007/s11892-016-0772-0

66. Biester T, Kordonouri O, Holder M, et al. "Let the Algorithm Do the Work": Reduction of Hypoglycemia Using Sensor-Augmented Pump Therapy with Predictive Insulin Suspension (SmartGuard) in Pediatric Type 1 Diabetes Patients. *Diabetes Technol Ther*. 2017;19(3):173-182. doi:10.1089/dia.2016.0349

67. Forlenza GP, Li Z, Buckingham BA, et al. Predictive low-glucose suspend reduces hypoglycemia in adults, adolescents, and children with type 1 diabetes in an at-home randomized crossover study: Results of the PROLOG trial. *Diabetes Care*. 2018;41(10):2155-2161. doi:10.2337/dc18-0771

68. Knebel T, Neumiller JJ. Medtronic MiniMed 670G Hybrid Closed-Loop System. *Clin Diabetes*. 2019;37(1):94-95. doi:10.2337/cd18-0067

69. Hughes CS, Patek SD, Breton M, Kovatchev BP. Anticipating the next meal using meal behavioral profiles: A hybrid model-based stochastic predictive control algorithm for T1DM. *Comput Methods Programs Biomed*. 2011;102(2):138-148. doi:10.1016/j.cmpb.2010.04.011

70. Patek SD, Hughes C, Breton M, Kovatchev BP. Anticipating Meals with Behavioral Profiles: Towards Stochastic Model Predictive Control of T1DM. *IFAC Proc Vol*. 2009;42(12):37-42. doi:10.3182/20090812-3-DK-2006.0059

71. DeBoer MD, Cherñavvsky DR, Topchyan K, Kovatchev BP, Francis GL, Breton MD. Heart rate informed artificial pancreas system enhances glycemic control during exercise in adolescents with T1D. *Pediatr Diabetes*. 2016;18(7):540-546. doi:10.1111/pedi.12454

72. Dassau E, Pinsker JE, Kudva YC, et al. Twelve-Week 24/7 Ambulatory Artificial Pancreas With Weekly Adaptation of Insulin Delivery Settings: Effect on Hemoglobin A1c and Hypoglycemia. *Diabetes Care*. 2017;40(12):1719-1726. doi:10.2337/dc17-1188

73. Huyett LM, Ly TT, Forlenza GP, et al. Outpatient Closed-Loop Control with Unannounced Moderate Exercise in Adolescents Using Zone Model Predictive Control. *Diabetes Technol Ther*. 2017;19(6):331-339. doi:10.1089/dia.2016.0399

74. Tagougui S, Taleb N, Rabasa-Lhoret R. The Benefits and Limits of Technological Advances in Glucose Management Around Physical Activity in Patients Type 1 Diabetes. *Front Endocrinol (Lausanne)*. 2018;9:818. doi:10.3389/fendo.2018.00818

75. Harvey RA, Dassau E, Bevier WC, et al. Clinical evaluation of an automated artificial pancreas using zone-model predictive control and health monitoring system. *Diabetes Technol Ther*. 2014;16(6):348-357. doi:10.1089/dia.2013.0231

76. Forlenza GP, Cameron FM, Ly TT, et al. Fully Closed-Loop Multiple Model Probabilistic Predictive Controller Artificial Pancreas Performance in Adolescents and Adults in a Supervised Hotel Setting. *Diabetes Technol Ther*. 2018;20(5):335-343. doi:10.1089/dia.2017.0424

77. Dovc K, Piona C, Mutlu GY, et al. Faster Compared with Standard Insulin Aspart during Day-And-Night Fully Closed-Loop Insulin Therapy in Type 1 Diabetes: A Double-Blind Randomized Crossover Trial. *Diabetes Care*. 2020;43(1):29-36. doi:10.2337/dc19-0895

78. Blauw H, Onvlee AJ, Klaassen M, van Bon AC, DeVries JH. Fully Closed Loop Glucose Control With a Bihormonal Artificial Pancreas in Adults With Type 1 Diabetes: An Outpatient, Randomized, Crossover Trial. *Diabetes Care*. 2021;44(3):836-838. doi:10.2337/dc20-2106

79. Haidar A, Yale JF, Lovblom LE, et al. Reducing the need for carbohydrate counting in type 1 diabetes using closed-loop automated insulin delivery (artificial pancreas) and empagliflozin: A randomized, controlled, non-inferiority, crossover pilot trial. *Diabetes, Obes Metab*. Published online 2021. doi:10.1111/dom.14335

80. Majdpour D, Tsoukas M, Yale J-F, et al. Fully Automated Artificial Pancreas for Adults with Type 1 Diabetes using Multiple Hormones: Exploratory Experiments. *Can J Diabetes*. Published online February 2021. doi:10.1016/j.jcjd.2021.02.002

81. Kovatchev BP, Breton M, Dalla Man C, Cobelli C. In Silico Preclinical Trials: A Proof of Concept in Closed-Loop Control of Type 1 Diabetes Boris. *J Diabetes Sci Technol*. 2009;3(1):44-55. doi:10.1177/193229680900300106

82. Visentin R, Campos-Náñez E, Schiavon M, et al. The UVA/Padova Type 1 Diabetes Simulator Goes From Single Meal to Single Day. *J Diabetes Sci Technol*. 2018;0(0):1-9. doi:10.1177/1932296818757747

83. Dalla Man C, Micheletto F, Lv D, Breton M, Kovatchev B, Cobelli C. The UVA/PADOVA Type 1 Diabetes Simulator: New Features. *J Diabetes Sci Technol*. 2014;8(1):26-34. doi:10.1177/1932296813514502

84. Dalla Man C, Camilleri M, Cobelli C. A System Model of Oral Glucose Absorption: Validation on Gold Standard Data. *IEEE Trans Biomed Eng*. 2006;53(12):2472-2478. doi:10.1109/TBME.2006.883792

85. Patek SD, Lv D, Ortiz EA, et al. Empirical Representation of Blood Glucose Variability in a Compartmental Model. In: Kirchsteiger H, Jørgensen JB, Renard E, del Re L, eds. *Prediction Methods for Blood Glucose Concentration*. Springer International Publishing; 2016:133-157. doi:10.1007/978-3-319-25913-0_8

86. Dalla Man C, Caumo A, Cobelli C. The oral glucose minimal model: Estimation of insulin sensitivity from a meal test. *IEEE Trans Biomed Eng*. 2002;49(5):419-429. doi:10.1109/10.995680

87. Bergman RN, Ider YZ, Bowden CR, Cobelli C. Quantitative estimation of insulin sensitivity. *Am J Physiol*. 1979;236(6):E667-77. doi:10.1152/ajpendo.1979.236.6.E667

88. J H, T G, P C, C F, MD B. Replay Simulations with Personalized Metabolic Model for Treatment Design and Evaluation in Type 1 Diabetes. *J Diabetes Sci Technol*. Published online 2020. doi:10.1177/1932296820973193

89. Sorensen JT. A physiologic model of glucose metabolism in man and its use to design and assess improved insulin therapies for diabetes. Published online 1985. Accessed April 27, 2019. https://www.semanticscholar.org/paper/A-physiologic-model-of-glucose-metabolism-in-man-to-Sorensen/4d1c156e1149b1f9ac629a951133b72ba0c05d34

90. Wilinska ME, Hovorka R. Simulation models for in silico testing of closed-loop glucose controllers in type 1 diabetes. *Drug Discov Today Dis Model*. 2008;5(4):289-298. doi:10.1016/J.DDMOD.2009.07.005

91. Oviedo S, Vehí J, Calm R, Armengol J. A review of personalized blood glucose prediction strategies

for T1DM patients. *Int j numer method biomed eng*. 2017;33(6):e2833. doi:10.1002/cnm.2833

92. Woldaregay AZ, Årsand E, Walderhaug S, et al. Data-driven modeling and prediction of blood glucose dynamics: Machine learning applications in type 1 diabetes. *Artif Intell Med*. 2019;98:109-134. doi:10.1016/J.ARTMED.2019.07.007

93. Lease M. *On Quality Control and Machine Learning in Crowdsourcing*. Accessed July 9, 2020. www.aaai.org

94. Gudivada VN, Ding J, Apon A. Data Quality Considerations for Big Data and Machine Learning: Going Beyond Data Cleaning and Transformations . *Int J Adv Softw*. Published online 2017:1-20. Accessed July 9, 2020. https://www.researchgate.net/publication/318432363

95. Bosu MF, MacDonell SG. Data quality in empirical software engineering: A targeted review. In: *ACM International Conference Proceeding Series*. ACM Press; 2013:171-176. doi:10.1145/2460999.2461024

96. Peters A, Van Name MA, Thorsted BL, Piltoft JS, Tamborlane W V. Postprandial Dosing of Bolus Insulin in Patients with Type 1 Diabetes: A Cross-sectional Study Using Data from the T1D Exchange Registry. *Endocr Pract*. 2017;23(10):1201-1209. doi:10.4158/EP171813.OR

97. Meade LT, Rushton WE. Accuracy of Carbohydrate Counting in Adults. *Clin Diabetes*. 2016;34(3):142. doi:10.2337/DIACLIN.34.3.142

98. Brazeau AS, Mircescu H, Desjardins K, et al. Carbohydrate counting accuracy and blood glucose variability in adults with type 1 diabetes. *Diabetes Res Clin Pract*. 2013;99(1):19-23. doi:10.1016/j.diabres.2012.10.024

99. Foster NC, Beck RW, Miller KM, et al. State of Type 1 Diabetes Management and Outcomes from the T1D Exchange in 2016–2018. *Diabetes Technol Ther*. 2019;21(2):66-72. doi:10.1089/dia.2018.0384

100. Randløv J, Poulsen JU. How Much Do Forgotten Insulin Injections Matter to Hemoglobin A1c in People with Diabetes? A Simulation Study. *J Diabetes Sci Technol*. 2008;2(2):229. doi:10.1177/193229680800200209

101. Dassau E, Bequette BW, Buckingham BA, Doyle FJ. Detection of a meal using continuous glucose monitoring: implications for an artificial beta-cell. *Diabetes Care*. 2008;31(2):295-300.

doi:10.2337/dc07-1293

102. Harvey RA, Dassau E, Zisser H, Seborg DE, Doyle FJ, III. Design of the Glucose Rate Increase Detector: A Meal Detection Module for the Health Monitoring System. *J Diabetes Sci Technol*. 2014;8(2):307-320. doi:10.1177/1932296814523881

103. Turksoy K, Samadi S, Feng J, Littlejohn E, Quinn L, Cinar A. Meal Detection in Patients With Type 1 Diabetes: A New Module for the Multivariable Adaptive Artificial Pancreas Control System. *IEEE J Biomed Heal Informatics*. 2016;20(1):47-54. doi:10.1109/JBHI.2015.2446413

104. Weimer J, Chen S, Peleckis A, Rickels MR, Lee I. Physiology-Invariant Meal Detection for Type 1 Diabetes. *Diabetes Technol Ther*. 2016;18(10):616-624. doi:10.1089/dia.2015.0266

105. Chang K, Liu S, Chu H, et al. The Diet-Aware Dining Table: Observing Dietary Behaviors over a Tabletop Surface. In: Springer, Berlin, Heidelberg; 2006:366-382. doi:10.1007/11748625_23

106. Zhou B, Cheng J, Sundholm M, et al. Smart table surface: A novel approach to pervasive dining monitoring. In: *2015 IEEE International Conference on Pervasive Computing and Communications (PerCom)*. IEEE; 2015:155-162. doi:10.1109/PERCOM.2015.7146522

107. Zhu F, Bosch M, Boushey CJ, Delp EJ. An image analysis system for dietary assessment and evaluation. In: *2010 IEEE International Conference on Image Processing*. IEEE; 2010:1853-1856. doi:10.1109/ICIP.2010.5650848

108. Zhu F, Bosch M, Schap T, et al. Segmentation Assisted Food Classification for Dietary Assessment. *Proc SPIE--the Int Soc Opt Eng*. 2011;7873:78730B. doi:10.1117/12.877036

109. Sun M, Burke LE, Mao Z-H, et al. eButton. In: *Proceedings of the The 51st Annual Design Automation Conference on Design Automation Conference - DAC '14*. Vol 2014. ACM Press; 2014:1-6. doi:10.1145/2593069.2596678

110. Chen H-C, Jia W, Yue Y, et al. Model-based measurement of food portion size for image-based dietary assessment using 3D/2D registration. *Meas Sci Technol*. 2013;24(10):105701. doi:10.1088/0957-0233/24/10/105701

111. Wenyan Jia, Yaofeng Yue, Fernstrom JD, Zhengnan Zhang, Yongquan Yang, Mingui Sun. 3D localization of circular feature in 2D image and application to food volume estimation. In: *2012 Annual International Conference of the IEEE Engineering in Medicine and Biology Society*. IEEE;

2012:4545-4548. doi:10.1109/EMBC.2012.6346978

112. Cadavid S, Abdel-Mottaleb M, Helal A. Exploiting visual quasi-periodicity for real-time chewing event detection using active appearance models and support vector machines. *Pers Ubiquitous Comput*. 2012;16(6):729-739. doi:10.1007/s00779-011-0425-x

113. Tanigawa S, Nishihara H, Kaneda S, Haga H. Detecting mastication by using microwave Doppler sensor. In: *Proceedings of the 1st ACM International Conference on PErvasive Technologies Related to Assistive Environments - PETRA '08*. ACM Press; 2008:1. doi:10.1145/1389586.1389686

114. Liu J, Johns E, Atallah L, et al. An Intelligent Food-Intake Monitoring System Using Wearable Sensors. In: *2012 Ninth International Conference on Wearable and Implantable Body Sensor Networks*. IEEE; 2012:154-160. doi:10.1109/BSN.2012.11

115. Sen S, Subbaraju V, Misra A, Balan RK, Youngki Lee. The case for smartwatch-based diet monitoring. In: *2015 IEEE International Conference on Pervasive Computing and Communication Workshops (PerCom Workshops)*. IEEE; 2015:585-590. doi:10.1109/PERCOMW.2015.7134103

116. Burke LE, Warziski M, Starrett T, et al. Self-Monitoring Dietary Intake: Current and Future Practices. *J Ren Nutr*. 2005;15(3):281-290. doi:10.1016/J.JRN.2005.04.002

117. Westerterp KR, Goris AHC. Validity of the assessment of dietary intake: problems of misreporting. *Curr Opin Clin Nutr Metab Care*. 2002;5(5):489-493. Accessed March 20, 2018. http://www.ncbi.nlm.nih.gov/pubmed/12172471

118. Dong Y, Scisco J, Wilson M, Muth E, Hoover A. Detecting Periods of Eating During Free-Living by Tracking Wrist Motion. *IEEE J Biomed Heal Informatics*. 2014;18(4):1253-1260. Accessed March 20, 2018. http://cecas.clemson.edu/~ahoover/bite-counter/IEEE-JBHI-2013.pdf

119. Thomaz E, Essa I, Abowd GD. A practical approach for recognizing eating moments with wrist-mounted inertial sensing. In: *Proceedings of the 2015 ACM International Joint Conference on Pervasive and Ubiquitous Computing - UbiComp '15*. ACM Press; 2015:1029-1040. doi:10.1145/2750858.2807545

120. Mendi E, Ozyavuz O, Pekesen E, Bayrak C. Food intake monitoring system for mobile devices. In: *5th IEEE International Workshop on Advances in Sensors and Interfaces IWASI*. IEEE; 2013:31-33.

doi:10.1109/IWASI.2013.6576082

121. Farooq M, Fontana JM, Sazonov E. A novel approach for food intake detection using electroglottography. *Physiol Meas*. 2014;35(5):739-751. doi:10.1088/0967-3334/35/5/739

122. Woda A, Mishellany A, Peyron M-A. The regulation of masticatory function and food bolus formation. *J Oral Rehabil*. 2006;33(11):840-849. doi:10.1111/j.1365-2842.2006.01626.x

123. Woda A, Foster K, Mishellany A, Peyron MA. Adaptation of healthy mastication to factors pertaining to the individual or to the food. *Physiol Behav*. 2006;89(1):28-35. doi:10.1016/j.physbeh.2006.02.013

124. Farooq M, Sazonov E. A Novel Wearable Device for Food Intake and Physical Activity Recognition. *Sensors*. 2016;16(7):1067. doi:10.3390/s16071067

125. Kalantarian H, Alshurafa N, Sarrafzadeh M. A Wearable Nutrition Monitoring System. In: *2014 11th International Conference on Wearable and Implantable Body Sensor Networks*. IEEE; 2014:75-80. doi:10.1109/BSN.2014.26

126. Fontana JM, Farooq M, Sazonov E. Automatic Ingestion Monitor: A Novel Wearable Device for Monitoring of Ingestive Behavior. *IEEE Trans Biomed Eng*. 2014;61(6):1772-1779. doi:10.1109/TBME.2014.2306773

127. Cramer JS. The Origins of Logistic Regression. *SSRN Electron J*. Published online November 2, 2005. doi:10.2139/ssrn.360300

128. Menard S. *Applied Logistic Regression Analysis*. Vol 106. Sage; 2002.

129. Garcia-Tirado J, Brown SA, Laichuthai N, et al. Anticipation of Historical Exercise Patterns by a Novel Artificial Pancreas System Reduces Hypoglycemia During and After Moderate-Intensity Physical Activity in People with Type 1 Diabetes. *Diabetes Technol Ther*. 2020;23(4). doi:10.1089/dia.2020.0516

130. Ellingsen C, Dassau E, Zisser H, et al. Safety constraints in an artificial pancreatic β cell: An implementation of model predictive control with insulin on board. *J Diabetes Sci Technol*. 2009;3(3):536-544. doi:10.1177/193229680900300319

131. Keith-Hynes P, Guerlain S, Mize B, et al. DiAs user interface: A patient-centric interface for mobile artificial pancreas systems. In: *Journal of Diabetes Science and Technology*. Vol 7. Diabetes

Technology Society; 2013:1416-1426. doi:10.1177/193229681300700602

132. Place J, Robert A, Ben Brahim N, et al. DiAs web monitoring: A real-time remote monitoring system designed for artificial pancreas outpatient trials. In: *Journal of Diabetes Science and Technology*. Vol 7. Diabetes Technology Society; 2013:1427-1435. doi:10.1177/193229681300700603

133. Brown SA, Kovatchev BP, Raghinaru D, et al. Six-Month Randomized, Multicenter Trial of Closed-Loop Control in Type 1 Diabetes. *N Engl J Med*. 2019;381(18):1707-1717. doi:10.1056/NEJMoa1907863

134. Isganaitis E, Raghinaru D, Ambler-Osborn L, et al. Closed-Loop Insulin Therapy Improves Glycemic Control in Adolescents and Young Adults: Outcomes from the International Diabetes Closed-Loop Trial. *Diabetes Technol Ther*. 2021;23(5). doi:10.1089/dia.2020.0572

135. Breton MD, Kanapka LG, Beck RW, et al. A Randomized Trial of Closed-Loop Control in Children with Type 1 Diabetes. *N Engl J Med*. 2020;383(9):836-845. doi:10.1056/nejmoa2004736

136. Ly TT, Breton MD, Keith-Hynes P, et al. Overnight glucose control with an automated, unified safety system in children and adolescents with type 1 diabetes at diabetes camp. *Diabetes Care*. 2014;37(8):2310-2316. doi:10.2337/dc14-0147

137. Anderson SM, Buckingham BA, Breton MD, et al. Hybrid Closed-Loop Control Is Safe and Effective for People with Type 1 Diabetes Who Are at Moderate to High Risk for Hypoglycemia. *Diabetes Technol Ther*. 2019;21(6):356-363. doi:10.1089/dia.2019.0018

138. Corbett JP, Garcia-Tirado JF, Colmegna P, Diaz C. JL, Breton MD. Using an Online Disturbance Rejection and Anticipation System to Reduce Hyperglycemia in a Fully Closed-loop Artificial Pancreas System (submitted). Published online 2021.

139. Breton MD, Patek SD, Lv D, et al. Continuous Glucose Monitoring and Insulin Informed Advisory System with Automated Titration and Dosing of Insulin Reduces Glucose Variability in Type 1 Diabetes Mellitus. *Diabetes Technol Ther*. 2018;20(8):531-540. doi:10.1089/dia.2018.0079

140. Bekiari E, Kitsios K, Thabit H, et al. Artificial pancreas treatment for outpatients with type 1 diabetes: systematic review and meta-analysis. *BMJ*. 2018;361:1310. doi:10.1136/BMJ.K1310

141. Lucia S, Finkler T, Engell S. Multi-stage nonlinear model predictive control applied to a semi-batch

polymerization reactor under uncertainty. *J Process Control*. 2013;23(9):1306-1319. doi:10.1016/j.jprocont.2013.08.008

142. Lucia S, Finkler T, Basak D, Engell S. A new Robust NMPC Scheme and its application to a semi-batch reactor example. In: *IFAC Proceedings Volumes (IFAC-PapersOnline)*. Vol 45. IFAC Secretariat; 2012:69-74. doi:10.3182/20120710-4-SG-2026.00035

143. Garcia-Tirado J, Corbett JP, Boiroux D, Jørgensen JB, Breton MD. Closed-loop control with unannounced exercise for adults with type 1 diabetes using the Ensemble Model Predictive Control. *J Process Control*. 2019;80:202-210. doi:10.1016/j.jprocont.2019.05.017

144. Garcia-Tirado JF, Colmegna P, Corbett JP, Ozaslan B, Breton MD. Ensemble Model Predictive Control Strategies Can Reduce Exercise Hypoglycemia in Type 1 Diabetes: In Silico Studies. In: *2019 American Control Conference (ACC)*. Vol 2019-July. ; 2019:4752-4758. doi:10.23919/acc.2019.8814728

145. Garcia-Tirado J, Colmegna P, Corbett JP, Ozaslan B, Breton MD. In Silico Analysis of an Exercise-Safe Artificial Pancreas With Multistage Model Predictive Control and Insulin Safety System. *J Diabetes Sci Technol*. 2019;13(6). doi:10.1177/1932296819879084

146. Corbett JP, Colmegna P, Garcia-Tirado J, Breton MD. Anticipating Meals with Behavioral Profiles in an Artificial Pancreas System - An Informed Multistage Model Predictive Control Approach. *IFAC-PapersOnLine*. 2020;53(2):16305-16310. doi:10.1016/j.ifacol.2020.12.652

147. Cameron F, Niemeyer G. Extended multiple model prediction with application to blood glucose regulation. *J Process Control*. 2012;22(8):1422-1432. doi:10.1016/J.JPROCONT.2012.05.014

148. Cameron F, Niemeyer G, Wilson D, et al. Inpatient trial of an artificial pancreas based on multiple model probabilistic predictive control with repeated large unannounced meals. *Diabetes Technol Ther*. 2014;16(11):728-734. doi:10.1089/DIA.2014.0093

149. Cameron F, Ly T, Buckingham B, et al. Closed-Loop Control Without Meal Announcement in Type 1 Diabetes. *Diabetes Technol Ther*. 2017;19(9):527-532. doi:10.1089/DIA.2017.0078

150. Steinhaus H. Sur la division des corps materiels en parties. *Bull Acad Pol Sci*. 1956;1(804):801.

151. Lloyd SP. *Least Squares Quantization in PCM*. Vol 28.; 1982. Accessed August 15, 2019. https://sites.cs.ucsb.edu/~veronika/MAE/kmeans_LLoyd_Least_Squares_Quantization_in_PCM.p

df

152. Macqueen J. Some methods for classification and analysis of multivariate observations. *5-TH BERKELEY Symp Math Stat Probab*. Published online 1967:281--297. Accessed September 10, 2020. http://citeseerx.ist.psu.edu/viewdoc/summary?doi=10.1.1.308.8619

153. Hamming RW. Error Detecting and Error Correcting Codes. *Bell Syst Tech J*. 1950;29(2):147-160. doi:10.1002/j.1538-7305.1950.tb00463.x

154. Caliñski T, Harabasz J. A Dendrite Method Foe Cluster Analysis. *Commun Stat*. 1974;3(1):1-27. doi:10.1080/03610927408827101

155. Davies DL, Bouldin DW. A Cluster Separation Measure. *IEEE Trans Pattern Anal Mach Intell*. 1979;PAMI-1(2):224-227. doi:10.1109/TPAMI.1979.4766909

156. Rousseeuw PJ. Silhouettes: A graphical aid to the interpretation and validation of cluster analysis. *J Comput Appl Math*. 1987;20:53-65. doi:10.1016/0377-0427(87)90125-7

157. Patek SD. Open-loop feedback control under multiple disturbance function hypotheses. In: *Proceedings of the IEEE Conference on Decision and Control*. ; 2010. doi:10.1109/CDC.2010.5717476

158. Maahs DM, Buckingham BA, Castle JR, et al. Outcome measures for artificial pancreas clinical trials: A consensus report. *Diabetes Care*. 2016;39(7):1175-1179. doi:10.2337/dc15-2716

159. White JW, Rassweiler A, Samhouri JF, Stier AC, White C. Ecologists should not use statistical significance tests to interpret simulation model results. *Oikos*. 2014;123(4):385-388. doi:10.1111/j.1600-0706.2013.01073.x